University of Alberta

Characterization of the C-terminal Domain of Human Sodium Bicarbonate Co-Transporter, NBC3

©

By
Frederick Benjamin Loiselle

A thesis submitted to the Faculty of Graduate Studies and Research in partial fulfilment of the requirements for the degree of Doctor of Philosophy

Department of Physiology

Edmonton, Alberta
Fall 2004

Library and Archives Canada

Published Heritage Branch

395 Wellington Street
Ottawa ON K1A 0N4
Canada

Bibliothèque et Archives Canada

Direction du Patrimoine de l'édition

395, rue Wellington
Ottawa ON K1A 0N4
Canada

Your file Votre référence
ISBN: 0-612-95976-7
Our file Notre référence
ISBN: 0-612-95976-7

The author has granted a non-exclusive license allowing the Library and Archives Canada to reproduce, loan, distribute or sell copies of this thesis in microform, paper or electronic formats.

L'auteur a accordé une licence non exclusive permettant à la Bibliothèque et Archives Canada de reproduire, prêter, distribuer ou vendre des copies de cette thèse sous la forme de microfiche/film, de reproduction sur papier ou sur format électronique.

The author retains ownership of the copyright in this thesis. Neither the thesis nor substantial extracts from it may be printed or otherwise reproduced without the author's permission.

L'auteur conserve la propriété du droit d'auteur qui protège cette thèse. Ni la thèse ni des extraits substantiels de celle-ci ne doivent être imprimés ou aturement reproduits sans son autorisation.

In compliance with the Canadian Privacy Act some supporting forms may have been removed from this thesis.

Conformément à la loi canadienne sur la protection de la vie privée, quelques formulaires secondaires ont été enlevés de cette thèse.

While these forms may be included in the document page count, their removal does not represent any loss of content from the thesis.

Bien que ces formulaires aient inclus dans la pagination, il n'y aura aucun contenu manquant.

Canada

Table of Contents

CHAPTER 1 1

. INTRODUCTION 1

1.1 OVERVIEW 1

1.1.1 Pancreatic duct cell bicarbonate secretion 3

1.1.2 Bicarbonate transport in the kidney 5

1.1.3 Bicarbonate transporter super family 9

1.2 THE NBC FAMILY OF TRANSPORTERS 13

1.2.1 NBC1 cloning 13

1.2.2 NBC1 localization 13

1.2.3 Stoichiometry of NBC1 in kidney and non-renal tissues 15

1.2.4 Regulation of NBC1 Activity 17

1.2.5 NBC4 Cloning and characterization 22

1.2.6 NBC3/NBCn1 cloning 24

1.2.7 NBC3/NBCn1 localization 26

1.2.8 Sodium bicarbonate co-transporters in familial disease 27

1.3 THE CARBONIC ANHYDRASE ENZYME FAMILY 28

1.4 CYTOPLASMIC DOMAINS OF BICARBONATE AND PROTON TRANSPORTERS 33

1.4.1 Characterization of the cytoplasmic domains of bicarbonate and proton transporters 33

1.4.2The cytoplasmic domain of the AE1 Cl^-/HCO_3^- exchanger 34

1.4.3 Role of AE1 cytoplasmic domain in regulation of transport 36

1.4.4 The cytoplasmic domain of the NHE1 Na^+/H^+ exchanger 38

1.4.5 The NBC3 C-terminal domain 39

1.5 RATIONALE AND SUMMARY OF PROJECT 41

CHAPTER 2. 43

STRUCTURAL AND FUNCTIONAL CHARACTERIZATION OF THE HUMAN NBC3 SODIUM/BICARBONATE CO-TRANSPORTER CARBOXYL-TERMINAL CYTOPLASMIC DOMAIN[1] 43

2.1 INTRODUCTION 44

2.2 METHODS AND MATERIALS 47

2.2.1 Materials 47

2.2.2 DNA constructs 47

2.2.3 Protein expression in mammalian cells 48

2.2.4 NBC3 transport assay 49

2.2.5 Immunodection 50

2.2.6 Confocal microscopy 51

2.2.7 GST-fusion protein purification 51

2.2.8 Analytical ultracentrifugation 53

2.2.9 Circular dichroism spectroscopy 53

2.2.10 Proteolysis 54

2.3 RESULTS 55

2.3.1 Effect of NBC3 C-terminal deletion on HCO_3^- transport 55

2.3.2 NBC3 expression and localization in HEK293 cells 57

2.3.3 Over-expression and purification of NBC3Ct 59

2.3.4 Hydrodynamic shape analysis of NBC3CT 63

2.3.5 NBC3Ct conformation is insensitive to changes in pH and temperature 63

2.3.6 Identification of surface exposed regions of NBC3Ct 66

2.4 DISCUSSION 69

CHAPTER 3. 74

REGULATION OF THE HUMAN NBC3 NA^+/HCO_3^- CO-TRANSPORTER BY CARBONIC ANHYDRASE II AND PROTEIN KINASE A 74

3.1 INTRODUCTION 75

3.2 MATERIALS AND METHODS 79

3.2.1 Materials 79

3.2.2 DNA constructs 79

3.2.3 Protein expression in mammalian cells 80

3.2.4 NBC3 transport assay 81

3.2.5 Measurement of intrinsic buffer capacity and proton flux 82

3.2.6 Antibody Preparation 82

3.2.7 Immunodection 83

3.2.8 Cell Surface processing assay 84

3.2.9 Confocal microscopy 84

3.2.10 GST-fusion protein purification 85

3.2.11 In vitro phosphorylation by PKA 85

3.2.12 Micro-titre plate binding assay 86

3.2.13 Sequence and statistical analysis 87

3.3 RESULTS 88

3.3.1 NBC3 transport activity and interaction with CAII 88

3.3.2 Effect of PKA on NBC3 transport activity 93

3.3.3 CAII physically interacts with NBC3Ct in a pH-dependent manner 95

3.3.4 NBC3 recruits CAII to the plasma membrane 98

3.3.5 PKA does not phosphorylate NBC3Ct in vitro 99

3.3.6 Identification of the site of CAII interaction on NBC3Ct 99

3.4 DISCUSSION 102

CHAPTER 4. 110

SUMMARY AND FUTURE DIRECTIONS 110

4.1 SUMMARY 111

4.1.1 Characterization of NBC3 Structure and Function 111

4.1.2 Regulation of NBC3 transport activity by CAII interaction and PKA-dependent phosphorylation 113

4.2 FUTURE DIRECTIONS 114

BIBLIOGRAPHY 117

List of Tables

Table 1.1. Bicarbonate transport proteins and their properties. 11

Table 1.2 Carbonic anhydrase isozyme catalytic activities and localizations. 29

Table 2.1. Summary of NBC3Ct purification data 62

List of Figures

FIGURE 1.1 MODEL DEPICTING HCO_3^- SECRETION BY PROXIMAL PANCREATIC DUCT CELLS. 4

FIGURE 1.2. MODEL OF HCO_3^- REABSORPTION/H^+ SECRETION IN KIDNEY PROXIMAL TUBULE CELLS. 7

FIGURE 1.3 MODEL OF HCO_3^- REABSORPTION/H^+ SECRETION FROM THE DISTAL TUBULE.. 9

FIGURE 1.4. ROOTED DENDROGRAM OF SLCA4 FAMILY 12

FIGURE 1.5 ESTABLISHMENT OF CONCENTRATION GRADIENT BY CA. 32

FIGURE 2.1. FUNCTIONAL ROLE OF NBC3CT 56

FIGURE 2.2. EXPRESSION AND LOCALIZATION OF HANBC3 AND HANBC3ΔCT. 58

FIGURE 2.3. ANALYSIS OF NBC3CT PURIFICATION. 60

FIGURE 2.4. SHAPE ANALYSIS OF NBC3CT. 64

FIGURE 2.5. CIRCULAR DICHROISM SPECTROSCOPY OF NBC3CT AT A RANGE OF PH VALUES. 65

FIGURE 2.6. LIMITED PROTEOLYSIS OF NBC3CT USING TRYPSIN AND CHYMOTRYPSIN. ... 68

FIGURE 3.1. CAII FUNCTIONALLY INTERACTS WITH NBC3 IN TRANSIENTLY TRANSFECTED CELLS. 89

FIGURE 3.2. EXPRESSION OF NBC3 AND CAII CONSTRUCTS IN HEK293 CELLS AND SUMMARY OF NBC3 ACTIVITY. 91

FIGURE 3.3. CAII BINDS GST.NBC3CT IN A PH-DEPENDENT MANNER 96

FIGURE 3.4. NBC3 RECRUITS OVER-EXPRESSED CAII TO THE PLASMA MEMBRANE IN TRANSIENTLY TRANSFECTED CELLS. 97

FIGURE 3.5. IDENTIFICATION OF THE CAII BINDING SITE WITHIN NBC3CT. 100

Abbreviations

AE, anion exchanger

AKAP, PKA associated protein

ANG II, angiotensin II

AT, angiotensin receptor

ATP, adenosine triphosphate

BCECF-AM, 2',7'-bis-(2-carboxyethyl)-5-(and-6)-carboxyfluorescein-acetoxymethyl ester

β_I, intracellular buffer capacity

BLM, basolateral membrane

bp, base pair

BT, bicarbonate transporter

CA, carbonic anhydrase

CAB, CAII consensus binding motif

cAMP, cyclic-adenosine monophosphate

CD, circular dichroism spectroscopy

CFTR, cystic fibrosis transmembrane conductance regulator

Ct, carboxyl-terminal

DMEM, Dulbecco's modified Eagle medium

dRTA, distal renal tubular acidosis

EBP50, ezrin binding protein 50

EIPA, 5-(N-ethyl-N-isopropyl) amiloride

EST, expressed sequence tag

GAPDH, glyceradehyde-3-phosphate dehydrogenase

GPC, gel permeation chromatography

GST, glutathione-S-transferase

GST.NBC3Ct, GST fusion of NBC3Ct

HA, hemagglutinin

HANBC3, HA tagged NBC3

HANBC3ΔCt, HANBC3 with NBC3Ct deletion

HEK, human embryonic kidney

HPLC, high performance liquid chromatography

IPTG, isopropylthiogalactoside

kDa, kiloDalton

LB, Luria broth

MAPK, mitogen activated protein kinase

MCT, monocarboxylate proton co-transport

NBC, sodium bicarbonate co-transporter

NBC3Ct, Ct domain of NBC3

NHE, sodium proton exchanger

NHERF, Na^+/H^+ exchange regulatory factor

Nt, amino-terminal

$OMCD_{is}$, outer medulla collecting duct inner stripe

PCR, polymerase chain reaction

PDZ, PSD-95/Dlg/ZO-1

PKA, protein kinase A

PKC, protein kinase C

Pyk2, non-receptor tyrosine kinase proline-rich tyrosine kinase II

PVDF, polyvinylidene difluoride

RACE, rapid amplification of cDNA end

RBCs, red blood cells

RT, reverse transcriptase

SDS, sodium dodecyl sulfate

SDS-PAGE, SDS-polyacrylamide gel electrophoresis

SLC, solute carrier family

SFKs, Src family kinases

Src, non-receptor protein tyrosine kinase

TK, tyrosine kinase

TMs, transmembrane segments

V_{max}, maximum transport rate

Chapter 1

Introduction

1.1 Overview

The pH of intra- and extracellular fluids is necessarily a tightly controlled variable in physiology. Changes in pH alter fundamental biological properties in the cell including protein-protein interactions, enzyme kinetics, and fluid osmolarity [1-4]. Intracellular pH (pH_i) regulation is critical for most cellular processes, including cell volume regulation, vesicle trafficking, cellular metabolism, cell membrane polarity, muscular contraction, and cytoskeletal interactions [1, 3-7]. The pH of a fluid compartment can be increased or decreased in one of two ways: metabolic generation or consumption of H^+ or transport of H^+ into or out of the cell.

Carbonic anhydrase, CA, is a ubiquitous enzyme found in both intracellular and extracellular compartments. CA catalyzes the reaction: $CO_2 + H_2O \leftrightarrow H^+ + HCO_3^-$. Thus, changes in the HCO_3^- concentration of a compartment bring about an indirect change in H^+ concentration through the mass action effect. In this way, moving a HCO_3^- ion from one compartment to another produces a "H^+ equivalent" in the original compartment. Cellular fuel metabolism converts nutrient molecules like glucose into CO_2, H_2O, and energy through a series of oxidative reactions. The newly generated CO_2 reacts with water to give HCO_3^- and H^+, resulting in cellular acidosis. Cellular transport processes then remove H^+ or H^+ equivalents to restore homeostatic pH.

There are four major mechanisms of pH_i recovery: monocarboxylate proton co-transport (MCT), sodium proton exchange (NHE), chloride bicarbonate anion exchange (AE), and sodium bicarbonate co-transport (NBC) [8-10]. After removal from the cell, protons or proton equivalents are temporarily

buffered in the blood, predominantly by CO_2/HCO_3^- and hemoglobin, then excreted from the body either through the action of the respiratory or urinary systems for CO_2-dependent or CO_2-independent acid respectively [11].

This thesis describes the intra- and extracellular metabolism of bicarbonate with an emphasis on the role of sodium bicarbonate transport proteins in that process. We will begin by detailing the movement of bicarbonate into and out of representative cell types for each process. We will then discuss the sodium bicarbonate and carbonic anhydrase families, emphasizing what is known about the cytoplasmic domains of the former. The main body of the thesis describes my work to determine the structure and function of the sodium bicarbonate transporter 3 C-terminal tail. The final chapter summarizes my work in the broader context of cellular physiology and suggest future avenues for exploration.

1.1.1 Pancreatic duct cell bicarbonate secretion

In addition to pH_i regulation, proton and proton equivalent transport processes are also required for several physiological processes involving the extracellular fluid. For example, in the gastrointestinal tract gastric HCl secretion acidifies the chyme to assist protein degradation. As the chyme passes through the pyloric sphincter, pancreatic duct cells secrete a HCO_3^- rich fluid that carries enzyme-rich fluid from the acini to the duodenum where the acidic chyme is neutralized [12]. This process is important to protect the small intestine mucosa and to optimize pancreatic enzyme kinetics [12]. In humans, pancreatic fluid

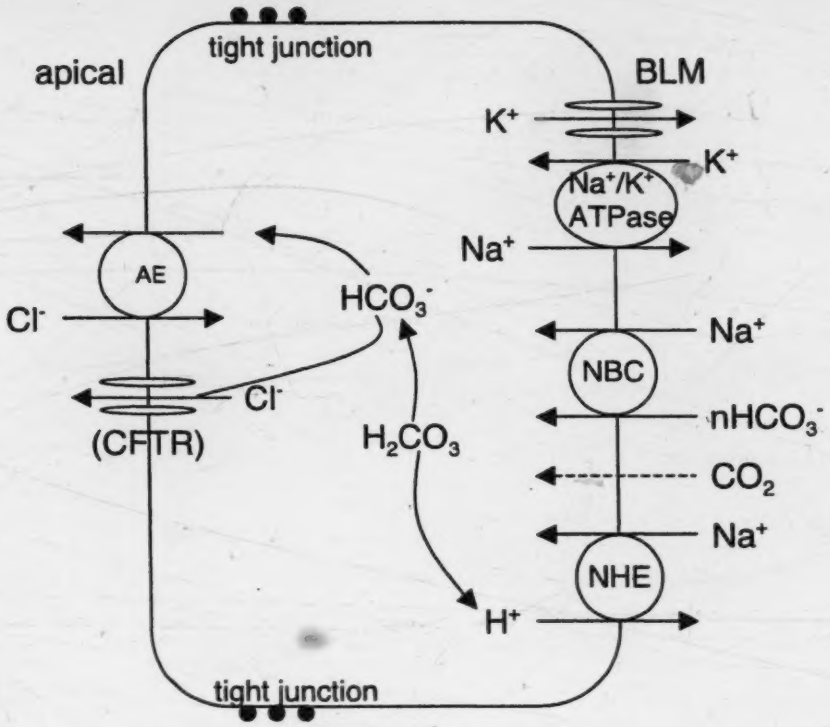

Figure 1.1 Model depicting HCO_3^- secretion by proximal pancreatic duct cells. Pancreatic duct cells possess BLM Na^+/K^+ ATPase, K^+ channel, NHE and NBC transport activity. The action of the Na^+/K^+ ATPase and K^+ channels produces an inward Na^+ gradient and polarizes the membrane. This provides the driving force for HCO_3^- entry and H^+ exit across the BLM via the NBC and NHE, respectively. Intracellular CA activity hydrates CO_2 to give HCO_3^- and H^+; the latter is removed from the cell by BLM NHE, thus provides a second route for HCO_3^- entry into the cell. The apical efflux of HCO_3^- has both Cl^- dependent and independent components, which utilize an AE and CFTR respectively [13]

secretions contain an average of 140 mM HCO_3^-, which is remarkable considering pancreatic duct cells have an intracellular HCO_3^- concentration of 10-15 mM [13]. Pancreatic HCO_3^- secretion requires transepithelial transport from the interstitial fluid to the lumen of the gland. At the basolateral membrane (BLM), HCO_3^- enters the cell directly via NBC activity with a stoichiometry of 1:2 or 1:3 (figure 1.1) [13]. An indirect pathway that involves CO_2 permeation followed by CA catalyzed hydration of H^+ and HCO_3^- also plays a role (figure 1.1). The resulting H^+ is extruded across the BLM via NHE activity and/or H^+-pump (figure 1.1) [13]. Transport across the luminal membrane involves a Cl^- channel, the cystic fibrosis transmembrane conductance regulator, CFTR, in most species, and an AE protein (figure 1.1). Upon stimulation by the gastric hormone secretin, a cyclic-adenosine monophosphate (cAMP) -dependent activation of CFTR occurs resulting in Cl^- flux into the luminal space. Cl^- is then taken back into the cell via AE activity in exchange for HCO_3^- resulting in a net HCO_3^- efflux [13]. This model accounts for secretion of 60 to 80 mM HCO_3^- observed in rat and mouse; however, in human and guinea pig total HCO_3^- secretion is 140 mM and an additional mechanism is required to achieve the extra HCO_3^- secretion [14]. Recently, a cAMP stimulated HCO_3^- flux has been demonstrated to occur through CFTR and it is believed that this pathway may account for the high pancreatic duct HCO_3^- concentration observed in some species (figure 1.1) [13].

1.1.2 Bicarbonate transport in the kidney

In contrast to the gastrointestinal tract, the kidneys perform net acid excretion. Transepithelial transport across the tubular cells, moves protons or

proton equivalents from the interstitial fluid into the lumen of the tubule, while in an obligatory fashion, bicarbonate is reabsorbed from the lumen and transferred to the interstitial fluid [15]. The proximal tubule reabsorbs approximately 80% of the filtered load of HCO_3^- by active H^+ secretion [16]. The majority of constitutive HCO_3^- reabsorption is carried out by a luminal sodium proton exchanger, NHE3, and a BLM sodium bicarbonate co-transporter, NBC1a [17]. The mechanism involves hydration of intracellular CO_2 by carbonic anhydrase to yield H^+ and HCO_3^- (figure1.2). The luminal NHE3 then transports H^+ into the tubular fluid in exchange for a Na^+ ion [17]. The resultant Na^+ ion is subsequently co-transported with HCO_3^- across the BLM by NBC1a. Thus in effect, a proton is secreted and a bicarbonate ion is reabsorbed by the same mechanism (figure 1.2). If the luminal proton is buffered by any system other than CO_2/HCO_3^- then instead of reabsorbing a HCO_3^- from the tubule, a new HCO_3^- ion is effectively produced. The new bicarbonate increases the buffering power of the blood. During metabolic acidosis the kidney actively secretes NH_3, which can buffer tubular protons, thereby increasing the tubular acid carrying capacity and blood buffer capacity.

The remaining 20% of bicarbonate reabsorption occurs in the distal tubule and collecting duct, and is less well understood. Type A intercalated cells in the outer medulla collecting duct inner stripe, $OMCD_{is}$, have been shown to have the highest rates of bicarbonate reabsorption and acid secretion [18]. Several transporters have been identified in this cell type and it is likely that multiple mechanisms of trans-epithelial transport contribute to proton and bicarbonate flux (figure 1.3). At the luminal membrane, the vacuolar H^+-ATPase, a P-type

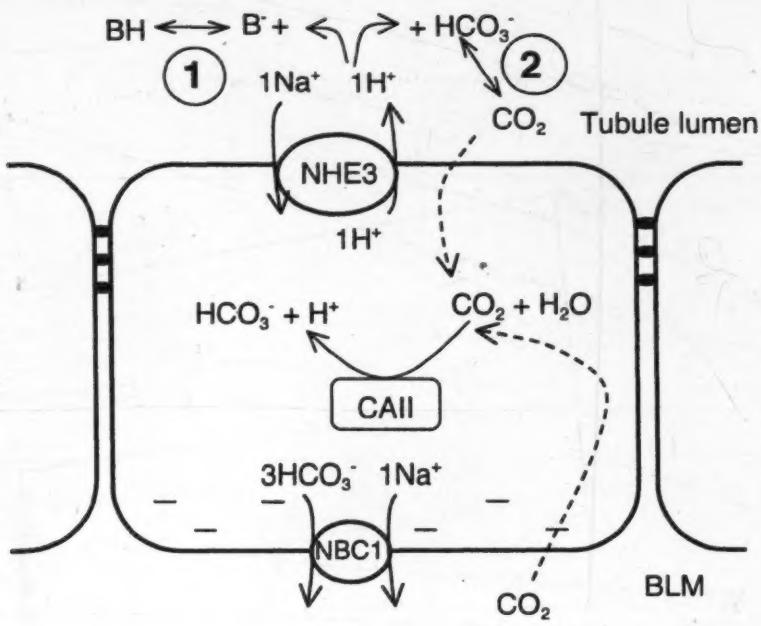

Figure 1.2. Model of HCO_3^- reabsorption/H^+ secretion in kidney proximal tubule cells.
CO_2 passively diffuses across the apical membrane and is hydrated to HCO_3^- and H^+ by intracellular CAII. Apical NHE3 then removes a H^+ from the cell in exchange for Na^+. If the efluxed H^+ is buffered by HCO_3^- then the resultant intracellular HCO_3^- generated was effectively reabsorbed from the tubule lumen (circled 2). However, if the efluxed H^+ is buffered by some other buffer (PO_4^- or NH_3) then the intracellular HCO_3^- generated by hydration of CO_2 is effectively a "new" molecule will ultimately increase the buffering strength of the blood. HCO_3^- exits the cell at the BLM via NBC1a operating with a 1:3, Na^+:HCO_3^- stoichiometry [19].

gastric-like H^+-K^+-ATPase, and the Na^+ HCO_3^- co-transporter, NBC3 are present [18]. At the BLM, an anion exchanger, kidney AE1, and a sodium proton exchanger are present and together with the apical transporters mediate proton secretion and bicarbonate reabsorption [20]. Naturally occurring mutations in some of these transporters have been identified in patients that present with distal renal tubular acidosis, dRTA [21]. For example, loss-of-function mutations in 116 kDa, or 58 kDa subunits of the vacuolar H^+-ATPase are associated with dRTA [21]. Mutations in kAE1 are also associated with both recessive and dominant forms of dRTA [21].

Until recently, proton secretion and bicarbonate reabsorption were believed to be Na^+-independent in $OMCD_{is}$ and mediated only by the apical H^+-ATPases and basolateral kAE1 [22]. The discovery of NBC3 in the apical membrane has prompted a re-evaluation of this belief. Using very sensitive techniques, a recent study has shown that approximately 15% of trans-epithelial H^+ flux results from apical membrane Na^+-dependent transporters [18]. Segments treated apically with EIPA, an inhibitor of NBC3 activity, also showed a 15% decrease in trans-epithelial H^+ flux [18]. There is some disagreement in the literature about the inhibitory effects of EIPA on NBC3. A review of all reports suggest that in the 0-10 μM range EIPA has little or no effect on NBC3 activity, yet at higher concentrations (50 μM and more) EIPA blocks NBC3 transport by 75% or more. The inhibitor and Na^+-dependent H^+ flux decrease were non-additive, which strongly suggests that this fraction of H^+ flux is due to apical NBC3 [18].

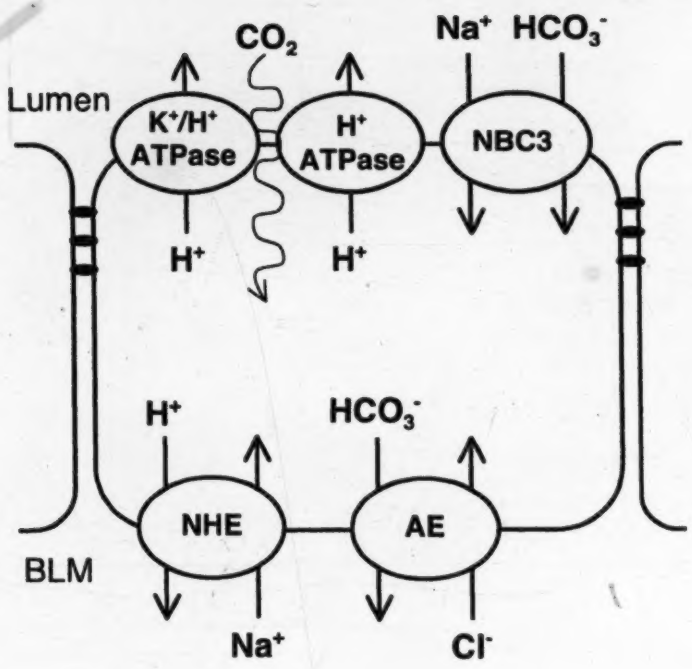

Figure 1.3 Model of HCO_3^- reabsorption/H^+ secretion from the distal tubule. Type A intercalated cells produce the highest rate of HCO_3^- reabsorption/H^+ secretion in the distal tubule. Several transporters are present in these cells; however, the percent contribution of each transporter to total flux is not known. Transporters that potentially play a role in flux include: the vacuolar H^+-ATPase, a P-type gastric-like H^+-K^+-ATPase, and the Na^+ HCO_3^- co-transporter, NBC3 at the apical membrane and, an anion exchanger (kidney AE1) and a sodium proton exchanger at the BLM [18]

1.1.3 Bicarbonate transporter super family

Alignment of the amino acid sequence of bicarbonate transporters (BT) from the solute carrier family 4, SLC4, and the more recently identified SLC26 families shows a significant degree of identity, which suggests the existence of a superfamily of BT. Table 1.1 summarizes the best-characterized BT superfamily members and their properties. The SLC26 family consists of anion exchangers that in general mediate halide/organic ion exchange including Cl^-/HCO_3^- exchange. One or more of these proteins may be the unidentified AE transporter present in the apical membrane of pancreatic duct cells (figure 1.1). Interestingly, a recent report has shown that CFTR interacts with the SLC26 family members DRA and Pendrin and suggests that one or more of these interactions may be physiologically significant [23].

The SLC4 family has two major branches, AE and NBC, as seen in figure 1.4. These transport families share substantial identity, especially within their membrane spanning domains. AE4 shares the greatest identity of all AEs with NBCs [24]. AE transporters exchange Cl^- for HCO_3^- across the membrane in a one-for-one electroneutral fashion. NBC proteins co-transport Na^+ and HCO_3^- across the membrane with a 1:1, 1:2, or 1:3 stoichiometry, depending on local regulatory factors and the specific isoforms. The following sections will discuss the cloning and characterization of the NBC and CA family members, with emphasis on cytoplasmic domain characterization.

Table 1.1. Bicarbonate transport proteins and their properties.

Protein	Other names	Tissue distribution	Mechanism	Net charge flux	Citation
AE1	SLC4A1, Band 3	Erythrocyte, kidney, heart	Cl^-/HCO_3^- exchange	0	[25]
AE2	SLC4A2	Widespread	Cl^-/HCO_3^- exchange	0	[26]
AE3	SLC4A3	Brain, heart, retina, gastrointestinal tract, kidney	Cl^-/HCO_3^- exchange	0	[27]
NBC1a	SLC4A4, kNBC	Kidney, cornea	Na^+/HCO_3^- co-transport	-2 or -1	[28, 29]
NBC1b	SLC4A4, hhNBC, pNBC, rb1NBC, splicing variant of NBC1	Heart, pancreas, kidney, cornea, prostate, colon, stomach, glia, thyroid, brain	Na^+/HCO_3^- co-transport	-2 or -1	[30-32]
NBC3	SLC4A7, NBC2, NBCn1a,b,c,d	Heart, kidney, skeletal muscle, pulmonary, artery, aorta, submandibular gland	Na^+/HCO_3^- co-transport	0	[33-35]
NBC4	SLC4A5, NBC4a,b,c	Liver, spleen, epididymis, heart, brain kidney	Na^+/HCO_3^- co-transport	-1 or 0	[36-39]
AE4	SLC4A9	Kidney, testis	Cl^-/HCO_3^- exchange? Na^+/HCO_3^- co-transport?	?	[40, 41]
NDCBE1	SLC4A8, NDAE1, NCBE, (NBC3)	Neurons, kidney, fibroblasts	Na^+-dependent Cl^-/HCO_3^- exchange	0 or +1	[42-44]
Btr1	SLC4A11	Kidney, salivary gland, testis, thyroid, trachea			[40]
DRA	SLC26A3, CLD	Colon, ileum, ecrine sweat gland	Cl^-/HCO_3^- exchange	0	[45, 46]
Pendrin	SLC26A4, PDS	Inner ear, thyroid, kidney	Cl^-/HCO_3^- exchange; also I^-	0	[47, 48]
PAT-1	SLC26A6, CFEX	Kidney, heart, pancreas, liver skeletal muscle, intestine, placenta	Cl^-/HCO_3^- exchange oxalate and formate	0	[49-51]
SLC26A7	SLC26A7	Kidney	Cl^-, SO_4^{2-}, HCO_3^-?		[52, 53]
Tat1	SLC26A8	Spermatocytes	Cl^-, SO_4^{2-}, HCO_3^-?		[52, 54]
SLC26A9	SLC26A9	Lung	Cl^-, SO_4^{2-}, HCO_3^-?		[52]

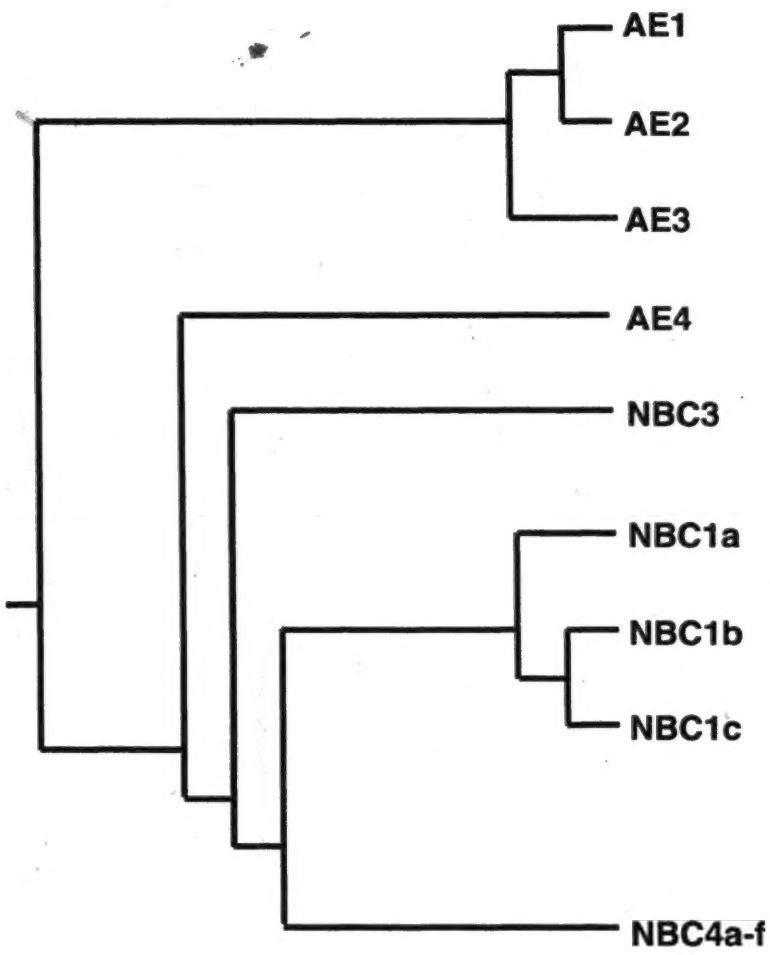

Figure 1.4. Rooted dendrogram of SLCA4 family.
The cartoon depicts the phylogenetic relationship between members of the human SLCA4 family of proteins. Dendrogram was produced using Phylip software.

1.2 The NBC family of transporters

1.2.1 NBC1 cloning

To date, four variant transcripts from the NBC1 gene have been identified. NBC1 was first cloned from amphibian and human kidney, and later from rat kidney. This variant will subsequently be referred to as NBC1a [24, 28, 29, 55]. A variant in which the first 41 amino acids of NBC1a N-terminal domain have been replaced by 85 unique amino acids has been cloned from human and rat pancreas, NBC1b [30, 56]. Another splice variant was identified from a human heart cDNA library, hNBC1 that is identical in amino acid sequence to NBC1b but differs in the mRNA 5′ un-translated region [32]. The preceding three variants have been shown to arise from differential splicing of the SLC4A4 gene, interestingly although NBC1b and hNBC1 share identical amino acid sequence, they differ in promoter usage, suggesting tissue-specific regulation of expression at the transcriptional level [57]. Finally, a variant that is identical to NBC1b except for 61 unique amino acids that replace 46 amino acids at the extreme C-terminus has been identified from rat brain (bNBC1) [31]. The amino acid sequence difference is due to a 97 base pair deletion that results in a frame shift and extension of the open reading frame [31], suggesting that the transcript may represent a cloning artefact.

1.2.2 NBC1 localization

Several groups have reported on the tissue distribution and membrane targeting of NBC1, each suggesting a different localization profile [12, 30, 58-69].

Some of this work was completed before the genetic organization of the SLC4A4 gene was characterized and thus does not account for variant specific profiling. There is still substantial disagreement on exact tissue distribution of each variant. Several factors contribute to this situation. First, many groups have performed multiple tissue Northern blots on various clones, but the completeness of each screen varies with each group. Second, some localization experiments have been carried out using antibodies on tissues known to transport HCO_3^- and not Northern blots. Finally, there are species-specific differences that complicate the matter further.

The emerging consensus is that NBC1a is found predominantly in the early proximal tubule with the S1 segment showing the strongest immunohistochemical staining [59, 64, 70]. Only a single study has identified the NBC1a variant in extra-renal tissue, specifically, the conjunctiva of rat eye [66]. By contrast, in the same study NBC1b was identified in cornea, conjunctiva, lens, ciliary body, and retina [66]. As this data suggests, NBC1b has a much broader distribution, and is likely involved with most HCO_3^- secreting systems of the body. In a comparative study, using human NBC1b and NBC1a variant specific mRNA probes, multiple tissue Northern blots identified a ~7.6-kb transcript for NBC1a only in kidney [30], while, the NBC1b probe identified ~7.7-kb transcripts in several tissues, including brain, pancreas, prostate, colon, stomach, thyroid, and spinal cord, with the strongest staining coming from pancreas [30]. In rat, an NBC1 variant has been identified in the initial segment and intermediate zone of the epididymis [58]. Strong staining was observed, in BLM of principle and apical/narrow cells in this region, using an antibody generated against the C-terminus of NBC1 [58]. *In Situ* hybridisation has also identified one or multiple

NBC1 variants in several brain structures in both glia and neurons [60]. In both studies the probes or antibodies used were directed against regions common to the variants, which makes it impossible to determine the variant that accounts for the observed staining. However, a multiple tissue Northern blot using a probe specifically against rat NBC1a did not identify a transcript in testis or brain [30]. In human pancreas, NBC1b localizes to the BLM of duct cells and is absent from acinar cells [61]. This finding is in contrast to a similar study of mouse pancreas that found NBC1b staining in the BLM of both duct and acinar cells [30]. Interestingly, in almost every epithelial tissue studied, NBC1b localizes exclusively to the BLM of HCO_3^- secreting cells suggesting that this variant is involved with HCO_3^- influx. One notable exception is the apical localization of NBC1 in rat parotid glands [62]. In these glands the primary fluid secreted by acini is higher in HCO_3^- than the final fluid, suggesting early secretion and later reabsorption of HCO_3^-.

1.2.3 Stoichiometry of NBC1 in kidney and non-renal tissues

In the kidney proximal tubule approximately 80% of the filtered HCO_3^- load is reabsorbed by the combined action of apical NHE3 and basolateral NBC1a (figure 1.2) [71]. Proximal tubule cells are hyperpolarized relative to the interstitial fluid, with a membrane potential around –60 mV [71]. Both the Na^+ and HCO_3^- gradients across this membrane are directed inward. Thus, it is a functional requirement that NBC1a transport stoichiometry have a net negative charge to facilitate HCO_3^- reabsorption from the tubule. In fact, a stoichiometry of 3:1, HCO_3^-: Na^+ is thermodynamically required for cellular efflux based on

what is known about the ionic gradients and membrane potential in the proximal tubule [72]. Several reports on isolated proximal tubule segments and vesicular preparations indicate that NBC1a functions with a 3:1 stoichiometry in the proximal tubule [73-75]. Three different transport models can account for a 3:1 HCO_3^-:Na^+ stoichiometry: 1Na^+ : 1CO_3^{2-} : 1HCO_3^-, 1$NaCO_3^-$: 1CO_3^{2-}, or 1Na^+ : 3HCO_3^-.

Electrophysiological studies of apical membrane permeablized proximal tubule segments have shown that NBC1a operates with a 3:1 stoichiometry in these cells [75]. Yet in transfected *Xenopus* oocytes or pancreatic duct cells NBC1a has a 2:1 HCO_3^-:Na^+ stoichiometry [2, 76]. In light of the fact that several physiological lines of evidence indicate that in the proximal tubule NBC1a operates with a 3:1 stoichiometry, it seems likely that an environmental factor influences the stoichiometry *in vivo*. In support of this idea a recent study found that when NBC1b and NBC1a were transfected into mouse proximal tubule and a collecting duct cell lines both exhibited 3:1 stoichiometry in the proximal tubule line and 2:1 stoichiometry in the collecting duct line [77]. This finding indicates that the stoichiometric difference in proximal tubule and pancreatic duct is not a property of the different NBC1 N-terminal domains, and that cellular factors are responsible for the difference.

Investigations into a possible role of second messengers in mediating this stoichiometric shift have shown that protein kinase A (PKA) -dependent phosphorylation of Ser^{982} of NBC1a causes this variant to switch from a 3:1 to a 2:1 stoichiometry [77]. This is consistent with the down-regulating effect of PKA stimulation on HCO_3^- reabsorption from the proximal tubule [78]. In the pancreas PKA stimulation activates the apical Cl^- channel function of CFTR [79].

This in turn will depolarise duct cells and facilitate HCO_3^- influx through NBC1b at the BLM. One suggested explanation for the inhibitory effect of phosphorylation at Ser^{982} involves an interaction with the cytosolic enzyme carbonic anhydrase II, CAII [15]. CAII has been shown to bind an acidic motif, LDADD, in AE1 and this interaction is required for the full HCO_3^- transport activity of this protein [80][81]. A similar acidic cluster, $D^{986}NDD$, in NBC1a may interact with CAII. The addition of another negative charge by phosphorylation at S^{982} may disrupt this interaction and form the basis of the stoichiometric shift. How phosphorylation affects the stoichiometric shift remains to be determined. An understanding of the exact ions transported to give a 3:1 or 2:1 stoichiometry would be useful in characterizing this effect.

1.2.4 Regulation of NBC1 Activity

The primary determinants of NBC activity are transmembrane Na^+ and HCO_3^- gradients and, for the electrogenic NBC1, membrane potential. In addition to these modulators, several lines of evidence suggest that NBCs are also regulated by other environmental factors, much like allosteric enzymes are. Specifically, NBC1 transport activity is subject to control by intracellular pH and P_{CO_2}, possibly through intrinsic sensor regions [82, 83]. Phosphorylation also modulates transport activity, either directly or through an accessory factor [17]. In addition, certain chronic conditions cause up-regulation of NBC1 expression both at the transcriptional and post-translational levels [71].

The effect of altered pH on NBC1 transport activity has been studied using *in vitro* models of metabolic acidosis and alkalosis. Isolated basolateral

vesicles from renal proximal tubule show NBC1 activity is up-regulated in acute metabolic acidosis but is insensitive to acute metabolic alkalosis, suggesting that the adaptive response of the kidney to metabolic alkalosis does not involve NBC1 [71]. The increased activity was caused by an increase in transporter maximum transport rate, V_{max}, consistent with an increase in either the number of transporters or the turnover rate of transporters already present in the membrane. In an independent study, acute metabolic acidosis activated NBC1 through a protein kinase C, PKC, -dependent pathway that involves an increase in V_{max} [71, 83-88]. Pre-treatment with the protein synthesis inhibitor, cycloheximide, did not inhibit the up regulation, which further indicates an increase in the number of transporters in the plasma membrane or activation of an inactive pool [89]. These effects could be mediated by recruitment of NBC-containing intracellular vesicles to the plasma membrane or activation of the existing plasma membrane pool of transporters. Proximal tubule cells grown to confluence on a permeable support, mounted in an Ussing-type chamber and apically permeablized with amphotericin B were used to study the pH-dependence of NBC1 transport activity. Using this method NBC1 transport activity was found to be sensitive to changes in intracellular but not extracellular pH, suggesting the existence of a pH sensor region on the intracellular surface of the transporter [90]. Recently, site-directed mutagenesis of NHE3 has identified two histidine residues in the cytoplasmic domain that are important to determine the pH responsiveness of this transporter [91]. Interestingly, the N-terminal cytoplasmic domain of NBC1 is rich in histidine residues, which suggests that this region may similarly act as a pH sensor.

Respiratory acidosis increases NBC1 activity both acutely and chronically [71].Kinetic analysis has demonstrated that up-regulation is mediated through changes in V_{max} and not substrate concentration at one-half V_{max}, Km [92]. Acute acidosis up-regulates NBC1 transport activity after only 5 minutes of exposure of transfected cells to high CO_2 and is reversible after 48 hours [92]. This mode of regulation is mediated through PKC and tyrosine kinase (TK) signalling pathways. Specifically, signalling through the TK pathway involves non-receptor protein tyrosine kinase family of kinases, SFKs, and the "classic" mitogen activated protein kinase, MAPK, pathway [83]. After 4 hours of exposure, protein synthesis inhibitors were able to block the stimulatory effect of high CO_2 [92]. These findings suggest that an extrinsic CO_2 sensor exists in the cell that signals through second messenger pathways and that acute regulation is mediated through phosphorylation while chronic (>4 hours) regulation involves and up-regulation of NBC1 expression.

Angiotensin II (ANG II) has direct effects on renal tubular functions. In the renal proximal tubule, its principle target is NBC1a [93]. Interestingly, the effects of ANG II are biphasic with respect to HCO_3^- reabsorption, in that at low concentrations (picomolar/nanomolar) ANG II is stimulatory, while at high concentrations (nanomolar/micromolar) it is inhibitory [94]. In the kidney, ANG II effects are mediated by angiotensin 1, AT_1 receptors, predominantly AT_{1A} [93]. Regulation of NBC1 in heart is more controversial; one report indicates that regulation is mediated through AT_1 receptors while another suggests AT_2 receptors are involved [86, 95]. This discrepancy may be due to methodological differences between the two studies. The group suggesting regulation through AT_2 receptors measured increases in expression at the mRNA, while the other

group looked at transport activity. It is possible that both pathways are important, with AT_1 being involved in acute regulation and AT_2 chronic regulation. Pharmacological dissection of the signalling pathway downstream of AT_1 receptor activation in proximal tubule cells has indicated that activation of SFKs and the classical MAPK pathway is involved [93]. Recently, a link between the acute activation of NBC1 by CO_2 and ANG II has been established. The non-receptor tyrosine kinase proline-rich tyrosine kinase II, Pyk2, is essential for the activation of NBC1 by both CO_2 and ANG II [96]. However, the mechanism that couples Pyk2 to NBC1 activation has not been elucidated.

Cholinergic agents have been shown to activate NBC1 through G protein-coupled M_1 muscarinic receptor activation in kidney proximal tubule cells [85]. Regulation involves the sequential activation of SFKs, Ras, and the classical MAPK pathways [85]. Cholinergic agents, insulin and epidermal growth factor activate NBC1 through receptor protein tyrosine kinases [83]. Glucose and Na^+ are important serum osmolytes. Thus, it is likely that regulation of NBC1a activity is linked to serum glucose levels. Increasing insulin concentration 100-fold did not further potentiate the stimulatory effect, which suggests that insulin has a permissive effect on TK activation [97].

High levels of glucocorticoids induce metabolic alkalosis, as seen in Cushing syndrome [98]. Consistent with this observation, NBC1a expression levels increase in the proximal tubule following four days of treatment with the dexamethasone, which suggests that NBC1a is at least partially responsible for the effect of glucocorticoids/metabolic alkalosis [98]. Conversely, treatment with mineralocorticoids (which have no receptors in the proximal tubule) had no effect on NBC1a levels in the proximal tubule, which suggests that proximal

tubule HCO_3^- reabsorption is up-regulated in response to stress but not hypertension [98]. A recent report has shown that dexamethasone treatment increases bicarbonate secretion in intrahepatic biliary epithelium. Therefore, it is likely that expression of the major extra-renal NBC protein, NBC1b, is upregulated under these conditions [99].

Potassium depletion has also been shown to up-regulate NBC1 expression. The regulation of plasma pH and potassium concentration is linked so that hypokalemia induces metabolic acidosis, which leads to up-regulated H^+ secretion and HCO_3^- reabsorption. Interestingly, increased expression could be detected as early as two days after the onset of potassium depletion in rats, and thus precedes hypokalemia, which suggests that NBC1 regulation is either extremely sensitive or mediated by an indirect mechanism [100]. This indicates that the signalling pathway initiating NBC1 expression up-regulation is sensitive to decreased intracellular potassium. Increased NBC1 expression is not limited to the proximal tubule but was also observed in the thick ascending limb and inner medullary collecting duct, which is consistent with the idea that K^+-sensing and secretion occurs in these regions of the tubule [100].

Activators of the cAMP second messenger pathway are inhibitory to NBC1 activity in the proximal tubule [101, 102]. Both norepinephrine and dopamine, which signal through activation of adenylate cyclase, inhibit NBC1 activity in proximal tubule cells [15]. The mechanism of transport inhibition by cAMP-dependent PKA activation is not well understood. However, in the proximal tubule the Na^+/H^+ exchange regulatory factor, NHERF, is required for PKA dependent inhibition of NBC [78].

1.2.5 NBC4 Cloning and characterization

NBC4 is the most recently identified member of the Na^+/HCO_3^- family of co-transporters [36, 103]. To date, 5 splice variants of this transporter have been identified, named NBC4a-e [36-38, 103]. NBC4a codes for a 1137 amino acid polypeptide with 12 to 14 putative membrane spanning domains [103]. NBC4b codes for 1074 amino acids and has a 16 base pair (bp) insertion in the third to last exon, which introduces a frame-shift mutation, resulting in premature truncation [103]. NBC4c codes for a 1121 amino acid polypeptide and is missing 16 amino acids, found in NBC4a and b, between putative transmembrane segments, TMs, 11 and 12 [37, 38]. NBC4d codes for a 1039 amino acid polypeptide and is missing two exons that code for the sequence between putative TMs 10 to 14 [38]. NBC4e truncates after only 18 bp of the second to last TM of NBC4a and codes for a 1051 amino acid polypeptide [39]. Using the technique of cysteine scanning mutagenesis our laboratory has generated several topology models for AE1, the first identified member of the BT super family [104-106]. Recently a topology model for NBC1b was also published [107]. Since all members of the BT super family share a high degree of identity within the membrane domain it is widely believed that the TM segment structure of the region is conserved. Therefore, it is difficult to believe that NBC4d, missing several functionally important TM segments, is capable of transporting ions. In addition, one group has questioned the authenticity of some of these variants on statistical grounds. Upon screening a mixed human cDNA library generated from several distinct tissues using polymerase chain reaction, PCR, probes, 9 consecutive clones of NBC4c were identified with no hits for any of the other

variants. Assuming even distribution of mRNA of each variant and equal PCR efficiencies the likelihood of this event is very low [38]. That is, it seems very unlikely that any real transcript expressed in human would be missed with the screening method used and that NBC4c is therefore the only real isoform of NBC4.

Determination of the tissue distribution of NBC4 is still in the early stages. On the basis of multiple tissue Northern blots variants NBC4a and or NBC4b show strong signals in liver, testes, and spleen and give moderate signals for heart [103]. Using cDNA libraries from heart and testis and PCR primers that amplify shared and unique regions of these variants it has been shown that both NBC4a and NBC4b are expressed in heart at approximately equal levels [103]. Only NBC4a was identified in the testis [103]. NBC4c shows wide distribution and is found, at the mRNA level, in tissues including brain heart, kidney, testis, pancreas muscle and white blood cells [37]. The tissue distribution of NBC4d has not been characterized. NBC4e was originally cloned from kidney and localizes to thick ascending limbs of the loop of Henle in both cortical and outer medullary segments [39].

The transport stoichiometry characteristics for NBC4c and e have been determined. Interestingly, NBC4c is electrogenic, when expressed in *Xenopus laevis* oocytes, with a stoichiometry of 2:1 HCO_3^-:Na^+ assessed by plotting E_{rev} versus $\log[Na^+]_o$ [38]. However, NBC4e has an electroneutral stoichiometry when expressed in the same system [39]. This finding is quite remarkable as it is the first example of a stoichiometric shift due to a structural difference between variants of the same gene in the BT superfamily. NBC4e contains a 16 amino acid insert between TM segments 11 and 12 (not present in variants a and b) and

is missing the C-terminal cytoplasmic domain. Functional characterization of the NBC4a and b variants will likely prove to be very instructive with respect to the nature of the stoichiometry shift of NBC4e. One possible explanation involves the binding of CAII to the C-terminal cytoplasmic domain. CAII binds the C-terminal domains of several members of the BT super family and is required for the full transport function of these proteins. In one study phosphorylation of the C-terminal domain of NBC1 decreased the transport stoichiometry from 3:1 HCO_3^-:Na^+ to 2:1 possibly by disrupting the interaction with CAII [19]. The absence of the C-terminal domain of NBC4e may also disrupt CAII binding and be responsible for the different transport stoichiometry from NBC4c.

1.2.6 NBC3/NBCn1 cloning

The contractile activity of muscle tissue is highly sensitive to changes in pH_i. During periods of high activity and ischemia large quantities of lactic acid are produced that need to be handled so as to prevent deleterious consequences. Several pH_i regulatory processes are believed to be involved in preventing intracellular acidosis in these cells, during times of increased metabolic acid production or increased ambient CO_2. Except for guinea pig femoral artery preparations, Na^+-dependent HCO_3^- transport has been demonstrated in all muscle preparations studied [108]. However, transport stoichiometry and pharmacological inhibition profiles differ between tissues, suggesting that multiple Na^+/HCO_3^- co-transporters are present in muscle. For example, Na^+/HCO_3^- co-transport in ventricular myocytes and smooth muscle cells is electroneutral [109, 110], while NBC1 mediates only electrogenic co-transport

with either a 2:1 or 3:1 HCO_3^-:Na^+ stoichiometry [16]. Also, NBC1 transport activity is stilbene-sensitive and amiloride-insensitive, yet in smooth muscle cell preparations stilbene-insensitive and amiloride-sensitive Na^+/HCO_3^- co-transport has been reported [108]. These findings set the stage for the identification of NBC3.

NBC3 was cloned from a human skeletal muscle cDNA library using probes generated from partial sequence information obtained from human expressed sequence tag, EST, clones and 5′ and 3′ rapid amplification of cDNA end, RACE, products [35]. Multiple tissue Northern blots originally indicated that NBC3 is expressed most strongly in skeletal muscle with approximately half as much expression in heart [35]. Subsequently, NBC3 was identified by reverse transcriptase, RT, -PCR in distal kidney tubule segments [111]. The NBC3 mRNA encodes a 1214 amino acid polypeptide with 12 putative transmembrane segments [35]. Its transport activity is electroneutral, stilbene-insensitive, and 5-(N-ethyl-N-isopropyl) amiloride, EIPA, -sensitive (50 μM) [35]. A rat orthologue to NBC3, called NBCn1 (n for electroneutral), has been cloned from smooth muscle [33]. Three C-terminal variants of this transporter (-B, -C, and -D) were identified and share 89-92 % identity at the amino acid level with human NBC3 [33]. Interestingly, NBCn1-B is ~25% sensitive to stilbene derivatives and essentially insensitive to EIPA (200 μM) [33]. The EIPA sensitivity of NBC3 requires some additional attention. Recently a report demonstrating an interaction between NBC3 and CFTR indicated that NBC3 is insensitive to low concentrations of EIPA [112], which has since been independently verified [113]. In this study, transport assays were carried out in human embryonic kidney,

HEK, 293 cells treated with 2.5-10 μM EIPA [112]. This concentration range was sufficient to block background NHE1 activity but did not adversely affect NBC3 mediated Na^+/HCO_3^- transport [112].

1.2.7 NBC3/NBCn1 localization

NBC3 localizes to the apical membrane of type A intercalated cells of collecting ducts in both the cortex and medulla, and co-localized with the 31 kDa subunit of the vacuolar H^+-ATPase [114]. A direct physical interaction was demonstrated by the bi-directional co-immunoprecipitation of these polypeptides [114]. The interaction was mediated by the PDZ binding site present at the NBC3 C-terminus, indicating a role of this region in formation of protein/protein complexes. In several reports the vacuolar H^+-ATPase has been identified in association with subcellular structures, where it plays a role in acidification, including clathrin-coated vesicles, endosomes, and lysosomes [115, 116]. This suggests that NBC3 may also localize to these structures. Alternatively, intracellular H^+-ATPase-containing vesicles are known to fuse to the plasma membrane in response to metabolic conditions. Type A intercalated cells are involved with acid secretion in the collecting duct, mediated by the apical vacuolar H^+-ATPase and H^+-K^+-ATPase and basolateral AE1 [117]. Type A intercalated cells also contain a BLM NHE and Na^+-K^+-ATPase, which opens the door for a Na^+-dependent mechanism of HCO_3^- reabsorption across these cells. A recent report evaluated the contribution of Na^+-dependent trans epithelial HCO_3^- flux in OMCD preparations and found that this mechanism provided only a minor contribution to the total trans-epithelial HCO_3^- flux [18]. This report also

found that pH_i recovery in type A intercalated cells was inhibited by greater than 50% in the absence of luminal Na^+, which suggests that the major function of NBC3 in these cells is associated with pH_i regulation [18]. Another report characterizing the distribution of NBC3 and NBCn1 in salivary glands also indicates a role for NBC3 in pH_i regulation. NBC3 localizes to the apical membranes of duct and acinar cells from both human and rat parotid and submandibular glands [118]. HCO_3^- secretion from salivary glands is generally believed to be mediated by duct cells and not acinar cells. Thus, the ubiquitous distribution of NBC3 suggests that its function is more likely to be pH_i regulation.

NBCn1 distribution in kidney has been determined by immunocytochemical and immunogold labelling techniques [119]. Strong labelling was detected in the inner strip of the renal outer medulla, with weak labelling in the outer strip of the outer medulla and inner medulla, and no labelling in the cortex [119]. Consistent with this finding, NBCn1 localized to the BLM of thick ascending limb cells in the outer medulla and the BLM of intercalated cells in the ISOM and inner medulla [119]. NBCn1 has also been localized to human striated duct cells in salivary glands [118].

1.2.8 Sodium bicarbonate co-transporters in familial disease

Mutation of the human NBC1 gene causes proximal renal tubular acidosis (PRTA) and blindness [120, 121], which underscores the functional importance of NBC1 in the kidney and eye. PRTA is caused by two different mutations of the NBC1 gene, R298S, which is in a region of the N-terminal cytoplasmic domain

that is conserved across NBCs, and R510H, which is predicted to be just before the insertion point of TM4 into the membrane. Although the mechanisms by which these mutations cause PRTA are not known it is seems likely disruption of NBC1 transport function is involved, possibly by interference with membrane targeting or transporter topology for R298S and R510H respectively. NBC4 has been proposed as a candidate gene for Alstrom syndrome, which is marked by retinitis pigmentosa, deafness, obesity, and diabetes mellitus [103]. Finally, two different cardiomyopathies map to the same chromosome interval as NBC3, making NBC3 a candidate gene in some heart disease [70, 122, 123]. A knock-out model of NBC exists only for the recently-described NBC3 null mouse line [124]. These mice manifest with retinal and auditory defects, which arise because other pathways in these tissues do not compensate for loss of the pH-regulatory activity of NBC3. Failure to accommodate the retinal H^+ load compromises Ca^{++}/H^+ exchange, which is required for Ca^{++} homeostasis, leading to blindness. The link between NBC3 deletion and auditory defect is not as easily explained. The retinal and auditory defects of the NBC3-deficient mouse led to the proposal that NBC3 is a candidate for Usher syndrome, which has symptoms similar to those of the NBC3 null mice [124].

1.3 The carbonic anhydrase enzyme family

The CA family of enzymes catalyses the reaction, $CO_2 + H_2O \leftrightarrow H_2CO_3 \leftrightarrow H^+ + HCO_3^-$ [125]. The first step is actively catalysed and the second occurs spontaneously in aqueous solution. To date, 10 enzymatically active isoforms of

Table 1.2 Carbonic anhydrase isozyme catalytic activities and localizations [126].

Isozyme	Catalytic Activity	Subcellular Localization
CAI	Low	Cytosol
CAII	High	Cytosol
CAIII	Very Low	Cytosol
CAVII	High	Cytosol
CAIV	High	Extracellular GPI-linked
CAIX	High	Extracellular TM-linked
CAXII	---	Extracellular TM-linked
CAXIV	Low	Extracellular TM-linked
CAV	Moderate High	Mitochondria
CAVI	Moderate	Secreted into saliva

CA have been identified (Table 1.2) [126]. CA isoforms have been implicated in several physiological processes including H^+ and HCO_3^- secretion, signal transduction, bone resorption, gluconeogenesis, cell proliferation and oncogenesis [127-130]. Recently, the role of CAII in bicarbonate metabolism and intracellular pH regulation has been identified in skeletal muscle, kidney type A intercalated cells, red blood cells (RBCs), and salivary glands but not cardiomyocytes [131][132][125][133]. Despite the fact that CAI is much more abundant in RBCs, CAII is believed to mediate the majority of CO_2 hydration/dehydration because of the low catalytic activity of CAI [128]. Furthermore CAII but not CAI binds the red cell anion exchanger, AE1 [134]. AE1 facilitates bicarbonate transport across the membrane, which is important for CO_2 transport in the blood as HCO_3^- accounts for ~60% of total blood CO_2 load [80]. The CAII/AE1 interaction increases the transport activity of AE1 in transiently transfected HEK293 cells as demonstrated by competitive inhibition of transport by a dominant-negative mutant of CAII [80].

The mechanism by which CAII increases bicarbonate transport activity is believed to be similar to the substrate shuttling system used in glycolysis, in this system the enzymes that carry out sequential catalytic reactions are physically linked so that substrate and product concentrations are kept high and low respectively near the active site of each enzyme, thereby maximizing the catalytic efficiency. Positioning CAII at the membrane surface linked to an AE1 transporter would effectively maximize the concentration of newly formed intracellular HCO_3^- at the transporter and thereby assist to drive HCO_3^- out of the cell. At the lungs the process could be reversed to assist in CO_2 off-loading. The preceding mechanism has recently been called the "bicarbonate transport

metabolon" [80]. CAII has been shown to interact with all three members of the anion exchange, AE, family of bicarbonate transporters as well as NBC1, and the cardiac sodium proton exchanger, NHE1, via an acidic cluster in the C-terminal region of these transporters. The consensus interaction motif consists of a leucine residue followed by at least two acidic residues within the next four amino acids in the chain. The reciprocal bicarbonate transporter binding motif on CAII has been localized to a basic patch of amino acids within the first 18 residues of the N-terminus of the enzyme [80].

CAIV is a catalytically active glycosylphosphatidylinositol linked carbonic anhydrase isoform located on the extracellular surface of the cell [135]. Recently this protein has been shown to interact with the fourth extracellular loop of AE1 and NBC1 [81, 136]. Transport experiments conducted in the presence of a dominant negative CAII mutant demonstrated that transfected CAIV could rescue the transport activity of NBC1 in HEK293 cells, suggesting a functional CAIV/NBC1 interaction. In this example of the bicarbonate transport metabolon, two CA isoforms and NBC1 are working together in a "push/pull" manner to move bicarbonate across the membrane (figure 1.5).

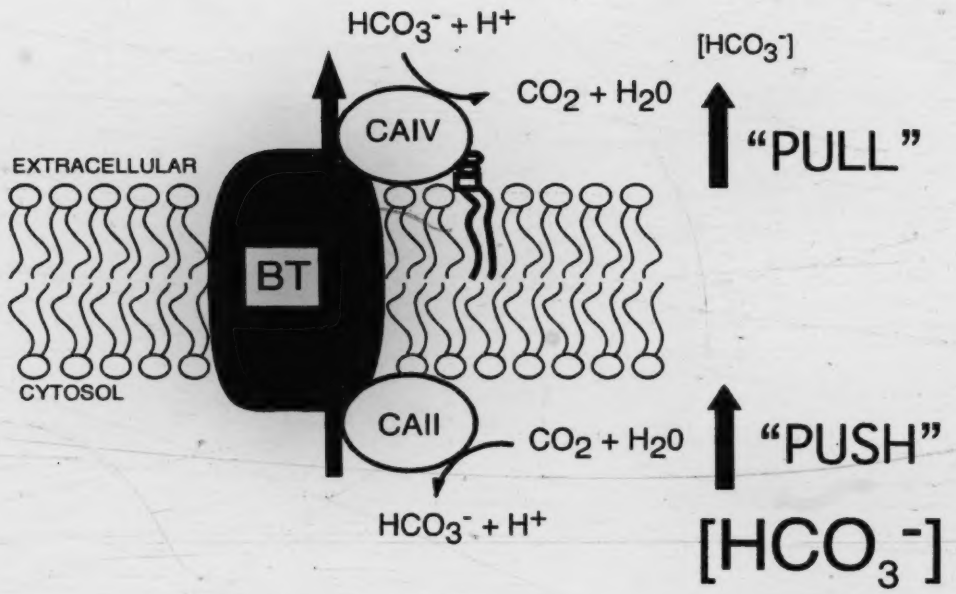

Figure 1.5 Establishment of concentration gradient by CA.
The carbonic anhydrases (CA) that interact with the bicarbonate transporters (BT) are responsible for the generation of a concentration gradient of HCO_3^- via a push-pull mechanism. At the cytosolic face, CAII rapidly converts CO_2 to HCO_3^- providing a high concentration to push transport of bicarbonate out of the cell. At the extracellular face, CAIV rapidly converts HCO_3^- + to CO_2, which depletes the extracellular HCO_3^- concentration, thereby pulling bicarbonate transport towards the extracellular space. These effects combined drive bicarbonate transport out of the cell. The reverse of this process can occur as well, to drive bicarbonate transport in to the cell.

1.4 Cytoplasmic domains of bicarbonate and proton transporters

1.4.1 Characterization of the cytoplasmic domains of bicarbonate and proton transporters

The transmembrane domains of transport proteins facilitate the flux of ions from one side of a membrane to the other, down an electrochemical gradient (or a net gradient in the case of co-transporters and exchangers). Generally speaking, these domains are predominantly hydrophobic especially within transmembrane spanning regions, with only a few polar or charged residues that likely face the translocation pore. In the case of proton or proton-equivalent transporters, the aqueous phase loops are usually too short to accommodate any substantial secondary structure and thus are limited in their role in transport function regulation. Many of these transporters have relatively large cytoplasmic domains, some of which have been well characterized. It is an emerging theme that cytoplasmic regions compose the major regulatory domains of pH regulating transporters. Possible regulatory functions of cytoplasmic domains include membrane targeting, cytoskeletal interaction, regulated recruitment to the plasma membrane, substrate concentration sensor, and response to second messengers (usually through phosphorylation). To date, specific information on regulation of transporter function by cytoplasmic domains has been sparse. The following section will discuss what is known about the cytoplasmic domains of the anion exchangers AE1 and 2 and the cardiac sodium proton exchanger.

1.4.2 *The cytoplasmic domain of the AE1 Cl^-/HCO_3^- exchanger*

The anion exchanger, AE1, cytoplasmic domain, AE1Nt, has been extensively characterized by biochemical, and crystallographic techniques [137][138, 139]. In the red cell, AE1 is believed to be an organizational hub; specifically, AE1Nt interacts with and anchors several membrane-associated proteins, including, ankyrin, protein 4.2, protein 4.1, glyceradehyde-3-phosphate dehydrogenase, GAPDH, phosphofructokinase, aldolase, hemoglobin, hemichromes, and protein tyrosine kinase [140-150]. These interactions have significant consequences for the structure and function of the cell. Interactions with cytoskeletal elements influence cell shape, flexibility, and lifespan while interaction with glycolytic enzymes influence glucose metabolism. More recently, interactions with signalling proteins and carbonic anhydrase have been shown to influence the transport activity of the membrane domain [80].

A crystal structure of AE1Nt has recently been reported at 2.6 Å resolution [138]. Analysis of the structure has provided insight into the architecture of AE1Nt interactions with peripheral membrane proteins. Several lines of evidence suggest that ankyrin interacts only with the tetrameric form of AE1 and has little or no affinity for the dimeric form [138]. It is thus likely that sequences from two dimers contribute to ankyrin binding thereby tethering the subunits together and forming a dimer of dimers [138]. Two regions of AE1Nt are involved with the interaction, the unresolved N-terminal region and residues 177-190 [138]. The latter region lies in the middle of a relatively exposed and convoluted segment between strands β5 and β8 on the main sheet [138]. Strands β6 and β7 consist of residues 177-185 and form a well-characterized β-hairpin

structure; such structures are commonly involved with protein-protein interactions [151]. Replacement of the wild-type residues 177-185 with a Gly-Gly dipeptide abolished binding to ankyrin, yet had no effect on the binding of other proteins [138]. In addition, the crystal-structure of another ankyrin binding protein, Na^+/K^+ ATPase, indicates a putative binding motif that is very similar in structure, consisting of a stalk-and-loop [138].

Although the structure of the N-terminal segment has not been resolved, the position of the last resolved residue, His 55, of dimer 1 lies within 31 to 41 Å of the β-hairpin structure of dimer 2 and on the same face of the putative tetramer [138]. Arranging the two sites on the same face and in close proximity is consistent with the requirement for two binding sites from two different dimers for interaction.

Support for the interaction of AE1Nt with other proteins including band 4.1, band 4.2, glycolytic enzymes and tyrosine kinases was not as clearly demonstrated by the crystal structure [138]. For example, biochemical studies have suggested that the motif, LRRRY, of AE1Nt is important for binding to band 4.1 [138]. However, the crystal structure indicates that residues L343, R346, and Y347 are on a buried face of a helix [138]. Thus interaction with band 4.1 would require partial unravelling of the structure. On the other hand, steric constraints and the N-termini of the tetramer require band 4.1 to overlap with the predicted position of ankyrin, such competition for binding has been observed by several groups [138].

Interestingly, the kidney variant of AE1 is identical to the RBC form except for a deletion of the extreme N-terminal 65 residues [152]. Some of these residues make up a central strand in crystal structure of RBC AE1Nt, and thus

removal of this strand would be expected to have severe consequences for the structure of this domain [138]. Consistent with this suggestion, the kidney variant no longer binds several peripheral membrane proteins including ankyrin, band 4.1 or glycolytic enzymes [137, 153].

1.4.3 Role of AE1 cytoplasmic domain in regulation of transport

The N-terminal cytoplasmic domain of AE2, AE2Nt, is larger than that of AE1, 705 residues versus 379, yet it still shares several similar core regions based on alignment. Interestingly, the regions of highest identity map onto the well-defined secondary structure elements of AE1Nt that constitute the main sheet [154]. The non-aligned residues of AE2Nt likely form additional sub-domain structures involved with the unique functionality of AE2. Thus, it is believed that the core structure of the N-terminal cytoplasmic domains of each protein is common. Consistent with this hypothesis, chimeric studies where the cytoplasmic domains of these proteins were swapped indicated isoform-specific regulation mediated by the N-terminal domains [154].

AE1 is relatively insensitive to regulation by protons, hypertonicity, and NH_4^+ [155, 156]. Conversely, AE2 is strongly inhibited by protons and activated by hypertonicity and low concentrations of NH_4^+ [155-158]. Initial experiments that investigated the pH-sensitivity profile of AE2 in transfected *Xenopus* oocytes varied pH_o over a 5 to 9 range, which in turn resulted in a pH_i range of 7.13 to 7.61 [154]. Under these conditions, chimeric analysis indicated that the transmembrane domain of AE2 was responsible for the majority of regulation by changes in pH_o. The $AE1_{cyto}/AE2_{memb}$ mutant showed an AE2-like profile that

differed only in an acid shifted pH_o (50) value [154]. In this way, the AE2 transmembrane domain was termed the pH sensor and AE2Nt the pH modifier [154]. Sequential truncation of AE2Nt has shown that removal of the N-terminal 510 residues produces a pH-sensitivity profile identical to the $AE1_{cyto}/AE2_{memb}$ chimera, thereby localizing pH modifier function to the initial segment [154]. Furthermore, additional experiments have identified two sub-regions that are important for pH modifier function, residues 328-347 and residues 391-510 [154]. In more recent experiments pH_i was varied at constant pH_o, which allowed for dissection of pH_i-dependent versus pH_o-dependent modifier function [154]. Removal of the N-terminal 328 residues abolished pH_i-sensitivity while near normal pH_o-sensitivity was retained [154]. Hexa-alanine block substitutions between residues 310-347 indicated that the residues required for pH_i-sensitivity lie between residues 336-341 and 342-347, which is in contrast to earlier N-terminal truncations experiments [154]. This region is highly conserved within the AE family and alignment with the AE1 sequence and mapping onto the AE1Nt crystal structure places these residues at the endofacial surface of the transmembrane domain at the cytoplasmic surface of the plasma membrane [154]. Such an arrangement would allow the modifier site to interact with the sensor region(s) of the transmembrane domain. Future studies aim to characterize site-specific mutation of residues in the pH-sensitivity modifier region.

1.4.4 The cytoplasmic domain of the NHE1 Na^+/H^+ exchanger

The cardiac sodium proton exchanger, NHE1, exchanges extracellular Na^+ for intracellular H^+ in a one-to-one electroneutral manner [159]. NHE1 plays an important role in pH_i recovery following an ischemic episode and may contribute to the accompanying Ca^{2+} loading and hypertrophy [160]. NHE1 is subject to regulation by the growth factors Angiotensin, endothelin, and α_1-adrenergic stimulation [159]. Interestingly, all of these factors are known to be involved with cardiac hypertrophy [161]. The 315 residue C-terminal cytoplasmic domain, NHE1Ct, has been shown to increase its phosphorylation state following stimulation by these factors [162]. In addition, NHE1 transport activity is modulated by interaction of NHE1Ct with cytoplasmic proteins including protein kinases and carbonic anhydrase II [162, 163].

Four functionally distinct sub-domains have been identified within the sequence of NHE1Ct [162]. NHE1 Transport activity is sensitive to changes in intracellular ATP concentration, although NHE1Ct does not bind ATP [162]. Residues 513-564 are responsible for at least some of this regulation, and the effect is likely mediated by phosphatidylinositol 4.5-bisphosphate [164]. Second, residues 567-637 contain a binding site for calcineurin homologous protein, which is believed to remain bound to NHE1Ct and down-regulate NHE1 transport activity until stimulated to leave by cellular exposure to growth factors [165]. Third, a calmodulin-binding domain containing high- and low-affinity sites, residues 636-656 and 657-700, respectively has been identified [166]. Calmodulin binding down regulates NHE1 activity [166]. Moreover, deletion of the high-affinity binding site results in a constitutively activated transporter

[166]. Finally, residues 700-815 compose the phosphorylation sub-domain. Several kinases are known to bind to and phosphorylate NHE1Ct within this region following cellular stimulation by growth factors [167].

NHE1 exhibits pH_i-dependent transport activity such that it is maximally active at low pH_i [163]. Phosphorylation of NHE1Ct as a result of stimulation by growth factors shifts the pH_i-dependence curve toward the alkaline, which results in an increased NHE1 transport rate for any given pH_i value [162]. Furthermore, growth factor stimulation results in intracellular alkalinization and an increased ability of the myocardium to recover from acid loads [162]. The intracellular signalling pathways responsible for these effects on NHE1 have yet to be elucidated. However, growth factor receptors are known to signal through G proteins [168]. Several kinases phosphorylate NHE1Ct, including mitogen activated protein kinases ERK1 and 2, p^{90rsk}, and p160ROCK [167, 169, 170]. However, the effect of phosphorylation by these kinases on transport activity has not been characterized.

1.4.5 The NBC3 C-terminal domain

Characterization of the C-terminal cytoplasmic domain of NBC3 is still in early stages. One of the most identifiable characteristics of this domain is the presence of a PSD-95/Dlg/ZO-1, PDZ, binding motif (human NBC3 C-terminal amino acid sequence is ETSL) at its extreme C-terminus. PDZ binding motifs are a common characteristic of most apically located proteins in epithelial tissues. One of the best characterized interactions of this type is between the proximal tubule apical NHE3 and NHE regulatory factor, NHERF, also called ezrin

binding protein 50 [171]. In this system NHERF acts as an adaptor linking the plasma membrane NHE3 to the cytoskeletal protein ezrin [172]. Ezrin in turn, binds the regulatory subunit of protein kinase A [172]. A substantial body of evidence indicates that this protein complex is responsible for mediating the inhibition of NHE3 by cAMP [173, 174]. For example, reconstitution of NHE3 into PS120 cells (a NHE3 and NHERF deficient cell line) alone is not sufficient for inhibition by PKA [175]. Co-transfection with both NHE3 and NHERF restores PKA-sensitive inhibition to the transporter [175]. Renal proximal tubule cells possess several receptors that signal through the cAMP second messenger pathway including, dopamine, parathyroid, and β_2-adrenergic receptors, each of which produces a unique profile of cellular effects.

Recently, the C-terminal PDZ binding motif of NBC3 was found to interact with NHERF and co-immunoprecipitate with CFTR both from transfected HEK293 cells and from pancreas and submandibular glands [112]. Mutation of the PDZ binding motifs in either NBC3 and CFTR blocked co-immunoprecipitation and prevented PKA dependent inhibition of NBC3 [112]. The authors conclude that this last effect involves an inhibitory role of CFTR on NBC3 function. In light of the work done on the NHE3/NHERF/ezrin/PKA signalling complex this conclusion needs to be re-examined. A study needs to be performed that determines which interacting proteins are required for the regulation of NBC3 by PKA *in vivo*. Furthermore, NHERF contains two distinct PDZ domains (PDZ I and PDZ II) and it remains to be determined which domain interacts with which transporter.

NHERF is involved with sorting of CFTR to the apical membrane of epithelial cells [176]. The existence of a NBC3/CFTR/NHERF complex suggests

that NHERF may also play a role in sorting NBC3 to apical membranes. In an independent report, the C-terminal 18 amino acids of NBC3 was bound to a Sepharose resin and incubated with kidney lysates. The peptide bound the 56 kDa and 70 kDa subunits of the vacuolar H^+-ATPase and NHERF [177]. Deletion of the final 5 amino acids of the peptide blocked the association. Performing the same assay with the last 18 amino acids of the 56 kDa vacuolar H^+-ATPase pulled down NHERF and NBC3. Once again deletion of the final 5 amino acids of this peptide prevented the pull down. These experiments provide convincing evidence of a direct interaction of both NBC3 and the vacuolar H^+-ATPase with NHERF. Mutation of the C-terminal PDZ consensus site (C-terminal leucine of NBC3) to glycine blocked the interaction of the 56 kDa subunit of the vacuolar H^+-ATPase with NHERF, which suggests that the H^+-ATPase binds NHERF by either PDZ domain I or II. The direct interaction of NBC3 with a PDZ domain on NHERF has yet to be determined. However, the ability of a point mutation of NBC3 C-terminus to block the interaction of another protein to one of the PDZ domains on NHERF suggests that wild-type NBC3 C-terminus has strong PDZ binding motif characteristics and is likely to bind the other PDZ domain on NHERF.

1.5 Rationale and summary of project

An emerging theme in transport physiology is that cytoplasmic domains are keystones linking the activities of the cytoplasm to the membrane and beyond. C-terminal domains form organizing centres for regulation of membrane transport through physical interactions and chemical modifications.

These domains also play a role in defining cellular architecture and directing membrane proteins to their final destinations on the plasma membrane or vesicular structures. The focus of this thesis is to characterize the C-terminal cytoplasmic domain of NBC3, NBC3Ct. We first established the functional necessity of the domain for NBC3 transport activity. Next, we characterized the structure of the domain using biochemical techniques that provided information on the shape, secondary structure and accessibility of particular residues. Finally, we identified binding partners for the domain by yeast-two-hybrid screen, and a microtitre dish assay. We characterized one of the resulting interactions, CAII and NBC3Ct. Specifically we looked at the effects of pH and phosphorylation by PKA and PKC on the physical and functional aspects of the interaction.

Chapter 2

Structural and Functional Characterization of the Human NBC3 Sodium/Bicarbonate Co-transporter Carboxyl-Terminal Cytoplasmic Domain[1]

[1]**Portions of this chapter have been previously published and are reproduced here with permission:**
Loiselle, F.B., P. Jaschke*, and J.R. Casey, Structural and functional characterization of the human NBC3 sodium/bicarbonate co-transporter carboxyl-terminal cytoplasmic domain. *Mol Membr Biol*, 2003. **20**(4): p. 307-17.
*Paul Jaschke assisted with NBC3 transport assays

2.1 Introduction

Regulation of intracellular pH (pH_i) is critically important in all cells as intracellular pH influences membrane transport, cell volume, metabolism, and intracellular messengers [178-180]. Physiological changes in metabolic proton production and ambient CO_2 make it necessary for cells to have a robust system to maintain pH_i homeostasis. Most cells experience transient alkalosis and acidosis, so that mechanisms for acid influx and efflux are required. Transport processes that regulate pH_i include: Na^+/H^+-exchange, Na^+-dependent and –independent Cl^-/HCO_3^- exchange, AE, and monocarboxylate/H^+ and Na^+/HCO_3^- co-transport, NBC [84, 181-187]. AE, Na^+-dependent AE, and NBC are part of a super-family of HCO_3^- transporters, BT [8, 154]. NBC participates in both alkalinization and acidification pathways [2]. For example, in kidney tubule epithelium, NBC activity is involved in HCO_3^- reabsorption (acid secretion), while in pancreatic duct cells, NBC activity facilitates HCO_3^- secretion into the lumen of the pancreatic duct.

NBC activity has been characterized in several tissues including kidney, pancreas, conjunctiva, heart, skeletal muscle, and respiratory epithelia [30, 35, 188]. The recent cloning of three isoforms, of NBC: NBC1, NBC3 and NBC4, each with several splicing variants, has enabled study of NBC activity at the molecular level [24, 29-33, 35, 36, 55, 56, 103, 189]. NBC1 exhibits electrogenic, 3:1 or 2:1 HCO_3^- : Na^+ co-transport in the kidney and pancreas respectively [2]. NBC3 functions with an electroneutral mechanism with a 1:1 stoichiometry [35]. NBC4 transport is either electroneutral or electrogenic depending on the spicing variant [37]. All three isoforms share a 3 domain structure with a large N-terminal

cytoplasmic domain, a highly conserved membrane domain of ~57 kDa, with 12 putative membrane spanning segments, and a small C-terminal domain of approximately 10 kDa. The N-terminal cytoplasmic domain of NBC3 is considerably larger than the other family members with a predicted molecular weight of 133 kDa, due in large part to an ~120 amino acid insert of unknown function that is absent from the other family members.

In the kidney NBC3 is expressed in the connecting tubule and the cortical and medullary collecting duct in both type A and B intercalated cells [111, 114]. Interestingly membrane targeting is cell type specific with apical or basolateral localization in type A or B cells respectively [111]. At the subcellular level, NBC3 co-localizes with the vacuolar H^+-ATPase to peri-membranous vesicular structures inside the plasma membrane [114]. This arrangement suggests that NBC3 undergoes regulated recruitment to the plasma membrane. These characteristics of NBC3 are likely mediated by interactions of its cytoplasmic domains with cytoskeletal scaffolding and targeting factors. The C-terminal domain of NBC1, NBC1Ct, has recently been implicated in the regulation of NBC1 transport function. NBC1Ct binds carbonic anhydrase II, CAII, and this binding is essential for full transport activity (Alvarez, Loiselle and Casey, submitted for publication). In addition, CAII binding shifts the transport stoichiometry from 1:2 to 1:3, Na^+:HCO_3^-, and likely accounts for the tissue-type specific stoichiometry of this transporter [19]. The NBC3 C-terminal domain also contains the consensus binding-motif for CAII and the possibility of a functional interaction is currently under investigation.

The objectives of this study were to determine the functional importance of the C-terminal cytoplasmic domain of human NBC3, NBC3Ct, and to

characterize its structure using biochemical techniques. Specifically, the functional role of NBC3Ct was characterized by measuring the rate of pH recovery from acid loads in cells expressing NBC3 variants. The effect of deletion of NBC3Ct on surface processing of NBC3 was examined by confocal microscopy and immunoblotting. The structure of recombinant over-expressed NBC3Ct was assessed by gel permeation chromatography (GPC) sedimentation velocity ultracentrifugation, circular dichroism spectroscopy, CD, and limited proteolysis. The data presented here provide a picture of NBC3Ct shape, secondary structure, and identify surface-exposed regions. This work also sets the stage for obtaining a crystal structure and allows for an independent verification of that structure.

2.2 Methods and Materials

2.2.1 Materials

Human NBC3 cDNA was a generous gift from Ira Kurtz (U.C.L.A.). PCR primers were from Life Technologies Inc. Recombinant expression vector, pGEX-6p-1, was from Pharmacia Biotech. Pwo DNA polymerase was from Roche and all other cloning enzymes were from New England Biolabs. *Escherichia coli* recombinant expression strain, BL21-CodonPlus was from Stratagene. Protein concentrators were from Millipore. GST fusion purification reagents, FPLC apparatus and HiLoad 26/60 Superdex 75 gel permeation columns were from Pharmacia Biotech. Protein quantification reagents were from Bio-Rad. Amino-acid analysis was provided by Alberta Peptide Institute. Transfection and cell culture reagents were from Invitrogen. Enhanced chemiluminescence, ECL, reagent was from Pharmacia Biotech.

2.2.2 DNA constructs

The NBC3 C-terminal domain (NBC3Ct) corresponding to codons 1127 to 1214 of the NBC3 cDNA was amplified by PCR using the forward and reverse primers 5′-GGAATTGAATTCATGACGAAGAGAGAACTTAGTTGGCTTGA and 3′-CCTTAAGGGCGGCCGCTACTATAATGAAGTTTCAGCATCCACGTA, respectively. pGEX-6p-1 and the PCR product were digested with BamH I and Not I and ligated together, yielding pNBC3Ct.

The carboxyl terminal deletion construct (NBC3ΔCt) was prepared by amplifying a region of the cDNA from a site on the 5′ side of an internal EcoR I

site to the end of the cDNA sequence corresponding to the membrane domain (nucleotides 2865 to 3378). A stop codon and a Not I site were introduced at the 3′ end of the product. The forward and reverse primers used were 5′-GCTCATGGTTGGCGTTATGTTGG and 3′-CCTTAACCGAATTCCTACTAGAAACACAGGTCCATGAGTTTGCGC, respectively. The PCR product and the NBC3 expression construct were digested with Eco R I and Not I, the fragments were ligated together, yielding pNBC3ΔCt.

An HA epitope tag was added to the end of the N-terminus of both NBC3 and NBC3ΔCt. An Nhe I restriction site, new start codon, and the HA epitope were built into the forward PCR primer, 5′-GGAACGAGCTAGCATGTACCCCTACGACGTGCCCGACTACGCC ATGGAAAGA TTTCGTCTGG AGAAG. The reverse primer, CCACATAAGGTTTACTCC, was selected to be just downstream from a BstE II site. The PCR product was amplified using human NBC3 cDNA as a template. Both NBC3 and NBC3ΔCt were digested with Nhe I and BstE II and were ligated together, yielding pHANBC3 and pHANBC3ΔCt, respectively. All constructs were sequenced after completion.

2.2.3 Protein expression in mammalian cells

NBC3 protein was expressed by transient transfection of HEK293 cells [32, 80], using the calcium phosphate method [190]. All experiments with transfected cells were carried out 48-hours post-transfection. Cells were grown at 37 °C in an air/CO_2 (19:1) environment in Dulbecco's modified Eagle media, DMEM, supplemented with 5% (v/v) fetal bovine serum and 5% (v/v) calf serum.

2.2.4 *NBC3 transport assay*

The transport activity of NBC3 was monitored using a fluorescence assay, as previously described [191]. Briefly, HEK293 cells grown on poly-L-lysine coated coverslips were transiently transfected as described in the previous section. Forty-eight hours post-transfection, coverslips were rinsed in serum free DMEM and incubated in 4 ml serum-free media, containing 2 μM 2',7'-bis-(2-carboxyethyl)-5-(and-6)-carboxyfluorescein-acetoxymethyl ester(37 °C, 20 min). Coverslips were then mounted in a fluorescence cuvette and perfused with Ringers buffer (5 mM glucose, 5 mM K gluconate, 1 mM Ca gluconate, 1 mM $MgSO_4$, 10 mM Hepes, 140 mM NaCl, 2.5 mM NaH_2PO_4, 25 mM $NaHCO_3$, pH 7.4), equilibrated with 5% CO_2 / air. The pH_i recovery activity of HANBC3 or HANBC3ΔCt was measured during the recovery from transient intracellular acidification. Acid loading was accomplished by transient perfusion with Ringers buffer, containing 40 mM NH_4Cl for 5 minutes, followed by the wash-out of NH_4Cl with Ringers buffer. All experiments were performed in the presence of 10 μM 5-(N-ethyl-N-isopropyl) amiloride, (Sigma), to block endogenous NHE activity. Fluorescence was monitored using a Photon Technologies International RCR fluorimeter, at excitation wavelengths 440 and 500 nm and emission wavelength 530 nm. Following calibration using the nigericin/high potassium technique [192] at three pH values between 6.5 and 7.5, fluorescence ratios were converted to pH_i. The initial rate of pH_i recovery from an acid load was calculated by linear regression of the first 1 min or the first 3 min of the pH_i recovery after maximum acidosis. The rates of HCO_3^- influx ($J_{HCO_3^-}$ in mM/min) were estimated according to the equation $J_{HCO3-} = \beta_{total} \times \Delta pH_i$ [193],

where $\beta_{total} = \beta_i + \beta_{CO2}$, $\beta_i = 10$ mM [194], and $\beta_{CO2} = 2.3 \times [HCO_3^-]$. In all cases the transport activity of cells transfected with empty vector was subtracted from the total rate, to ensure that these rates consisted only of HANBC3 or HANBC3ΔCt transport activity.

2.2.5 *Immunodetection*

Transfected cells were washed in PBS buffer (140 mM NaCl, 3 mM KCl, 6.5 mM Na_2HPO_4, 1.5 mM KH_2PO_4, pH 7.5) and lysates of the whole tissue culture cells were prepared by addition of 150 µl SDS-PAGE sample buffer (20% (v/v) glycerol, 2% (v/v) 2-mercaptoethanol, 4% (w/v) SDS, 1% (w/v) Bromophenol Blue, 150 mM Tris, pH 6.8) containing complete mini protease inhibitor cocktail (Roche). Prior to analysis, samples were heated to 65 °C for 5 min and sheared through a 26-gauge needle (Becton Dickinson). Insoluble material was then sedimented by centrifugation at 16 000 x g for 10 min. Total protein content was measured using the Bradford protein assay [195]. Samples (5 µg) were resolved by SDS-PAGE on 8% acrylamide gels [196]. Proteins were transferred to PVDF membranes by electrophoresis for 2 h at 100 V at room temperature, in buffer composed of 20% (v/v) methanol, 25 mM Tris and 192 mM glycine [197]. PVDF membranes were blocked by incubation for 1 h in TBST-M buffer (TBST buffer (0.1% (v/v) Tween-20, 137 mM NaCl, 20 mM Tris, pH 7.5), containing 5% (w/v) nonfat dry milk) and then incubated overnight in 10 ml TBST-M, containing 20 µl rabbit anti-HA antibody. The next day, blots were washed 3 times with TBST, and then incubated with TBSTM containing 1:3000 diluted donkey anti-rabbit IgG conjugated to horseradish peroxidase.

After a final wash with TBST buffer (3 times), blots were visualized using ECL reagent and a Kodak Image Station 440CF.

2.2.6 *Confocal microscopy*

Cells grown on poly-L-Lysine-coated, 18 mm diameter coverslips were transiently transfected as described. The coverslips were transferred to 35 mm petri dishes. Cells were fixed for 30 min in 2% (w/v) paraformaldehyde in PBSC (1 mM $CaCl_2$, 140 mM NaCl, 3 mM KCl, 6.5 mM Na_2HPO_4, 1.5 mM KH_2PO_4, pH 7.5). After two washes with PBSC the cells were incubated for 25 min in permeabilisation buffer (300 mM sucrose, 50 mM NaCl, 3 mM $MgCl_2$, 0.5% (v/v) Triton X-100, 20 mM Hepes, pH 7.4). The coverslips were washed three times with PBSC and blocked for 25 min in 10% serum in PBSC. Coverslips were incubated with 1/50 dilution of rabbit anti-HA antibody SC805 in PBSC, 4% serum. Coverslips were washed three times with PBSC, 4% serum, and incubated for 45 min in a dark chamber with 1/100 dilution of biotinylated anti-rabbit IgG antibody in PBSC, 4% serum. After three washes with PBSC, 4% serum, the coverslips were incubated for 45 min in a dark chamber with 1/100 dilution of streptavidin fluorescein conjugate. Images were collected using a Zeiss LSM 510 laser scanning confocal microscope mounted on an Axiovert 100M, with a 63X (NA1.4) lens.

2.2.7 *GST-fusion protein purification*

pGST.NBC3Ct in *E. coli* BL21 codon plus was inoculated into 50 ml of Luria broth, LB, medium. Following overnight growth at 37 °C with shaking, 1.2 liters of LB media was inoculated with the culture (5 ml/200 ml). Cultures were

grown at 37 °C with shaking until A_{600} was 0.6-1.0. Isopropylthiogalactoside, IPTG, (1 mM final) was added and growth allowed to continue for 3 hours. The culture was then centrifuged at 10 000 x g, 10 min and bacterial pellets were resuspended in 4 °C PBS buffer, pH 7.40), containing complete mini protease inhibitor cocktail. Suspended cells were disrupted by sonication ((4 times 1 min, power level 9.5 with model W185 probe sonifier (Heat systems-Ultrasonics Inc., Plainview, N.Y.)) and Triton X-100 was added to a final concentration of 1% (v/v), with slow stirring for 30 min. Following centrifugation (15 000 × g, 10 min) the supernatant was added to 1.3 ml glutathione Sepharose 4B (50% slurry equilibrated with PBS) and incubated at room temperature with gentle agitation for 1-2 hours. The sample was centrifuged (500 × g, 5 min) and the pellet washed three times with PBS. The fusion protein was then washed 3 times with PreScission cleavage buffer (150 mM NaCl, 1 mM EDTA, 1 mM dithiothreitol, 50 mM Tris-HCl, pH 7.0), and reduced to a 50% slurry. PreScission Protease (60 units/ml resin) was then added and the sample incubated at 4 °C for forty-eight hours with rotation. Following cleavage the resin was centrifuged at 500 × g for 5 minutes and the supernatant collected. The resin was washed once with an equal volume of cleavage buffer and the supernatants pooled. The cleaved fusion protein was then further purified by FPLC gel permeation chromatography using a HiLoad 26/60 Superdex 75 column, eluted with GPC buffer (150 mM NaCl, 1 mM DTT, 50 mM Tris-HCl, pH 7.5). Fractions (5 ml) were collected. Peak fractions were pooled and designated Peak A and Peak B.

2.2.8 Analytical ultracentrifugation

Sedimentation velocity experiments were conducted at 5 °C in a Beckman XL-I analytical ultracentrifuge using absorbance optics following the procedures described by Laue and Stafford [198]. Aliquots (400 μl) of sample were loaded into 2-sector CFE sample cells and runs were performed at 60 000 rpm for approximately 3 hours, during which a minimum of 50 scans were taken to monitor the sedimentation rate of the protein. The sedimentation velocity data was analyzed to determine sedimentation coefficients, using the program SVEDBERG [199], which incorporates a modified Fujita-MacCosham function into a non-linear least squares fitting routine to fit the sedimentation boundaries to either single species or multiple species models. The program SEDNTERP was employed to calculate the protein's partial specific volume, $S_{20,w}$, axial ratio and the solvent density and viscosity [198].

2.2.9 Circular dichroism spectroscopy

pH titration experiments were performed using a JASCO J-720 Spectropolarimeter. NBC3Ct at 7.1 mM in CD buffer (100 mM KCl, 15 mM Hepes) was scanned at pH values 6.2, 6.8, 7.0, 7.2, and 7.8, at 25 °C. Experiments were performed with the following conditions: cell length 0.2 mm, scan range 196 nm to 250 nm, resolution 1 nm, sensitivity 50 mdeg, response 0.25 sec, speed, 50 nm/minute, and 8 accumulations per sample.

In thermal denaturation experiments 2.2 mM NBC3Ct in TDCD buffer (50 mM NaCl, 25 mM $NaPO_4$, pH 7.5) were scanned at 5 °C, 15 °C, 25 °C, 35 °C, 45 °C, 55 °C, 65 °C, and 75 °C. Experiments were performed under the following

conditions: cell length 1 mm, scan range 203 nm to 250 nm, resolution 1 nm, sensitivity 20 mdeg, response 0.25 sec, speed 100 nm/minute, and 8 accumulations per sample. All data were analyzed using JASCO J700 analysis software.

2.2.10 Proteolysis

Trypsin and chymotrypsin concentrations were optimized by digesting 200 μg/ml samples of NBC3Ct in GPC buffer with a range of trypsin and chymotrypsin concentrations spanning 50 to 400 μg/ml and 0.63 to 40 μg/ml, respectively, at 25 °C for 20 minutes. In this way 1 μg/ml chymotrypsin and 40 μg/ml trypsin was chosen to perform the digestion time courses. Each time course was run until NBC3Ct had been completely digested to smaller fragments. Reactions were quenched by the addition of 2 times SDS-PAGE sample buffer and immediately boiling samples for 5 minutes. Alternatively, samples for mass spectroscopy analysis were quenched by transferring aliquots to glacial acetic acid (25% final concentration). Mass spectroscopy samples were analyzed by matrix-assisted laser desorption/ionisation-time of flight (Voyager De-Pro from ABI) and dominant fragment weights were screened against a library of predicted fragment weights, and fragment designations assigned. Samples (20 μg) were also loaded onto 15% SDS-PAGE gels, electrophoresed and stained with Coomassie Blue.

2.3 Results

2.3.1 *Effect of NBC3 C-terminal deletion on HCO_3^- transport*

Cl^-/HCO_3^- exchangers of the AE family share up to 40% amino acid identity with NBC isoforms [24]. Alignment of the NBC3 amino acid sequence with AE1, whose C-terminal domain has been structurally characterized [106, 200], indicates that the C-terminal tail of NBC3 spans T1127 to L1214. To examine the functional role of the NBC3 C-terminal tail, the hemagglutinin (HA) tagged mutant HANBC3ΔCt with T1127-L1214 deleted was prepared. Transfected HEK293 cells were loaded with the pH sensitive dye, 2',7'-bis-(2-carboxyethyl)-5-(and-6)-carboxyfluorescein-acetoxymethyl ester, subjected to acid loading and their rate of pH_i recovery was assessed (figure 2.1a). All experiments were performed in the presence of 10 μM 5-(N-Ethyl-N-isopropyl)amiloride (EIPA) to inhibit endogenous Na^+/H^+-exchange activity of the HEK293 cells. HANBC3 transport activity was 2.2 mM ± 0.3 mM HCO_3^- /minute, which is about 2-fold over background (figure 2.1a). The transport rate of HANBC3ΔCt was determined by normalizing HANBC3 transport to 100% for each day of experiments. HANBC3ΔCt transport rate was 12 % ± 5 % of HANBC3 ($n=9$, $p < 0.05$ (unpaired, 2 tailed *t-test*)) (figure 2.1b) indicating that loss of NBC3Ct greatly reduced transport activity. Comparison of the rate of pH_i recovery is shown in figure 2.1c. The minimum pH of cells transfected with HANBC3 and HANBC3ΔCt cDNAs was the same (pH 6.5). However, the empty vector control acidified to pH 6.7 and thus recovery was less affected by

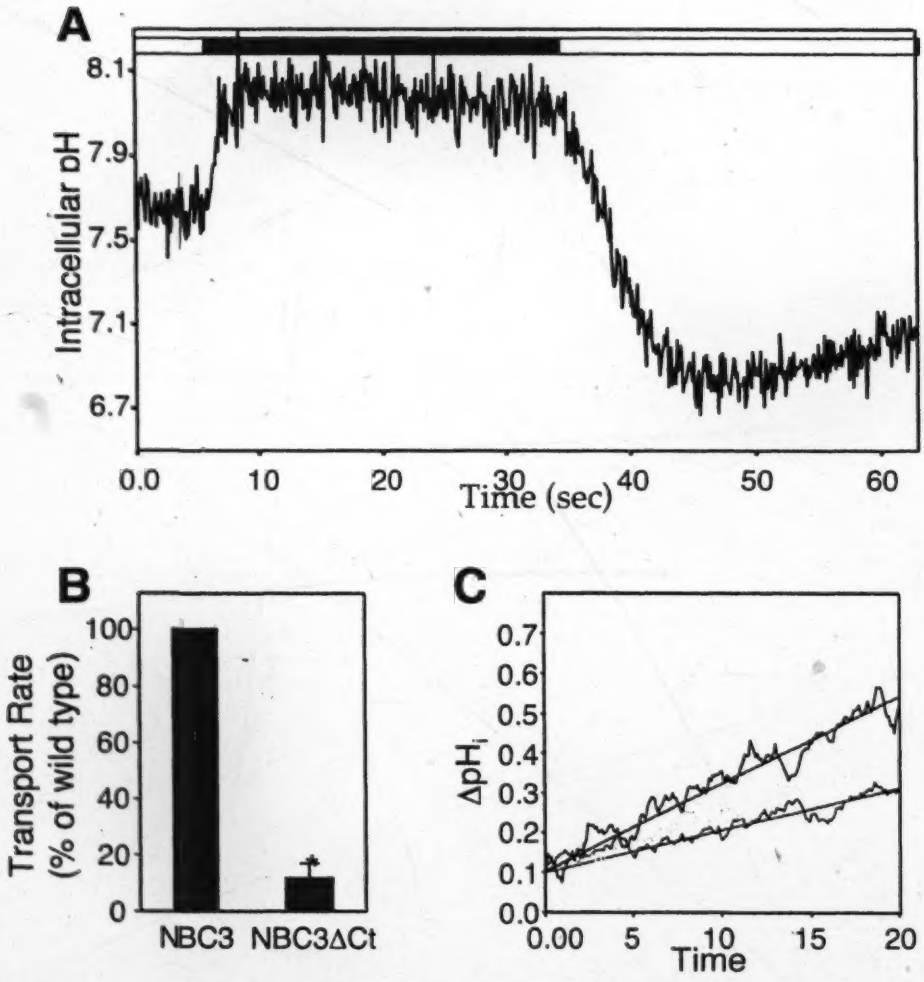

Figure 2.1. Functional role of NBC3Ct.
A, HEK293 cells grown on coverslips were transiently transfected with empty vector, HANBC3, or HANBC3ΔCt cDNAs. Transfected cells were loaded with 2',7'-bis-(2-carboxyethyl)-5-(and-6)-carboxyfluorescein-acetoxymethyl ester, and placed into a cuvette to monitor pH_i. Cells were perfused alternately with Ringers buffer (open box), or Ringers buffer, containing 40 mM NH_4Cl (shaded box). Representative plot of pH versus time for cells transfected with HANBC3, where pH_i recovery rate was 0.045 ΔpH/minute or 3.0 mM HCO_3^-/minute. B, The average pH_i recovery rate of HANBC3ΔCt is expressed as a percent of the wild-type rate. Error bars represent standard error of the mean (n=9). Asterisk represents statistical difference $p<0.05$ (unpaired, 2 tailed *t-test*). C, representative pH_i recovery of empty vector (light grey), HANBC3 (black), and HANBC3ΔCt (dark grey) transfected cells.

intracellular buffer capacity, β_i, which accounts for the sub-background recovery of the deletion construct in this example.

2.3.2 NBC3 expression and localization in HEK293 cells

The diminished HCO_3- transport activity of HANBC3ΔCt could result from reduced expression or processing of the protein to the cell surface, or an effect on transport catalysis. The expression and localization of wild type NBC3 and NBC3ΔCt were assessed by immunoblotting and confocal microscopy. Immunoblots were also prepared in parallel with transport assays for each day of experiments to ensure consistent expression levels. Figure 2.2a, shows an immunoblot of lysates prepared from the same transfection used to generate the transport data shown in figure 2.1c. HANBC3 migrated as two bands: a strong band at 168 kDa, and a weaker band at 156 kDa. HANBC3ΔCt expression level was much lower than HANBC3 and migrated as a single weaker band at 146 kDa. The two band pattern of HANBC3 suggests that some of the protein is retained intracellularly, either unglycosylated or only core glycosylated. Since deletion of the C-terminal domain of NBC3 removes ~10 kDa, the single HANBC3ΔCt band migrating at 10 kDa less than the lower NBC3 band suggests that the deletion is not glycosylated and may be completely retained within the cell. The dramatically lower expression level of HANBC3ΔCt may be attributable to degradation of destabilized, intracellular-retained protein, which suggests that NBC3Ct plays a role in targeting and/or folding of the transporter.

Confocal immunofluorescence microscopy of transiently transfected HEK293 cells showed that HANBC3ΔCt is completely contained within the cell

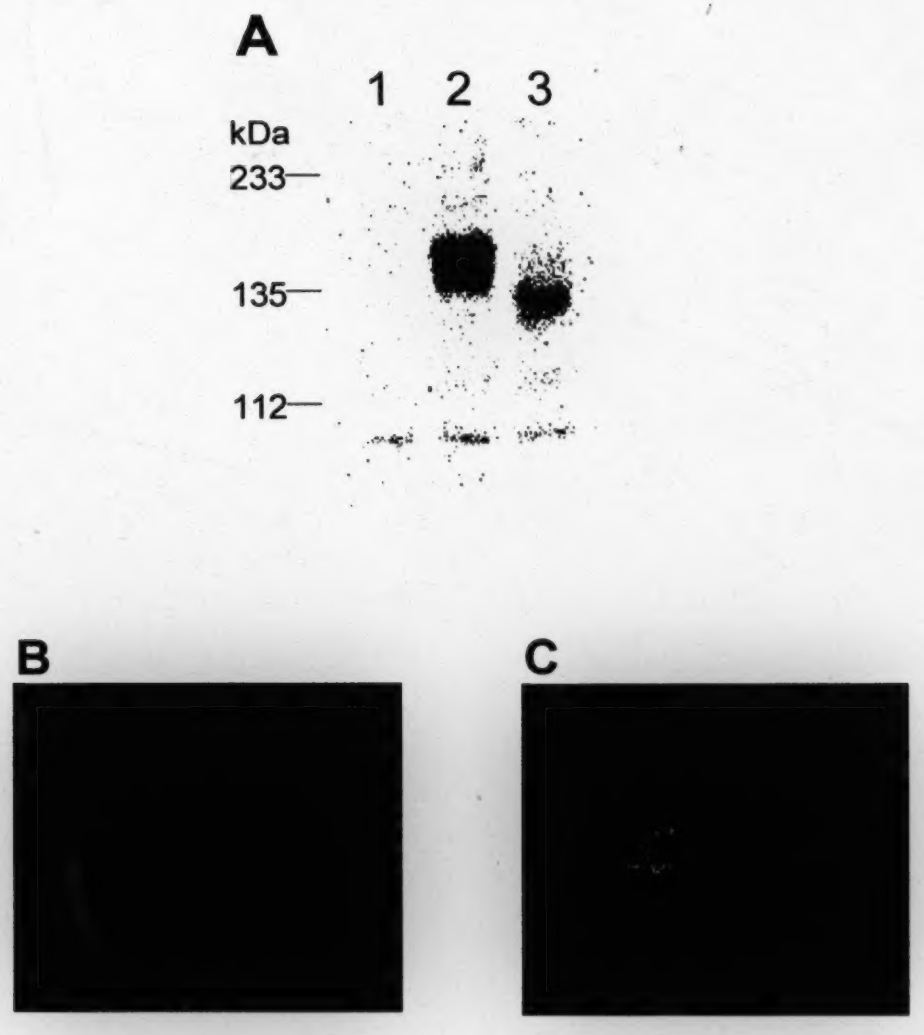

Figure 2.2. Expression and localization of HANBC3 and HANBC3ΔCt.
A, HEK 293 cells transfected with empty vector (lane 1), HANBC3 (lane 2), or HANBC3ΔCt (lane 3) were solubilized and samples (5 μg protein) were resolved by SDS-PAGE and transferred to PVDF membrane. Immunoblot as probed with rabbit polyclonal anti-HA antibody. Localization of HANBC3 (B) and HANBC3ΔCt (C) was assessed by confocal microscopy of transiently transfected HEK293. Coverslips were fixed, permeablized, and stained with the same anti-HA antibody as above, a biotinylated goat anti-rabbit secondary antibody, and finally streptavidin-FITC dye.

(figure 2.2c). HANBC3 also appears to be slightly intracellular-retained; however, the majority of the protein localizes to the plasma membrane (figure 2.2b), consistent with a previous report that showed NBC3 localization both to the plasma membrane and to a peri-plasma membrane subcellular pool in type A intercalated cells [114]. Taken together the expression data and confocal microscopy suggest that deletion of the NBC3 C-terminal domain blocks the ability of the protein to reach the plasma membrane, leading to protein degradation and reduced steady-state accumulation.

2.3.3 *Over-expression and purification of NBC3Ct*

Since NBC3Ct is required for NBC3 plasma membrane localization and transport activity, we chose to characterize the domain's properties. Codons 1127 to 1214 of human NBC3 cDNA, encoding NBC3Ct, were sub-cloned in frame, with an N-terminal, glutathione-S-transferase, GST, fusion partner into the pGEX-6p-1 prokaryotic expression vector. In this construct a PreScission protease consensus cleavage linker-sequence separates GST from NBC3Ct. GST.NBC3Ct was expressed to about 20% of total protein in *E. coli* (Table 2.1 and figure 2.3a). GST.NBC3Ct was almost completely soluble as seen by the small difference in purity between the re-suspended culture and the cleared lysates (Table 2.1 and figure 2.3a). During purification the GST-Sepharose was completely saturated with GST-NBC3Ct (~8 mg GST/ml resin), so that most of the fusion protein was lost during the wash steps, which accounts for the large decrease in yield. Following cleavage with PreScission protease the apparent purity of the preparation dropped somewhat, which was expected as about 2/3

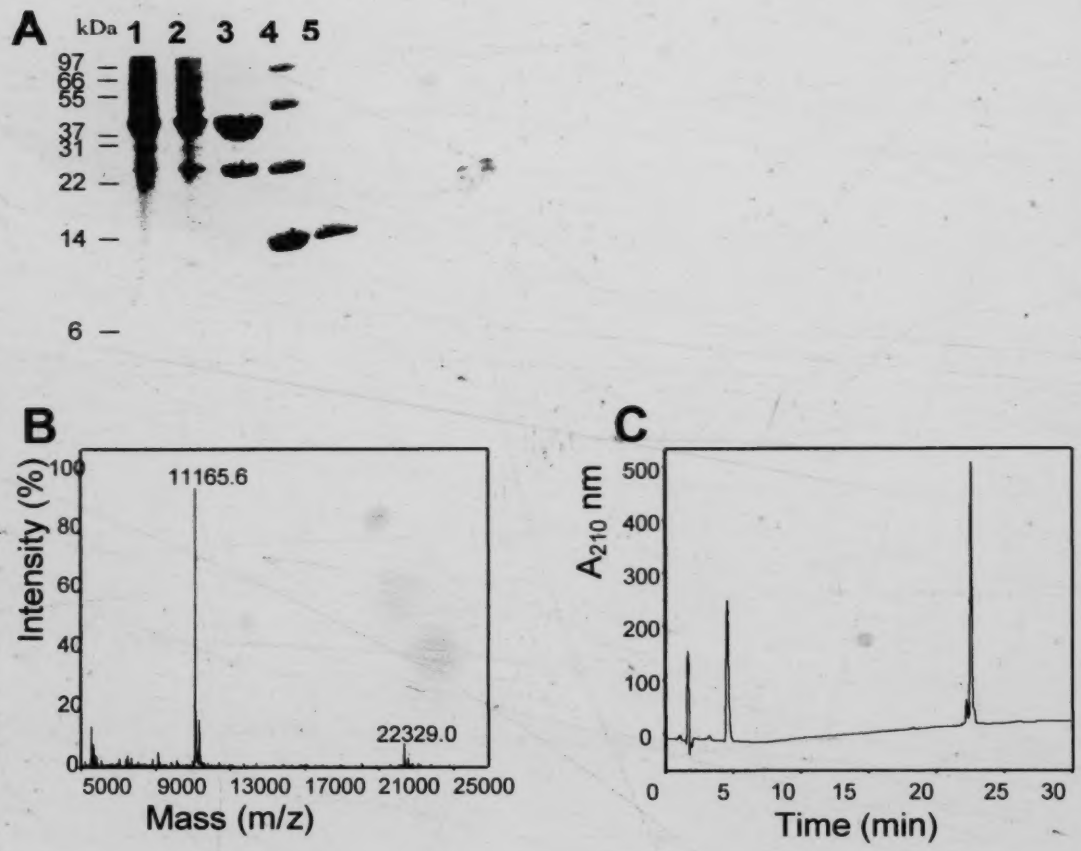

Figure 2.3. Analysis of NBC3Ct purification.
A, samples from stages of the purification procedure were subjected to SDS-PAGE on 15 % acrylamide gels and Coomassie blue staining. An equal fraction of total protein was loaded in each lane. Sample analyses were: resuspended culture following 3 hours of induction with 1 mM IPTG (lane 1), Triton X-100 treated lysate (lane 2), Glutathione Sepharose® 4B resin incubated with the lysate and washed extensively (lane 3), supernatant from PreScission™ protease treated resin (lane 4), and GPC chromatography purified sample (lane 5). B, the purified sample was analyzed by matrix-assisted laser desorption/ionisation-time of flight mass spectrometry, which indicated a nearly pure protein at the predicted molecular weight of 11,165 Da. C, reverse phase high performance liquid chromatography analysis of the purified sample. Fractions were analyzed my mass spectroscopy, the NBC3Ct peak was found to elute at ~23 minutes and showed 97% purity.

of the molecular weight of the fusion protein was lost following removal of the GST moiety; in addition, the presence of a band at ~ 46 kDa suggests that some of the PreScission protease (which contain a GST domain) did not remain bound to the resin (Table 2.1, figure 2.3a). A final step of GPC effectively purified NBC3Ct (figure 2.3a). Two major peaks (pools A and B) were observed during GPC (figure 2.4a). SDS-PAGE revealed three major bands in Pool A, likely corresponding to GST, a bacterial protein product of the *E. coli* gene dnaK known to bind GST [201], and PreScission protease. SDS-PAGE of Pool B indicated a strong band with a molecular weight of 14 kDa, and a much weaker slightly lower band, likely a truncated version of NBC3Ct (figure 2.3a). Immunoblotting of the pools with an anti-NBC3 antibody indicated that the band from pool B corresponds to NBC3Ct. Scanning and densitometry of Coomassie blue-stained SDS-PAGE gels showed that pool A protein was 94% pure NBC3Ct (Table 2.1, figure 2.3a). Purity was also assessed by mass spectrometry and reverse phase high performance liquid chromatography (figure 2.3b and c). Mass spectrometry showed that the major peak had mass 11165.6 Da, consistent with NBC3Ct. The small peak with m/z 22329.0 is consistent with dimeric NBC3Ct and likely represents a mass spectrometry artefact caused by the high concentration of the sample. Fractions from reverse phase, high performance liquid chromatography, HPLC, peaks were analyzed by mass spectrometry and the NBC3Ct peak was found to elute at ~23 minutes. Integration of this peak indicated a sample purity of ~97%, which is slightly greater than densitometry showed.

Table 2.1. Summary of NBC3Ct purification data.
Purification units were based on the densitometric analysis of the appropriate bands in figure 3. * Units were assigned based on the number of pixels counted during densitometry of the scanned gel. Each count was normalized for the fraction of total protein used and divided by 10,000,000 pixels. Percent yield was calculated from the units remaining compared to the resuspended culture. Percent purity was determined by comparing the pixels representing the band of interest to the total pixels for a given lane.

step	culture	cleared lysate	affinity resin	cleaved fusion	post GPC
units*	206	188	7.27	7.66	6.20
% yield	/	91.3	3.5	3.7	3.0
% purity	20	18	67	48	94
yield (mg)	/	151	/	/	4.30

2.3.4 Hydrodynamic shape analysis of NBC3CT

The Stokes radius, which is a mathematical value indicating the apparent radius of a hard sphere (determined by its rate of movement though aqueous solution) of NBC3Ct was 26 Å on the basis of elution from GPC columns. This was surprising since this is greater than the Stokes radius of the carbonic anhydrase standard, which has more than twice the molecular weight of NBC3Ct. The observation was verified independently by sedimentation velocity analysis, which indicated a Stokes radius of 30 Å and an axial ratio of 12:1. Shape modelling using the Teller method indicated a prolate molecule with long and short axial diameters of 19 and 2 nm respectively (figure 2.4b).

2.3.5 NBC3Ct conformation is insensitive to changes in pH and temperature

Purified NBC3Ct was analyzed by CD spectroscopy over the pH range 6.2 to 7.8 (figure 2.5a). The conformation of NBC3Ct was insensitive to changes in pH over the patho/physiological range, as indicated by the nearly super-imposable CD spectra from 5 pH values assessed. Best fit de-convolution modelling, as analyzed using the Contin program of Provencher and Glockner [202], indicated 60% β-sheet, 33% β-turn, and 7% random coil at pH 7.0. The range of $\Delta\varepsilon$ seen was not very large, ~-2500 $M^{-1}cm^{-1}$ at 215 nm compared to a fully β-structured protein (~-30,000 $M^{-1}cm^{-1}$ at 215 nm), which suggests that although the total structure is predominantly β, NBC3Ct likely does not form a single continuous β-sheet. Interestingly, thermal denaturation CD scans indicated a

subtle loss of β-structure in the 5 to 25 °C range but the majority of structure was retained up to 85 °C, which suggests that NBC3Ct is very stable.

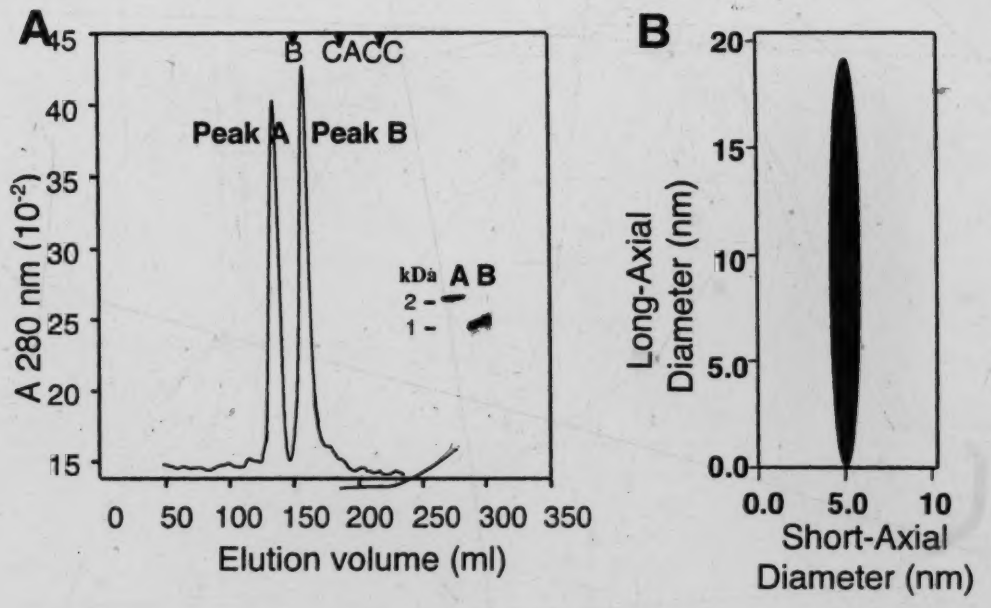

Figure 2.4. Shape analysis of NBC3Ct.
A, PreScission™ protease treated GST.NBC3Ct was applied to a Superdex® 75 column via a Pharmacia Biotech FPLC apparatus, and 5 ml fractions were collected. The fractions corresponding to peaks A and B were pooled separately and analyzed by SDS-PAGE with Coomassie blue staining (inset) and immunoblotting. Arrows indicate the elution position of bovine serum albumin (B, 36 Å, 66 kDa), carbonic anhydrase (CA, 20 Å, 29 kDa), cytochrome C (CC, 16 Å, 12.4 kDa). The Stokes radius for peak B was found to be 26 Å. B, Shape modeling by Sedimentation Velocity. Purified NBC3Ct was subjected to analytical ultracentrifugation in a Beckman XL-I ultracentrifuge. Data was analyzed using the program, SEDNTERP. Analysis indicated a Stokes radius of 29.6 Å and an axial ratio of 12.2. The model was generated by SEDNTERP on the basis of these parameters, and the amino acid sequence of the domain; it indicates a prolate shape with a long axis of 19 nm and a short axis of 1.6 nm.

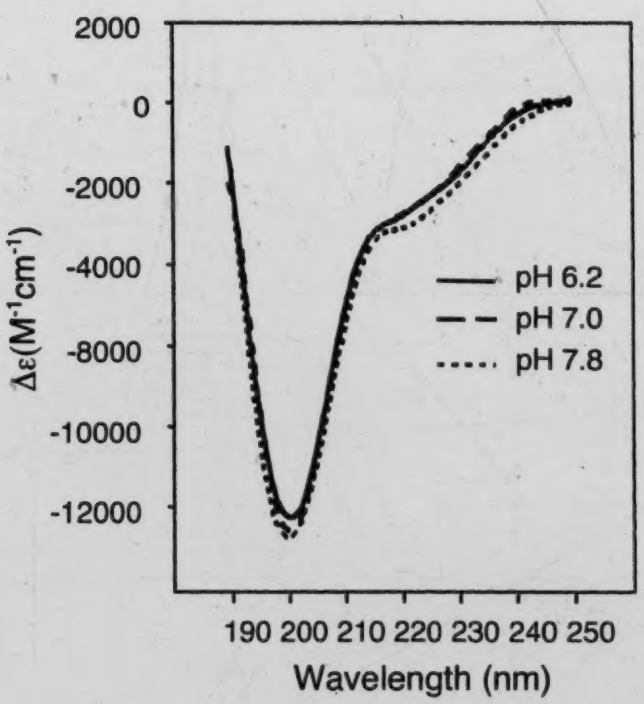

Figure 2.5. Circular dichroism spectroscopy of NBC3Ct at a range of pH values.
Circular dichroism spectra were collected in Phosphate buffers at pH 6.2, 7.0, and 7.8. Each curve was generated from the average of 8 scans of the same sample.

2.3.6 Identification of surface exposed regions of NBC3Ct

Limited proteolysis was used to identify regions of the domain that are sensitive to proteolysis, suggesting an extended or open structure. The amino acid sequence of NBC3Ct contains 19 and 17 potential trypsin and chymotrypsin cleavage sites respectively, distributed throughout the length of the domain (figure 2.6d). Thus, digestion with these enzymes should identify open-structured parts of the whole domain. Tryptic digests were optimized to identify the concentration of trypsin producing a ladder of fragments following 20 minutes of digestion. Using this method 40 μg/ml trypsin was selected for longer time courses. Figure 2.6a shows the results of a 64 minute digestion, which resulted in nearly complete cleavage of the starting material. When the same optimization protocol was used to identify an appropriate chymotrypsin concentration, even at low concentrations of enzyme, all starting material had been digested by 20 minutes. A stable fragment appeared within the first 30 seconds of digestion (figure 2.6b).

Samples of both reactions from each time point were analyzed by matrix-assisted laser desorption/ionization-time of flight mass spectroscopy for fragments between 5 and 25 kDa (m/z). Resolution of the technique was ± 4 Da, which was sufficient to determine the sites of cleavage of NBC3Ct (figure 2.6c). Also, the relative intensity of each fragment at each time point indicated the order of degradation and relative site sensitivity (figure 2.6c). That is, more sensitive sites rise in intensity earlier than less sensitive sites. In order of cleavage, trypsin cleaved at sites R1129, K1186, and K1183. After 8 minutes the fragment cleaved at R1129 and K1183 (6341 Da) was stable and persisted through

until the end of the experiment (64 minutes). Chymotrypsin cleaved only at one site (yielding a fragment greater than 5 kDa), at L1185.

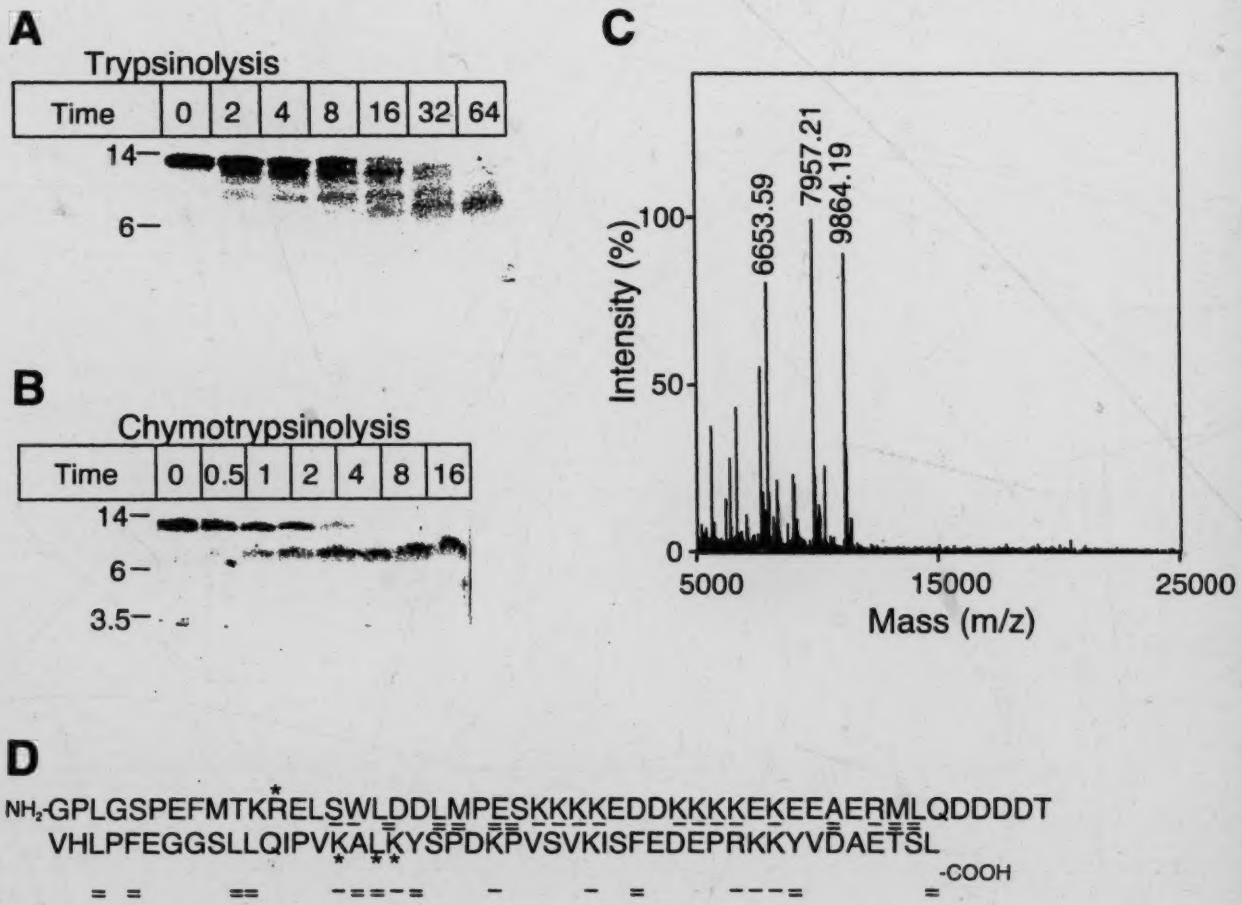

Figure 2.6. Limited proteolysis of NBC3Ct using trypsin and chymotrypsin. Coomassie Blue stained SDS-PAGE gels of the progression of trypsinolysis (A) and chymotrypinolysis (B), respectively, of NBC3Ct. Three and one distinct proteolytic fragments are observed during trypsinolysis and chymotrypsinolysis, respectively. C, the molecular weight of each fragment was determined by matrix-assisted laser desorption/ionisation-time of flight mass spectrometry; a sample output for the 4 minute time point (trypsinolysis) is shown . D, model of the sequence of NBC3Ct with the observed cleavage sites denoted by * above the bar. Potential cleavage sites are indicated under the bar by - and = for trypsin and chymotrypsin, respectively.

2.4 Discussion

The C-terminal domains of bicarbonate transporter super-family members play an important role in the regulation of transport function [103, 125, 203]. AE1, AE2, AE3 [19, 125], and NBC1 [81] bind the cytosolic enzyme, carbonic anhydrase II. Mutation of the CAII binding site or competitive displacement of CAII from its binding site diminished HCO_3^- transport activity by ~40 % for these transporters. Recently it has been suggested that phosphorylation of the C-terminal domain of NBC1 may modulate the HCO_3^-/Na^+ coupling ratio by displacement of CAII from its binding site [19]. This finding suggests that the bicarbonate transporter/CAII interaction may be regulated in a phosphorylation-state dependant manner. The C-terminal domain of NBC3 likely plays a similarly important role. In the present report we found that deletion of the C-terminal domain of NBC3 reduced transport by almost 90% (figure 2.1), consistent with an important role for the domain. NBC3Ct has an open structure, well suited to act as a binding site for peripheral proteins, but the domain does not undergo conformational alterations with changes of cytosolic pH. If NBC3Ct mediates regulation of transport in response to changes of cytosolic pH, it does not do so by changes of its secondary structure.

Immunoblotting of transiently transfected HEK293 cells identified two specific bands for NBC3, migrating at ~168 and ~156 kDa. The higher molecular weight band is not as large as previously reported, but this likely reflects a tissue-type specific glycosylation pattern and not a difference in primary sequence. The deletion mutant migrated at ~10 kDa less than the lower NBC3 band, as expected based on the predicted molecular weight of the C-terminal

domain. The lack of a corresponding higher molecular weight band for the C-terminal deletion mutant suggests that the deletion is either un- or incompletely glycosylated. This suggests that the lower NBC3 band and the deletion mutant band are equally glycosylated or unglycosylated. Thus, it is likely that the poor transport activity of the C-terminal deletion mutant is secondary to poor processing to the plasma membrane. Consistent with this idea, confocal microscopy of HEK293 cells transiently transfected with either NBC3 or the deletion mutant showed greater subcellular retention of the deletion mutant (figure 2.2b and c).

The fusion protein, GST.NBC3Ct, which was over-expressed to 20 % of total protein (figure 2.3a) was almost completely soluble as assessed by densitometry. The very high purity of NBC3Ct gave us confidence that our biochemical characterizations were accurate and not influenced to any significant extent by impurities. During purification we found that NBC3Ct eluted from the GPC column much earlier than was expected based on its molecular weight. The Stokes radius of 26 Å was independently verified by velocity ultracentrifugation, which indicated a Stokes radius of 30 Å. Using modelling software a rod-like shape ~19 nm long by ~2 nm wide was predicted. NBC3Ct possesses a PDZ consensus binding motif that shares strong homology to the PDZ motif of Na^+/H^+-exchanger 3, which has been shown to interact with cytoskeletal scaffolding elements and A kinase anchor proteins [204]. An extended structure would be ideal to bind such regulatory proteins and to form sites for anchorage to the cytoskeleton.

NBC1 activity was sensitive to changes in intracellular pH but not extracellular pH [90]. It thus seems likely that pH sensitivity is conferred by one

or more of the cytoplasmic domains or and intracellular loop of the membrane domain. We hypothesized that the C-terminal domain could undergo a pH-dependent conformational change within the physiological or pathophysiological range. Measuring secondary structure as an indication of conformation, we could not detect any change within the pH range examined. This finding suggests either a) that the C-terminal domain does not contain a pH sensor or b) a C-terminal pH sensor does not function via large conformational changes.

NBC3Ct has a large number of trypsin and chymotrypsin sites distributed throughout the length of the polypeptide, which makes it particularly amenable to study by limited proteolysis. Digestion experiments were designed to identify the first few cleavage sites utilized because these are most likely to be surface exposed residues. Since trypsin and chymotrypsin cleave at basic and hydrophobic residues, respectively, we expected that trypsin would generate more fragments than chymotrypsin. Hydrophilic residues are more prevalent at the surface of proteins, while hydrophobic residues generally make up the core of proteins. Indeed, trypsin and chymotrypsin cleavage generated one and three fragments respectively, under similar conditions. Given that NBC3Ct has such a long shape it was surprising that proteolysis generated so few cleavages under the experimental conditions, especially for trypsin. NBC3Ct also contains several acidic residues, leading to an isoelectric pH of 6.20 with 22% basic residues and 25% acidic residues. One explanation for the low number of sites used may be that the majority of basic residues are ion paired with acidic residues and therefore less susceptible to cleavage.

Identified proteolytic cleavage sites clustered around two regions. One was at the N-terminal end of NBC3Ct just after the membrane domain (figure 6d). The accessibility the N-terminal region suggests that the purified domain has assumed a native conformation since this region is required to be at the surface of the C-terminal domain because of its attachment to the membrane domain. Interestingly, sequence analysis indicates that a consensus PKA phosphorylation site, S1132, is 3 residues C-terminal to the cleavage site and a consensus CAII binding site lies 5 residues C-terminal to the cleavage site. Taken together this data suggests a model in which a CAII binding site and a PKA phosphorylation site localize to an open region on the extended rod structure of the NBC3 C-terminal tail. A similar region was recently identified in NBC1. Mutation of D986 or D988 blocked the S982 phosphorylation-state dependent shift from 2:1 to 3:1, HCO_3^-:Na^+ transport stoichiometry for NBC1 [19]. It seems possible that the NBC3 C-terminal tail also undergoes a phosphorylation-state-dependent interaction with CAII. We are currently investigating this possibility.

The second exposed region spans K1183 to K1186. Chymotrypsin also cleaved at L1185, between the two lysine residues. Chymotrypsin cleaves aromatic residues at a higher rate than leucine, which suggests that the exposed motif is limited at its C-terminal end by K1186 since no detectable cleavage occurred at Y1187. NBC3 shows cell type specific membrane targeting, apical or basolateral in type A and B intercalated cells respectively [111, 114]. Assuming that the N-terminal exposed binding region is involved in regulation of transport activity through binding to CAII, region 2 may be involved in cell surface targeting.

In conclusion, deletion of NBC3Ct prevents membrane. Consistent with observations of NBC3 localization in the kidney, we also found that NBC3 localizes both to the plasma membrane and to an intracellular pool. Structural analysis revealed NBC3Ct as a stable elongated rod-like shape with two proteolytically sensitive regions. This structure is well-suited to a role in binding of regulatory proteins. NBC3Ct did not change structure over the pH range tested, suggesting that conformational changes do not serve to signal changes of NBC3 activity. NBC3Ct proximal to the membrane domain contains consensus CAII binding and PKA phosphorylation motifs and had an open, accessible structure. Thus the region could be involved in mediation of a phosphorylation state dependent interaction with CAII. The membrane-distal region of NBC3Ct may be involved in membrane targeting.

Chapter 3

Regulation of the human NBC3 Na^+/HCO_3^- Co-transporter by Carbonic Anhydrase II and Protein Kinase A

[2]**Portions of this chapter have been previously published and are reproduced with permission: Loiselle, F.B.**, P.E. Morgan[*], B.V. Alvarez[*], and J.R. Casey, Regulation of the human NBC3 Na^+/HCO_3^- Co-transporter by Carbonic Anhydrase II and Protein Kinase A. Am J Physiol Cell Physiol, 2004. 286: C1423-33.

[*]Patricio Morgan and Bernardo Alvarez assisted with NBC transport assays.

3.1 Introduction

Regulation of intracellular pH, pH_i, is critically important in all cells as pH_i influences membrane transport, cell volume, metabolism, and intracellular messengers [178-180]. Physiological changes in metabolic proton production and ambient CO_2 make it necessary for cells to have a robust system to maintain pH_i homeostasis. Most cells experience transient alkalosis and acidosis, so that mechanisms for acid influx and efflux are required. NBC3 contributes to pH_i regulation in striated myocytes and HCO_3^- secreting epithelial cells [18, 35]. NBC3, originally cloned from human skeletal muscle, was also localized by multiple tissue northern-blot to heart [35]. Subsequently, NBC3 has been identified at the apical surface of several epithelial cell types including renal outer medullary collecting duct type A intercalated cells, and duct and acinar cells of parotid and submandibular glands [111, 114, 118]. A recent report evaluated the contribution of Na^+-dependent trans-epithelial HCO_3^- flux in outer medullary collecting duct preparations and found that this transport mechanism provided only a minor contribution to the total trans-epithelial HCO_3^- flux [18]. However, pH_i recovery in acid-secreting type A intercalated cells was inhibited by greater than 50% in the absence of lumenal Na^+, which suggests that the major function of NBC3 in these cells is associated with pH_i regulation [18]. In addition, NBC3 has a widespread distribution in salivary glands, yet HCO_3^- secretion from these glands is believed to be mediated by duct cells and not acinar cells, which further supports the role of pH_i regulation. By comparison, the rat orthologue of NBC3, NBCn1, localizes specifically to the basolateral

membrane of duct cells, which leaves open the possibility that this protein may participate in trans-epithelial HCO_3^- flux [118, 119].

The carbonic anhydrase, CA, family of enzymes catalyse the reversible hydration of CO_2 to yield HCO_3^- and a H^+ by the following mechanism, $CO_2 + H_2O \leftrightarrow H_2CO_3 \leftrightarrow H^+ + HCO_3^-$ [132]. The first reaction step is actively catalysed and the second occurs spontaneously in aqueous solution. To date, 10 enzymatically active isoforms of CA have been identified [132]. CA isoforms are involved in many physiological processes including H^+/HCO_3^- secretion, signal transduction, bone resorption, gluconeogenesis, cell proliferation and oncogenesis. CAII is a cytosolic isoform and has been identified in skeletal muscle, kidney type A intercalated cells and salivary glands, but not adult cardiomyocytes.

CAII interacts functionally with all three members of the anion exchange, AE, family of bicarbonate transporters and interacts physically via an acidic motif in the C-terminal region of these transporters [134, 205]. The consensus interaction motif consists of a hydrophobic residue followed by at least two acidic residues within the next four amino acids [205]. The reciprocal bicarbonate transporter-binding motif on CAII has been localized to a basic patch of amino acids within the first 18 residues of N-terminus of the enzyme [206]. This interaction is essential for the full HCO_3^- transport activity of anion exchangers in transiently transfected HEK293 cells as demonstrated by inhibition of transport by a dominant-negative mutant of CAII, presumably by displacement of wild-type CAII from binding sites on the intracellular surface of the anion exchangers [80].

Recently, members of two other families of pH regulating transporters have been shown to interact with CAII. Na^+/H^+ exchanger 1, NHE1 is a ubiquitously expressed electroneutral transporter, with a two-domain structure consisting of an N-terminal ion translocation domain of ~500 amino acids, and a C-terminal regulatory domain of ~300 amino acids. NHE1 reciprocally co-immunoprecipitates with CAII from Chinese hamster ovary, CHO, cells [163]. The last 178 amino acids of NHE1 C-terminal domain are sufficient for the CAII interaction, as shown by a micro-titre binding assay [163]. Interestingly, phosphorylation of NHE1 C-terminal domain enhanced CAII binding [163]. In the presence of a dominant negative CAII mutant, NHE1 transport rate was reduced by ~50%. The kidney electrogenic Na^+/HCO_3^- co-transporter, NBC1a, binds to CAII via its C-terminal domain [19, 81] and also interacts with the extracellular anchored CAIV isoform [81]. The transport stoichiometry of NBC1a or pancreatic spliceform NBC1b is shifted from 3:1 $HCO_3^-:Na^+$ to 2:1 by cAMP-dependent protein kinase A, PKA, phosphorylation at Ser^{982} or Ser^{1026}, respectively [207]. PKA-dependent phosphorylation of Thr^{49} of NBC1b increased transport activity without altering transport stoichiometry [207]. Interestingly, the CAII inhibitor, acetazolamide, reduces short-circuit current through NBC1a by 65% when operating in the 3:1 (unphosphorylated) mode but has no effect on the 2:1 transport mode [19], suggesting a link between the effects of PKA and CAII on NBC1 transport. However, the effect of phosphorylation on CAII binding has not been investigated.

Recently we characterized the structure of the C-terminal domain of NBC3, NBC3Ct, and discovered that the region close to the membrane domain is proteolytically sensitive. Interestingly, the consensus PKA phosphorylation

motif and CAII binding consensus motifs are present in this same region. Taken together with previous work on CA/AE interactions, we decided to explore the possibility that NBC3 interacts with CAII and that the interaction is phosphorylation state dependent, so that phosphorylation reduces the binding affinity. To examine the regulation of NBC3 activity by CAII and PKA, we first addressed the question of physical and functional interaction of CAII and NBC3, by performing micro-titre binding assays and dominant negative competition assays in transiently transfected HEK293 cells, respectively. Next we addressed the physical and functional effects of PKA phosphorylation, using the micro-titre binding assay and two pulse pH recovery experiments in transiently transfected HEK293 cells. Finally PKA and CAII binding, CAB, motif mutants were constructed and their effects on transport activity analysed.

3.2 Materials and Methods

3.2.1 Materials

Human NBC3 cDNA was a generous gift from Dr. Ira Kurtz (U.C.L.A.). PCR primers were from Invitrogen Inc (Burlington, ON, Canada). Recombinant expression vector, pGEX-6p-1, ECL reagent, and GST fusion purification reagents were from Amersham Biosciences (Piscataway, NJ). Pwo DNA polymerase was from Roche (Laval, QC, Canada) and all other cloning enzymes, as well as the PKA catalytic subunit, were from New England Biolabs (Mississauga, ON, Canada). *E. coli* recombinant expression strain, BL21-CodonPlus, was from Stratagene (La Jolla, CA). Protein concentrators were from Millipore (Billerica, MA). Protein quantification reagent was from Bio-Rad (Hercules, CA). Transfection and cell culture reagents were from Invitrogen (Burlington, ON, Canada). Forskolin, 5-(N-ethyl-N-isopropyl) amiloride and protein kinase A inhibitor, H89, were from Sigma-Aldrich Canada (Oakville, Canada). The antibodies against NBC3, CAII, and GST, were from SynPrep (Dublin, CA), Serotec (Raleigh, NC), and Santa Cruz (Santa Cruz, CA), respectively.

3.2.2 DNA constructs

Expression constructs for NBC3, NBC3Ct, CAII, and CAII V143Y, have been described previously [80, 113]. PKA phosphorylation site mutants, NBC3-S1132A and CAB site mutants, NBC3-CAB1 (D1135N and D1136N) and NBC3-CAB2 (D1163N and D1165N) were constructed using the mega-primer mutagenesis strategy [208]. First round PCR forward primer for all mutants was

5′-GCTCATGGTTGGCGTTATGTTGG-3′. First round PCR mutagenic reverse primers were 5′-CTGGCATAAGATTATTAAGCCAACTAAGTTC-3′, and 5′-GCACAGTATCATTATTGTTTTGAAGCATCCG-3′ for NBC3-CAB1 and NBC3-CAB2, respectively. Amino acid sequences of consensus CAII binding motifs were therefore mutated to $L^{1134}NNLM^{1138}$ and $L^{1162}QNNN^{1166}$, for CAB1 and CAB2, respectively. The products from the first round of PCR were used as forward mega-primers for the second round of PCR and 5′-TAGAAGGCACAGTCGAGG-3′ was used for the reverse primer. Second round products were sub-cloned back into the NBC3 cDNA (pNBC3) using Eco RI and Not I at 5′ and 3′ ends, respectively. GST fusion mutant constructs, GST.NBC3CtCAB1, GST.NBC3CtCAB2, and GST.NBC3CtS1132A, were engineered using the respective expression constructs as PCR templates. The sub-cloning strategy had previously been described [113]. All constructs were sequenced prior to initiation of experiments.

3.2.3 Protein expression in mammalian cells

NBC3, NBC3-CAB1, NBC3-CAB2, CAII and CAII V143Y proteins were expressed by transient transfection of HEK293 cells [32, 80], using the calcium phosphate method [190]. All experiments with transfected cells were carried out 48-hours post-transfection. Cells were grown at 37 °C in an air/CO_2 (19:1) environment in Dulbecco's modified Eagle media (DMEM), supplemented with 5% (v/v) fetal bovine serum, (v/v) calf serum and penicillin-streptomycin-glutamine.

3.2.4 NBC3 transport assay

The transport activity of NBC3 was monitored using a fluorescence assay, as previously described [209]. Briefly, HEK293 cells grown on poly-L-lysine coated coverslips were transiently transfected as described in the previous section. Forty-eight hours post-transfection, coverslips were rinsed in serum free DMEM and incubated in 4 ml serum-free media, containing 2 μM 2',7'-bis-(2-carboxyethyl)-5-(and-6)-carboxyfluorescein-acetoxymethyl ester (BCECF-AM) (37 °C, 20 min). Coverslips were then mounted in a fluorescence cuvette and perfused with Ringers buffer (5 mM glucose, 5 mM K gluconate, 1 mM Ca gluconate, 1 mM $MgSO_4$, 140 mM NaCl, 2.5 mM NaH_2PO_4, 25 mM $NaHCO_3$, and, 10 mM Hepes, pH 7.4), equilibrated with 5% CO_2 / air. The pH_i recovery activity of HEK293 cells transfected with NBC3, NBC3-CAB1, NBC3-CAB2 or NBC3 plus CAII V143Y was measured during the recovery from transient intracellular acidification. Acid loading was accomplished using the NH_4Cl pulse technique [210]. Cells were transiently perfused with Ringer's buffer, containing 40 mM NH_4Cl for 5 minutes, followed by the wash-out of NH_4Cl with Ringers buffer. All perfusion was performed with flow rate 3.5 ml/min. All experiments were performed in the presence of 5 μM 5-(N-ethyl-N-isopropyl) amiloride, (Sigma), to block endogenous NHE activity. Fluorescence was monitored using a Photon Technologies International RCR fluorimeter, at excitation wavelengths 440 and 500 nm and emission wavelength 530 nm. Following calibration using the nigericin/high potassium technique [192] at three pH values between 6.5 and 7.5, fluorescence ratios were converted to pH_i. The initial rate of pH_i recovery from an acid load was calculated by linear regression of the first 1-3 min of the initial

linear phase of pH_i recovery after maximum acidosis. In all cases the pH_i recovery of cells transfected with empty vector was subtracted from the total recovery, to ensure that these recoveries were only due to the transiently expressed proteins.

3.2.5 Measurement of intrinsic buffer capacity and proton flux

Intracellular buffering capacity measurements were made by the ammonium pulse method [210]. HEK293 cells grown on coverslips were sham transfected as described previously. Two days post-transfection, cells were loaded with BCECF-AM as described above. Coverslips were mounted in a fluorescence cuvette and allowed to equilibrate in Ringer's buffer containing 1 mM amiloride, bubbled with oxygen to ensure bicarbonate-free conditions. Cells were then perfused consecutively for 200 s with Ringer's buffer, without sodium bicarbonate, containing varying concentrations of NH_4Cl. $[NH_4^+]_i$ was calculated from the Henderson-Hasselbalch equation, and the intrinsic buffering capacity (β_i) was then calculated as $\Delta[NH_4^+]_i / \Delta pH_i$ [211]. The total buffering capacity of the system (β_{total}) was then determined as $\beta_{total} = \beta_i + \beta_{CO2}$, where $\beta_{CO2} = 2.3\ [HCO_3^-]$ [193]. Total proton flux was calculated as:

$J_{H^+} = \beta_{total} \times \Delta pH_i$ [193].

3.2.6 Antibody Preparation

A synthetic peptide comprised of the C-terminal 18 amino acids of human NBC3 was synthesized, yielding peptide: NH_2-ISFEDEPRKKYVDAETSL-COOH. The peptide was coupled to keyhole limpet hemocyanin and subsequently

injected into two rabbits numbered SN 338-1 and 2. Serum from each rabbit was monitored, on immunoblots containing NBC3 protein, until a maximal immune response was observed. Rabbits were sacrificed, exsanguinated and sera designated SN 338-1 and 2 were isolated. Only the SN 338-1 has a high anti-NBC3 titre. Peptide synthesis and antiserum production were completed by SynPep (Dublin, CA).

3.2.7 Immunodetection

Transfected cells were washed in PBS buffer (140 mM NaCl, 3 mM KCl, 6.5 mM Na_2HPO_4, 1.5 mM KH_2PO_4, pH 7.5) and lysates of the whole tissue culture cells from one 60 mm Petri dish were prepared by addition of 150 µl SDS-PAGE sample buffer, containing, complete mini protease inhibitor cocktail (Roche). Total protein content was measured using the Bradford protein assay [195]. Samples (5 µg) were resolved by SDS-PAGE on 8% acrylamide gels [196]. Proteins were transferred to PVDF membranes [197]. Membranes were blocked by incubation for 1 h in TBST-M buffer (TBST buffer (0.1% (v/v) Tween-20, 137 mM NaCl, 20 mM Tris, pH 7.5), containing 5% (w/v) non-fat dry milk) and then incubated overnight in 10 ml TBST-M, containing 1:5000 diluted affinity purified rabbit anti-NBC3 antibody or 1:3000 diluted sheep anti-CAII antibody, then incubated with TBSTM containing 1:3000 diluted donkey anti-rabbit IgG (Santa Cruz) or donkey anti-sheep IgG (Santa Cruz) conjugated to horseradish peroxidase. After a final wash with TBST buffer (3 times), blots were visualized using ECL reagent, and a Kodak Image Station 440CF.

3.2.8 *Cell Surface processing assay*

The fraction of protein processed to the cell surface was quantified as described [212], using the membrane-impermeant biotinylating reagent, Sulfo NHS-SS Biotin.

3.2.9 *Confocal microscopy*

Cells grown on poly-L-Lysine-coated, 18 mm diameter coverslips were transiently transfected, as described above. The coverslips were transferred to 35 mm Petri dishes. Cells were fixed for 30 min in 2% (w/v) paraformaldehyde in PBSC (1 mM $CaCl_2$, 140 mM NaCl, 3 mM KCl, 6.5 mM Na_2HPO_4, 1.5 mM KH_2PO_4, pH 7.5). After two washes with PBSC the cells were incubated for 25 min in permeabilisation buffer (300 mM sucrose, 50 mM NaCl, 3 mM $MgCl_2$, 0.5% (v/v) Triton X-100, 20 mM Hepes, pH 7.4). The coverslips were washed three times with PBSC and blocked for 25 min in 10% serum in PBSC. Coverslips were incubated with 1/50 dilution of sheep anti-CAII antibody (Serotec) in PBSC, 4% calf serum. Coverslips were washed three times with PBSC, 4% calf serum, and incubated for 45 min in a dark chamber with 1/100 dilution of biotinylated anti-rabbit IgG antibody (Santa Cruz) in PBSC, 4% serum. After three washes with PBSC, 4% serum, the coverslips were incubated for 45 min in a dark chamber with 1/100 dilution of streptavidin fluorescein conjugate (Amersham). Images were collected using a Zeiss LSM 510 laser scanning confocal microscope mounted on an Axiovert 100M controller, with a 63X (NA1.4) lens.

3.2.10 GST-fusion protein purification

GST constructs (NBC3Ct, CAB1, CAB2, or S1132A) were expressed in *E. coli* BL21 Codon Plus and purified, as previously described [80]. Note that NBC3Ct corresponds to amino acids 1127-1214 of human NBC3.

3.2.11 In vitro phosphorylation by PKA

GST or GST.NBC3Ct were treated with PKA in either of two ways: 1. with γ-labelled ^{32}P-ATP to measure incorporation of phosphate by scintillation counting and 2. with non-radioactive ATP, for analysis by mass spectrometry and microtitre plate binding assays. GST or GST.NBC3Ct (0.1 nmol) was mixed with 2500 units of PKA catalytic subunit (or equivalent volume of water), in PKA reaction buffer (200 μM ATP, 10 mM $MgCl_2$, 50 mM Tris-HCl, pH 7.5) or PKA reaction buffer supplemented with 500 μCi/μmol γ-labeled ^{32}P-ATP. Samples were then incubated at 30 °C for 10 minutes. Non-radioactive samples were characterized by matrix-assisted laser desorption/ionisation-time of flight, using a Voyager De-Pro mass spectrometer from Applied Biosystems (Foster City, CA). Radioactive samples were precipitated with TCA/DOC (5% trichloroacetic acid containing 0.03% deoxycholate), centrifuged at 14,000 rpm for 5 minutes, and washed twice with saturated TCA/DOC solution. Samples were then resuspended in 0.5 M NaOH and radioactivity counted by a Beckman LS 6500 scintillation system (Fullerton, CA).

3.2.12 Micro-titre plate binding assay

The micro-titre plate CAII binding assay is modified from an assay previously reported [134]. Purified CAII (200 ng/well) was immobilized onto 96-well micro-titre plates by 30 minutes of incubation at room temperature in ELISA buffer (150 mM NaCl, 100 mM Na_2HPO_4, pH 6.0) containing 1.25 mg/ml 1-cyclohexyl-3-(2-morpholinoethyl) carbodiimide metho-p-toluene sulphate. Plates were then washed (3 times 5 minutes) with PBS and blocked at room temperature for 1.5 hours with PBS containing 2% BSA. Plates were then washed twice with Antibody buffer (100 mM NaCl, 5 mM EDTA, 0.25% (w/v) gelatin, 0.05% (v/v) Triton X-100, 50 mM Tris-HCl, pH 7.5) then once with Antibody buffer, containing 1 mM DTT. Plates were then incubated with varied concentrations of GST or GST.NBC3Ct with or without PKA phosphorylation, overnight at room temperature. For pH titration experiments Antibody buffer was prepared containing 25 mM MES and 25 mM MOPS, in place of 50 mM Tris-HCl, and the buffer pH was adjusted appropriately. The following day plates were washed with Antibody buffer (3 x 5 minutes), then incubated with rabbit polyclonal anti-GST (1:5000 dilution) in Antibody buffer at room temperature for two hours. Plates were washed, then incubated with donkey anti-rabbit IgG (1:5000 dilution) in Antibody buffer at room temperature for 2 hours. Plates were washed, then incubated with streptavidin-biotinylated horseradish peroxidase complex (1:5000 dilution) in Antibody buffer at room temperature for 2 hours. Plates were washed a final time then developed with orthophenylenediamine dihydrochloride substrate with absorbance at A_{450}, read using a Labsystem Multiskan MCC ELISA micro-plate reader (MTX lab system

Inc., McLean, VA), when sufficient colour had developed. To estimate the affinity of the association between CAII and NBC3Ct, double reciprocal plots of [NBC3Ct] versus % binding were prepared. The Kd for the interaction was estimated from the negative inverse of the x-intercept.

3.2.13 Sequence and statistical analysis

The amino acid sequence of the NBC3 C-terminal tail was analyzed for the presence of consensus protein kinase A phosphorylation sites, using Peptools software. Statistical analysis was performed using Excel Software (Microsoft). Groups were compared with one-way ANOVA, followed by Tukey test, with $p < 0.05$ considered significant. For other experiments paired T-test was used with $p < 0.05$ considered significant.

3.3 Results

3.3.1 NBC3 transport activity and interaction with CAII

To measure NBC3 HCO_3^- transport activity HEK293 cells were transiently transfected with NBC3 and the recovery rate from an acid load induced by 40 mM NH_4Cl pre-pulse assessed (figure 3.1A). Although the initial characterization of human NBC3 [35] suggested that the protein is amiloride sensitive, a subsequent report (confirmed here) showed that NBC3 is not amiloride sensitive [112]. Thus, all NBC3 transport assays were performed in the presence of 5 μM EIPA to block activity of the endogenous Na^+/H^+ exchanger. The average rate of recovery from acid load was 0.080 ± 0.007 pH/min (2.1 mM/min) for NBC3 transfected cells and 0.037 ± 0.004 pH/min (0.97 mM/min) for vector-alone transfected cells. The background recovery rate of the sham cells may be attributable to the endogenous NBC3 expression that has been reported in HEK293 cells [112]. Background activity was subtracted from all measurements of NBC3 pH_i recovery activity.

In other experiments NBC3 activity was measured using the same assay as above, except using Na^+-free Ringer's buffer (Na^+ replaced by choline), containing 1 mM amiloride. After maximum acidification was achieved, the rate of pH_i recovery was measured for one minute, as 0.021 ± 0.003 pH/min (n=3). Three minutes after maximum acidification, perfusion solution was switched to Na^+-containing Ringer's buffer, containing 1 mM amiloride. The recovery rate then accelerated to 0.113 ± 0.008 pH/min. Peak acidification was pH 6.64 ±0.04. We conclude that NBC3-transfected cells express a pH recovery activity that is

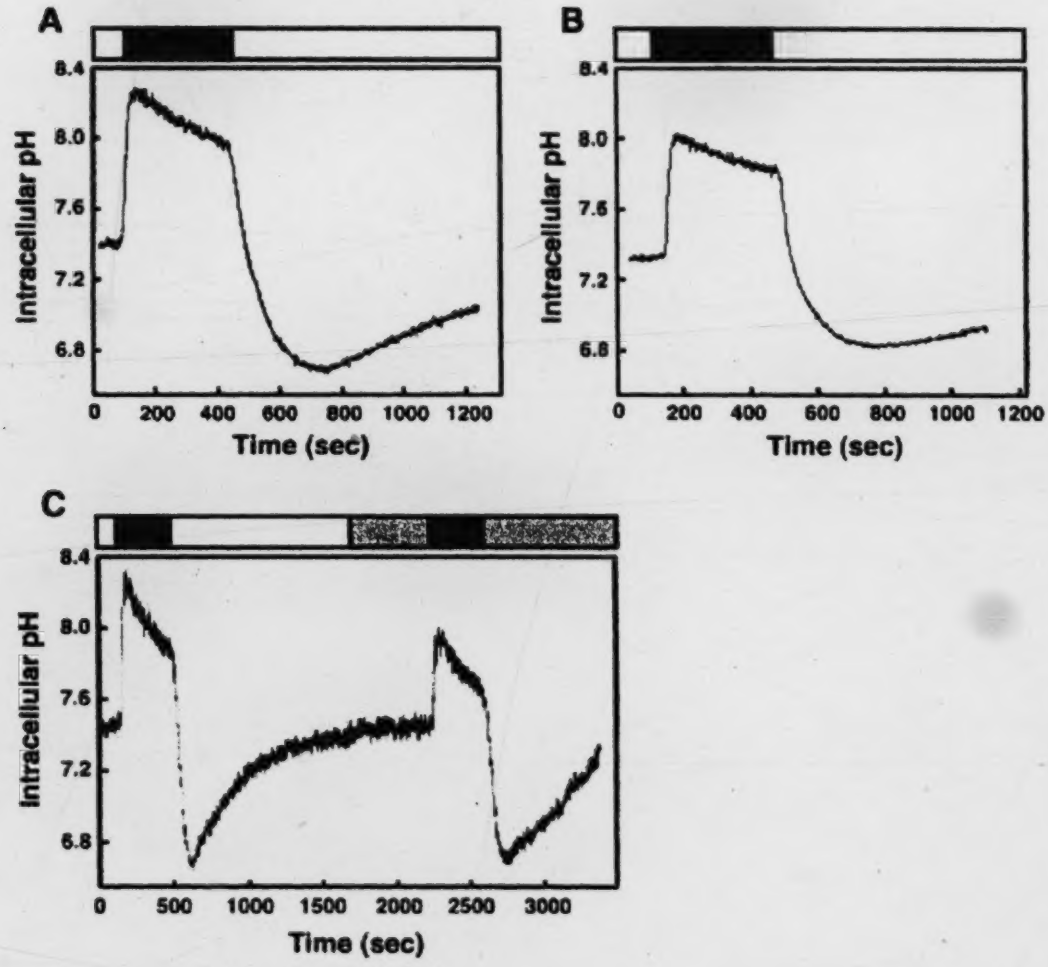

Figure 3.1- CAII functionally interacts with NBC3 in transiently transfected cells.

HEK293 cells grown on coverslips were transiently transfected with A, C NBC3 alone and B, NBC3 and CAII V143Y. Forty-eight hours post-transfection cells were loaded with the pH-sensitive dye BCECF-AM, and placed into a cuvette to monitor pH_i. Cells were perfused with the following solutions Ringers Buffer plus 5 μM EIPA (white bar), or Ringers Buffer plus EIPA containing 40 mM NH_4Cl (black bar). NBC3 activity was measured from the initial rate of pH_i recovery from the acid load. The effect of 100 μM 8-Br-cAMP (grey bar) on pH recovery was assessed by performing a second acid loading pulse and monitoring the rate of pH_i recovery. Note that the data in panels A and B were collected on the same day, with similar levels of transfection efficiency. Data in C were collected on a different day.

Na^+-dependent and amiloride insensitive, consistent with NBC3 [112]. The low level of pH recovery in the absence of Na^+, underscores the absence of Na^+-independent pH recovery activity. NBC3 contains two CAII binding motifs in its cytoplasmic C-terminus [8]. Functional assays were performed to assess the effects of CAII binding on NBC3 transport activity (figures 3.1, 3.2). To examine whether CAII binding affects NBC3 HCO_3^- transport activity we assayed NBC3 activity in the absence and presence of the functionally inactive CAII V143Y mutant. CAII is endogenously expressed in HEK293 cells (figure 3.2A) at sufficient levels that over-expression has previously been shown to have no effect on HCO_3^- transport activity [80]. However, over-expression of the V143Y mutant will displace wild-type CAII from its cytoplasmic binding sites. The V143Y point-mutation reduces CAII catalytic activity to $1/3000^{th}$ of wild-type activity yet preserves wild-type structure [213], so that the mutant is able to compete with wild-type protein for interactions with physiological binding partners [80]. Transfection of HEK293 cells with the V143Y CAII mutant, increased total CAII expression ~20-fold, as assessed by densitometry, compared to untransfected cells, which indicates that the amount of mutant CAII greatly exceeds wild-type in transfected cells (figure 3.2A). Anti-NBC3 antibody, SN 338-1, recognized a band with molecular weight consistent with NBC3 in NBC3-transfected HEK293 cells, but not in untransfected cells (figure 3.2B). This indicates the specificity of antibody SN 338-1 to recognize NBC3. The doublet band likely arises from differential glycosylation of NBC3, but was not further characterized.

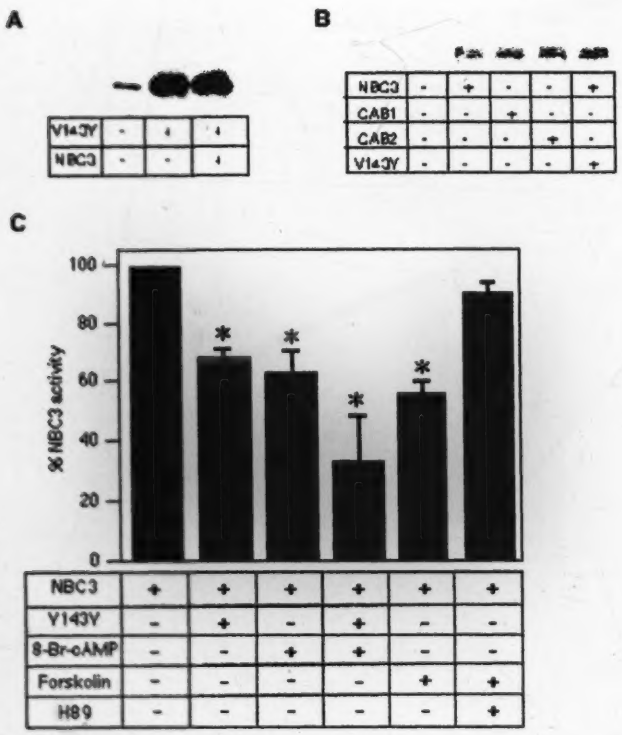

Figure 3.2- Expression of NBC3 and CAII constructs in HEK293 cells and summary of NBC3 activity.
A, expression of CAII V143Y relative to endogenous wild-type CAII expression was measured in lysates from HEK293 cells either sham-transfected or expressing NBC3 or NBC3 and CAII V143Y used for transport experiments, and probed on immunoblots for CAII as indicated at the bottom. B, expression of NBC3 and NBC3 CAB1 and CAB2 mutants measured in lysates used for transport experiments, and probed on immunoblots using the SN 338-2 antibody. The major immunoreactive band shown migrated between the 233 kDa myosin marker and the 135 kDa β-galactosidase marker and had Mr of approximately 150 kDa. C, average pH_i recovery rate is expressed as a percent of wild-type NBC3 recovery. Forskolin, 8-Br-cAMP and H89 were used at 5 μM, 100 μM and 10 μM, respectively. Error bars represent standard error (n=3-4). Asterisk represents statistical difference $p<0.05$ relative to wild-type NBC3 (unpaired, 2 tailed t-test).

Co-transfection of CAII V143Y and NBC3 had no effect on the level of NBC3 expression (figure 3.2B). However, co-transfection with the V143Y mutant reduced NBC3 transport activity by 31% ± 3% (Figs 1, 2C). The reduction of NBC3 activity in the presence of V143Y CAII suggests that displacement of wildtype CAII from a binding site on NBC3 reduces NBC3 transport activity. Localization of wildtype CAII to a binding site on NBC3 is thus required for full transport. Rates of change of pH_i are highly dependent on buffer capacity of the cell. Intrinsic buffer capacity (β_i) was measured for HEK293 cells transfected with NBC3, or co-transfected with NBC3 and CAII. In the pH region where measurements of NBC3 transport rate were made β_i was 11.2 ± 4.5 mM/pH at pH 6.82 ± 0.08 and 13.3 ± 1.3 mM/pH at pH 6.84 ± 0.06 for cells transfected with NBC3 alone and NBC3/CAII co-transfected cells, respectively. β_i measurements for NBC3 and NBC3/CAII are representative of all experiments performed here, since NBC3 transfected cells are likely to have the same β_i as cells transfected with NBC3 mutants. Similarly, cells are likely to have the same β_i whether transfected with wild-type or point mutant CAII. We conclude that there is no significant difference in β_i for the HEK293 cells under the various transfections states studied in these experiments. At pH 6.83 the buffer capacity resulting from bicarbonate (β_{CO2}) is 14.1 mM/pH; β_{total} is thus estimated as 26.3 mM/pH. In order to compare rates of pH_i recovery mediated by NBC3 it is essential that the pH recovery be measured from the same pH value. In the experiments described above the minimum pH_i in experiments to measure NBC3 activity was 6.67 ± 0.09 and 6.59 ± 0.06 for NBC3 and NBC3/V143Y CAII co-transfections,

respectively. There was no statistically significant difference between these values.

3.3.2 Effect of PKA on NBC3 transport activity

In the proximal tubule, PKA-dependent phosphorylation of NBC1 reduces transport activity and HCO_3^- reabsorption [71]. Recently, an important phosphorylation site S^{982} has been identified that shifts the NBC1a transport stoichiometry from 3:1 to 2:1 (HCO_3^-:Na^+) in proximal tubule cells [214]. Interestingly, analysis of the NBC3Ct sequence with Peptools software revealed the presence of a consensus PKA phosphorylation site (S1132) in NBC3Ct. Notably this site was identified as a low stringency site and does not form a strong consensus site. The presence of a potential PKA phosphorylation site, however weak, suggested the possibility that PKA could phosphorylate NBC3Ct, reducing activity through displacement of CAII or by other means. We therefore characterized the effect of PKA on NBC3 transport activity. HEK293 cells, transiently transfected with NBC3, were incubated with the membrane-permeant PKA agonist, 8-Br-cAMP (100 μM). The compound reduced pH_i recovery rate by 38% ± 7%, compared to the rate of pH_i recovery following an initial acid load without treatment (figure 3.1C, 3.2C). As a control the rate of pH_i recovery was measured following two successive acid loads, without 8-Br-cAMP treatment. The rates of pH_i recovery were indistinguishable (ΔpHi/min= 0.072 ± 0.001 (acidotic pH_i= 6.70 ± 0.05) and 0.071 ± 0.003 (acidotic pH_i= 6.71 ± 0.03) for recovery from the first and second pulse, respectively). Treatment with 8-Br-cAMP in the presence of CAII V143Y reduced pH_i recovery by 69% ± 12%

compared to untreated NBC3 transfected cells (figure 3.2C). The additive nature of the CAII V143Y and 8-Br-cAMP effects suggests that cAMP does not mediate its effects on NBC3 transport activity through modulation of CAII/NBC3 interaction.

To verify the results with 8-Br-cAMP, experiments were also performed with the adrenergic agonist, forskolin (5 μM). Cells treated with forskolin for 10 min prior to recovery from acid load had pH_i recovery rate 44% ± 3% lower than the rate before forskolin treatment (figure 3.2C). This indicates that mobilization of cAMP at physiological levels inhibits NBC3 to an extent similar to 100 μM 8-Br-cAMP. To examine whether the inhibitory effects of cAMP on NBC3 are mediated through protein kinase A, NBC3-transfected cells were pre-incubated with the PKA inhibitor, H89 (10 μM), for 5 min then for a further 10 min with H89 together with forskolin (5 μM). Treatment with H89 reduced the inhibitory effect of forskolin on NBC3 activity to 10% ± 3% (figure 3.2C) which was not significantly different from untreated NBC3. There was no difference in the level of acidification between the groups of transfected cells in these experiments. Average minimum pH_i was 6.67 ± 0.09, 6.69 ± 0.11, 6.61 ± 0.04, 6.69 ± 0.01 and 6.74 ± 0.02 for NBC3 alone, NBC3/8-Br-cAMP, NBC3/8-Br-cAMP/V143Y CAII, NBC3/forskolin and NBC3/H89/forskolin, respectively. We conclude that physiological levels of cAMP inhibit NBC3 activity and that PKA is responsible for the inhibition.

3.3.3 CAII physically interacts with NBC3Ct in a pH-dependent manner

We next examined the possibility that the functional interaction between CAII and NBC3 may be mediated by a direct physical interaction between these two proteins. A micro-titre-binding assay was performed in which CAII was immobilized to the bottom of a micro-titre dish well. Plates were then washed, overlaid with GST fusion proteins, and the amount of bound protein quantified using an anti-GST antibody and a tertiary development system [134]. We performed the assay using GST alone and GST.NBC3Ct (NBC3Ct corresponds to amino acids 1127-1214 of human NBC3) at concentrations from 0- 200 nM. Four wells were prepared for each experiment without bound CAII to control for test protein binding to the wells, no appreciable binding was observed. We observed saturation binding kinetics for GST.NBC3Ct with a K_d value of 101 nM (figure 3.3A). The V143Y mutant also bound GST.NBC3Ct, but with a K_d value of 227 nM, which is still well within the range of normal protein-protein interaction affinities. The CAII/NBC3Ct interaction was verified by dot-blot assay with purified NBC3Ct bound to a nylon membrane, overlaid with a cellular extract from HEK293 cells, and developed with an anti-CAII antibody. As shown in figure 3.3B, the NBC3Ct/CAII interaction is pH-dependent, with greater binding at acid pH, which is consistent with a role in pH-dependent regulation of NBC3 activity. Pre-treatment of the GST.NBC3Ct fusion protein with PKA had no significant effect on NBC3Ct/CAII binding over the pH 5-8 range (figure 3.3B). For example, at pH 7.25 binding of CAII was 17.2 ± 3.6% and 13.6 ± 2.5% of

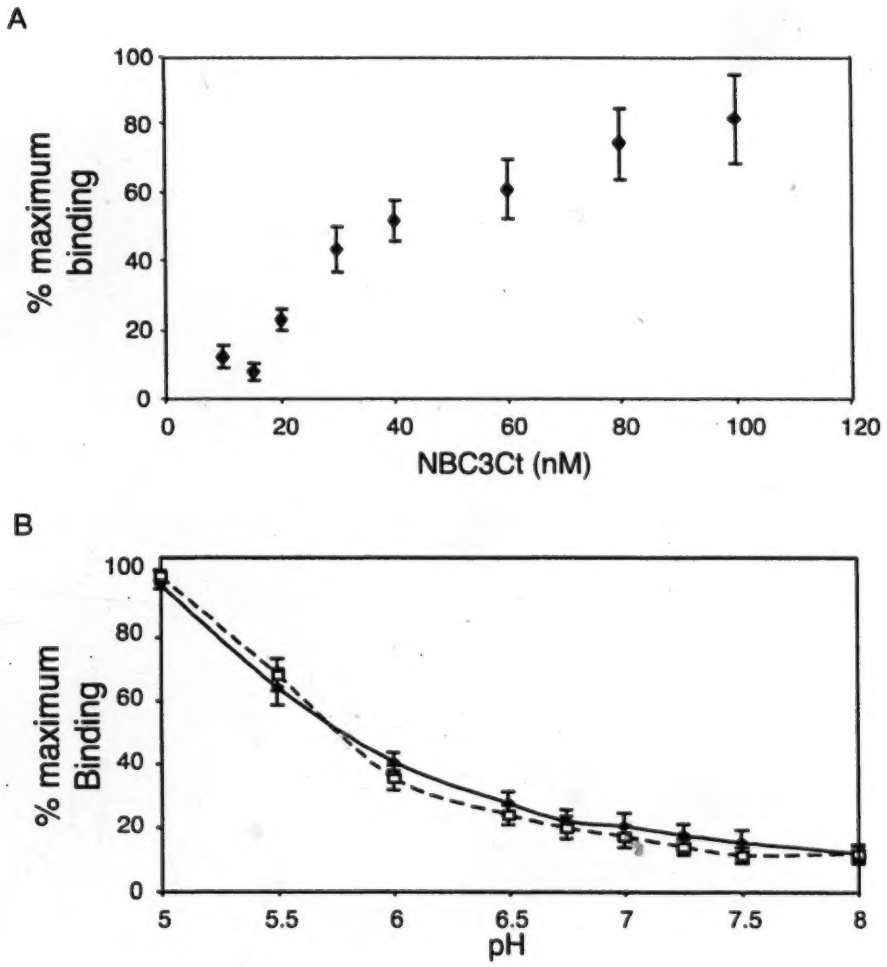

Figure 3.3- CAII binds GST.NBC3Ct in a pH-dependent manner
Purified CAII (50 ng/well) was bound to the bottom of micro-titre dish wells using a carbodiimide compound, and non-specific binding sites blocked by pre-treatment with 2% BSA in PBS. Wells were overlaid with GST test proteins in Antibody buffer and color developed by sequential treatment with rabbit anti-GST antibody, donkey anti-rabbit biotinylated antibody, finally HRP-conjugated streptavidin, and finally OPD substrate. For each data point (n=4) background binding of GST alone was subtracted from GST.NBC3Ct for each concentration or pH value tested and the respective data set normalized to the maximum A_{450} observed. A, binding of CAII and GST.NBC3Ct at a range of GST.NBC3Ct concentrations. B, GST.NBC3Ct binding over a range of pH values and fixed 100 nM GST.NBC3Ct, with and without pre-phosphorylation, "□" and "♦", respectively. Curves were manually fitted through the data points.

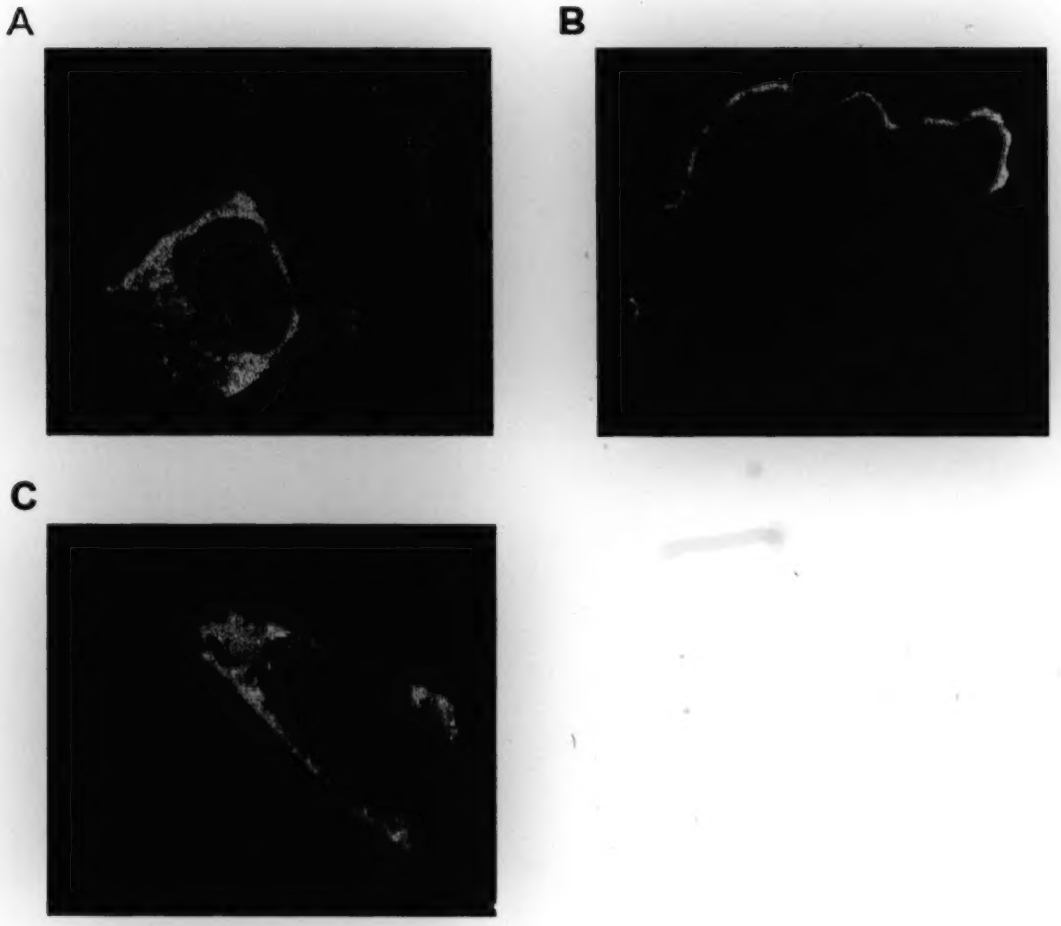

Figure 3.4. NBC3 recruits over-expressed CAII to the plasma membrane in transiently transfected cells.
The localization of CAII within HEK293 cells was assessed by immunofluorescence confocal microscopy. Cells were transiently transfected or co-transfected with A, CAII, B, CAII and NBC3, or C, CAII and NBC3ΔCt. Transfected cells were fixed and permeabilized 48 hours post transfection. Coverslips were incubated with anti-CAII antibody, a biotinylated goat anti-rabbit secondary antibody, and finally streptavidin-FITC dye. All images were collected at 630 times magnification. Data are representative of results found in 6-9 coverslips at each condition.

maximum binding for GST.NBC3Ct without and with PKA treatment, respectively, which was statistically indistinguishable. We conclude that PKA does not alter CAII/NBC3 binding kinetics by phosphorylation of NBC3Ct.

3.3.4 NBC3 recruits CAII to the plasma membrane

We further investigated the CAII/NBC3 physical interaction in transiently transfected HEK293 cells. CAII was over-expressed by transient transfection and cells were then treated with an anti-CAII antibody. Confocal immunofluorescence indicated a predominant cytoplasmic localization for CAII figure 3.4A. In contrast, co-transfection of CAII with NBC3 recruited CAII to the plasma membrane, consistent with association with NBC3 (figure 3.4B). Co-transfection of CAII with a deletion mutant of NBC3, lacking the C-terminal domain, restored the diffuse cytoplasmic localization of CAII (figure 3.4C). At the exposure levels used in these experiments endogenous CAII (expressed at levels 20-fold lower than the level induced by transfection with CAII cDNA) was not visible. These experiments demonstrate that NBC3 expression recruits CAII to the plasma membrane and that the NBC3 C-terminal domain is required to mediate this interaction.

In figure 3.4B it is surprising that while there is intense membrane staining, cytosolic CAII staining is weak, in spite of the fact that the cells are transfected with CAII. We suspect that the fixation methods used in the immunocytochemistry experiments result in some loss of cytosolic contents. It stands to reason that free cytosolic components will be more labile than membrane proteins, fixed in a bilayer, or proteins bound to membrane proteins. Thus, the lower than expected cytosolic staining may reflect loss of free cytosolic

CAII during slide processing. It may also reflect the result that localized CAII, at the membrane, will stain much more intently than diffuse cytosolic CAII.

3.3.5 PKA does not phosphorylate NBC3Ct in vitro

NBC3 interacts with the membrane scaffolding protein, NHE regulatory factor, NHERF, via a PDZ binding motif at the extreme C-terminus of NBC3 [112]. NHERF in turn interacts with the PKA associated protein, AKAP, ezrin, which binds the regulatory domain of PKA [175]. The NBC3Ct/NHERF interaction suggests that NBC3Ct may be a substrate for PKA, especially in light of our finding that 8-Br-cAMP treatment reduces NBC3 transport activity. We therefore investigated the possibility that PKA phosphorylates NBC3Ct. GST.NBC3Ct was treated *in vitro* with the catalytic subunit of PKA. PKA-mediated phosphorylation of NBC3Ct was first assessed by mass spectrometry. Addition of phosphate adds 80 Da to a protein's mass, yet no 80 Da-shifted peak could be detected when PKA-treated NBC3Ct was analysed. To verify this finding NBC3Ct was PKA-treated in the presence of γ-^{32}P-ATP. Again, no phosphorylation of NBC3Ct was detected. We conclude that the effect of PKA on NBC3 activity in transiently transfected HEK293 cells does not involve phosphorylation of the NBC3 C-terminal domain.

3.3.5 Identification of the site of CAII interaction on NBC3Ct

Site-directed mutagenesis of the putative CAII binding motif of AE1 has shown that the minimum binding requirements for CAII are a hydrophobic residue (usually leucine) followed by at least two acidic residues within the next four amino acids [205]. The C-terminus of AE1 contains 4 putative motifs yet

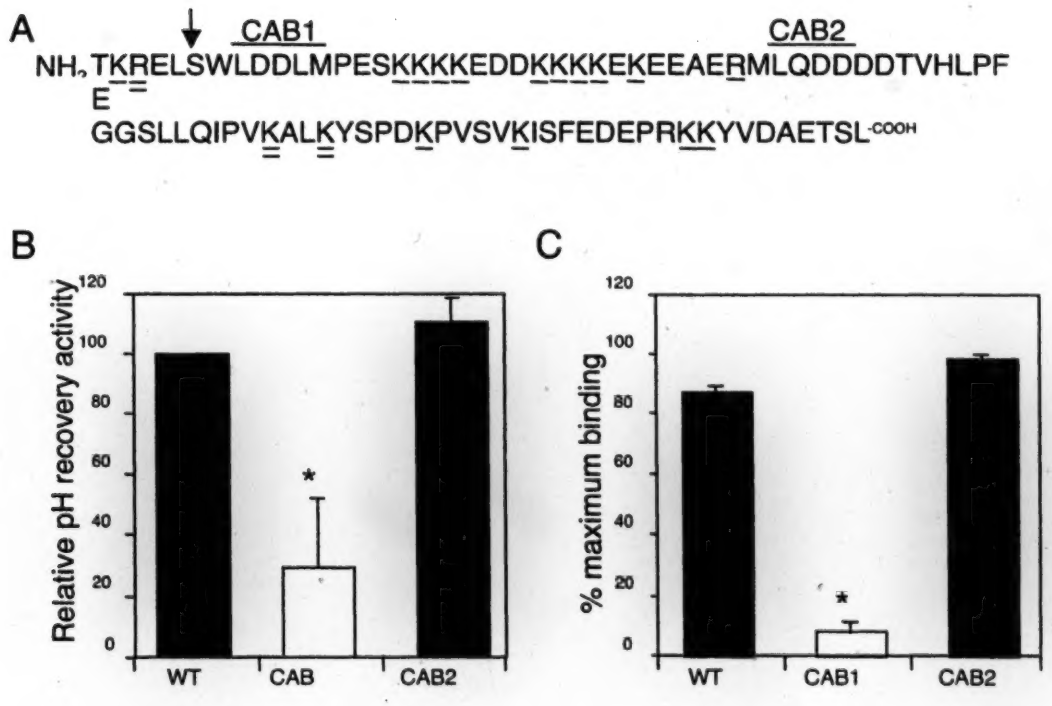

Figure 3.5- Identification of the CAII binding site within NBC3Ct.
A, The amino acid sequence of NBC3Ct (residues 1127 to 1214) with potential and utilized cleavage sites for trypsin indicated by single and double lines under the bar, respectively [113]. Putative carbonic anhydrase binding (CAB) motifs, CAB1 and CAB2 are indicated above the bar. Vertical arrow represents potential PKA phosphorylation site identified by Peptools software. B, rate of pH_i recovery from acid loads was measured for HEK293 cells transfected with wild-type NBC3 (WT) or NBC3-CAB1 (CAB1 was mutated to LNNLM) and NBC3-CAB2 mutants (CAB2 was mutated to LQNNN). C, binding of wild-type NBC3 and NBC3-CAB1 and CAB2 mutants to CAII, measured using micro-titre plate assay. Error bars represent standard error (n=3). Asterisk represents statistical difference $p<0.05$ relative to wild-type NBC3 (unpaired, 2 tailed t-test).

only the most membrane proximal motif binds CAII [205]. The C-terminal domain of NBC3 contains two consensus CAII binding motifs, CAB1 and CAB2 (figure 3.5A). In a previous report, limited proteolysis revealed two proteolytically sensitive regions in NBC3Ct (figure 3.5A), which were interpreted to be conformationally-open, potential protein binding sites [113]. The most membrane-proximal protease-sensitive region is very close to CAB1. To examine the role of CAB1 and CAB2 we replaced the acidic residues within the putative CAB motifs with the corresponding amide residue (mutation to LNNLM and LQNNN for CAB1 and CAB2) (Fig. 5A), to neutralize charge in the CAB site with the simplest change possible. The pH_i recovery rates of the NBC3-CAB1 and CAB2 mutants were measured in transiently transfected HEK293 cells using the NH_4Cl pre-pulse method of acid loading. The NBC3-CAB1 mutant had a transport rate that was 29% ± 22% of wild-type, while the CAB2 mutant recovery rate was not statistically different from wild-type (Fig. 5B). The dramatic effect of the CAB1 mutations is not explained by a failure of the protein to be processed appropriately to the cell surface, since assays of cell surface processing revealed that the fraction of total cellular NBC3 expressed at the plasma membrane was 48%, 67% and 53% (n=2) for wild-type NBC3, NBC3-CAB1 and NBC3-CAB2, respectively. The difference in rate of change of pH_i mediated by the CAB1 mutants also did not result from differences in the starting pH_i in transport assays; minimum pH_i values were 6.62 ± 0.03 and 6.55 ± 0.06 for the CAB1 and CAB2 mutants, respectively, which represents no statistically significant difference.

CAB mutations were recapitulated into NBC3 C-terminal domain GST fusion proteins, GST.NBC3CtCAB1 and GST.NBC3CtCAB2, and the effect of CAII/NBC3 physical interaction assessed. Micro-titre dish CAII-binding assays revealed that GST.NBC3CtCAB1 mutant bound 7% ± 2% of the amount of CAII bound by wild-type NBC3, while GST.NBC3CtCAB2 binding was not statistically different from wild-type binding (Fig. 5C). We conclude that the CAB1 motif meditates the CAII/NBC3 interaction.

3.4 Discussion

Mechanisms to regulate the activity of membrane transport proteins are limited because much of the protein is buried in the lipid bilayer, inaccessible to direct interaction with modulators. Compounding the problem, only one surface of plasma membrane transporters is accessible to the cytosol. Membrane transport can be chronically regulated by changes of expression level or acutely regulated by insertion of previously-translated vesicle-localized transporters into the membrane, as occurs for Glut4 [215] and renal H^+-ATPase. How else can membrane transport be regulated acutely? Renal HCO_3^- transport is acutely inhibited by cAMP-coupled agonists [78, 216]. In this report we examined the acute regulation of the NBC3 Na^+/HCO_3^- co-transporter by cAMP and by the cytosolic enzyme, CAII, which catalyzes the reaction, $HCO_3^- + H^+ \leftrightarrows CO_2 + H_2O$, to produce the substrate for transport by NBC3, or in reverse mode to consume HCO_3^-. CAII binding has large effects on the Cl^-/HCO_3^- exchange activity of AE family members [80, 136]. [80]. The presence of a consensus protein kinase A (PKA) site beside a consensus CAII binding site in NBC3 (Fig. 5), led to the following potential regulatory model for NBC3: cAMP-coupled agonists activate PKA, which in turn phosphorylates the NBC3 C-terminus, displacing CAII from

its binding site and thereby decreasing transport activity. Here we explored this regulatory mechanism and found that while parts were accurate, the model on the whole did not hold together.

We explored the interaction between CAII and NBC3. Consistent with what was found for Cl^-/HCO_3^- exchangers, a single CAII binding site in the cytosolic C-terminus was sufficient to stabilize the NBC3/CAII interaction. Micro-titre plate binding assays revealed that the CAII/NBC3 binding had sufficient affinity (101 nM) to be physiologically relevant. Mutation of two aspartic acid residues (D1135 and D1136) in the CAB1 consensus CAII binding site of the NBC3 C-terminus was sufficient to reduce CAII interaction with the C-terminal domain to only 7% of wild-type levels. The presence of only this single CAII binding site on NBC3 is supported by immunofluorescence data, which showed that while wild-type NBC3 induced CAII to localize to the plasma membrane, cells transfected with an NBC3 deletion mutant lacking its C-terminus, previously shown to localize to intracellular membranes [113], showed a broad cytosolic CAII distribution, as found for cells not transfected with NBC3. Since the CAII/NBC3 interaction occurred *in vitro*, we conclude that the interaction is direct and does not require accessory factors.

Interaction between CAII and NBC3 is highly significant to NBC3 activity. Displacement of wild-type CAII from its binding site on the NBC3 C-terminus was accomplished by expression of functionally inactive V143Y mutant CAII at levels 20-fold higher than wild-type CAII. V143Y CAII expression reduced NBC3 HCO_3^- transport activity by 31% ± 3%, in the absence of effects on NBC3 expression level or cell surface processing. More profound was the effect of mutation of the CAII binding site (CAB1) on NBC3 activity; NBC3 activity was

inhibited by 71%. The significance of the result was underscored by the lack of effect on transport activity of mutation of the second consensus CAII binding site, CAB2, which did not bind CAII. The larger effect of CA binding site mutation than V143Y CAII on NBC3 activity was also found for AE1 [80]. This likely reflects the fact that V143Y CAII was expressed at only 20-fold higher levels than wild-type CAII, so that about 5% of NBC3 molecules would be occupied by wild-type CAII. Also, V143Y CAII retains $1/3000^{th}$ of its catalytic activity. CAII, with turnover of 10^6 s^{-1}, still retains a turnover rate that is significant relative to the turnover rate for NBC3, which is likely to be 10^3-10^4 s^{-1}.

Interaction between CAII and NBC3 increases the rate of pH_i recovery mediated by NBC3 in transfected cells. NBC3 is an electroneutral co-transporter that does not transport ions that can be detected with fluorescent dyes, which eliminates electrophysiological and fluorescent techniques for direct measurement of ion flux, respectively. Instead, we used the pH sensitive dye, BCECF, to determine changes in pH_i, which in turn was an indirect measurement of HCO_3^- flux because of the equilibrium reaction $HCO_3^- + H^+ \leftrightarrows CO_2 + H_2O$. Concentration gradients are often thought not to exist within the cytosol because the rate of diffusion within free solution is much greater than across the plasma membrane. However, Vaughan-Jones has established that H^+ movement in biological systems is much slower than in non-physiological solvents, because of fixed buffer molecules, viscosity and other factors [217, 218]. How does CAII/NBC3 interaction facilitate NBC3 HCO_3^- transport? The acceleration of transport rate we observed with CAII requires direct binding by NBC3 since the expression of dominant negative V143Y CAII and mutation of the NBC3 CAB1 site both reduced transport rate, in the presence of endogenous wild-type CAII

expression. Since NBC3 transport is driven by the Na^+ and HCO_3^- gradients present at the surfaces of NBC3, localization of CAII to the C-terminus of NBC3 will maximize the rate of HCO_3^- conversion to CO_2 at the site where NBC3 brings HCO_3^- into the cell. This minimises the local [HCO_3^-] and maximizes the transmembrane [HCO_3^-] gradient across each individual NBC3 molecule, maximizing the transport rate.

In this report we did not examine the effect of V143Y CAII on the efficiency of processing of NBC3 to the cell surface. If V143Y CAII inhibited NBC3 cell surface processing, we would observe a decrease in transport activity, as we found. Although we did not measure the level of cell surface expression of NBC3 in the presence and absence of V143Y CAII, we believe that this is unnecessary for the following reasons: 1. We have measured the effect of V143Y CAII on the level of cell surface expression for AE1 [80] and NBC1 [81]. In neither case, with transporters related to NBC3, did we see an effect of V143Y CAII on surface processing efficiency. 2. We determined the cell surface processing of NBC3 versus the NBC3 CAB1 and CAB2 mutants. Since the mutants were as well processed as wildtype NBC3, we were able to conclude that the impairment of NBC3 CAB1 function resulted from impaired transport rate, not inefficient cell surface processing. The NBC3 CAB1 data support the role of CAII interaction in activation of NBC3, consistent with the V143Y/ NBC3 data. Taken together we cannot absolutely rule out the possibility the V143Y CAII acts through effects on NBC3 cell surface processing. However, the balance of data is consistent with a model in which interaction of CAII with the NBC3 C-terminal region activates NBC3 transport function.

We found that treatment of NBC3-expressing HEK293 cells with the membrane-permeant cAMP derivative, 8-Br-cAMP, and the adrenergic agonist, forskolin, inhibited NBC3-mediated pH_i recovery rate by 38% ± 7% and 44% ± 3%, respectively, representing a strong, acute regulation of transport activity. Transport inhibition resulted from cAMP stimulation of protein kinase A, since the PKA inhibitor, H89, blocked the cAMP effect. The presence of a consensus PKA phosphorylation site adjacent to CAB1 suggested that PKA might mediate NBC3 inhibition by displacement of CAII binding. However, three lines of evidence showed that this was not the case. *In vitro* treatment of a GST fusion protein of the NBC3 C-terminus with PKA did not result in any phosphorylation of the protein, as measured by mass spectrometry and radioactive phosphate incorporation. Second, treatment with PKA did not affect the *in vitro* interaction between CAII and NBC3Ct. Finally, the effects of V143Y CAII and 8-Br-cAMP were additive, suggesting that they act through independent pathways. These data need to be interpreted carefully. Since the phosphorylation experiment was performed *in vitro,* it is possible that some cytosolic factor, like the PKA scaffolding protein ezrin [175] and NHERF [112], may be required for phosphorylation of NBC3. Indeed, NHERF has already been shown to interact with NBC3 [112]. Second, the definitive experiment would be to assay the effect of 8-Br-cAMP on the NBC3-CAB1 mutant, which cannot bind CAII. If cAMP acts by PKA-mediated displacement of CAII, then 8-Br-cAMP would have no effect on the CAB1 mutant. Conversely, if cAMP acts independently of CAII, it would still inhibit transport activity. Unfortunately this experiment could not be reliably performed because the activity of the CAB1 mutant is already too low to be able to observe further reductions of activity. If the NBC3 C-terminal domain

is not required for regulation by PKA, then it suggests that the N-terminal cytoplasmic domain is the site of action of PKA. Consistent with this possibility, analysis of the human NBC3 sequence reveals that while the C-terminal domain has a single consensus PKA phosphorylation site (S1132, Fig. 5A), the N-terminal cytoplasmic domain has six, at amino acids 182, 225, 242, 260, 276 and 301. It is also possible that PKA does not act directly on NBC3; PKA may phosphorylate some protein, which is able to regulate NBC3 transport activity.

One other report has examined the effect of cAMP on NBC3 transport activity [112]. In that study cAMP was mobilized by forskolin treatment of NBC3-transfected HEK293 cells, the same used in the present report. The results of that paper are difficult to compare directly to the present study. In the previous report it was found that expression of the CFTR Cl^- channel did not affect NBC3 activity. However, treatment of NBC3/CFTR co-transfected cells with forskolin inhibited the rate of NBC3-mediated HCO_3^- transport by 67 ± 11%, in comparison to forskolin treated cells that expressed NBC3 alone. The paper did not report on the effect of forskolin on NBC3 in the absence of CFTR. The report also differed in methodology. In the present report cells were incubated with forskolin or 8-Br-cAMP for 10-15 minutes prior to measuring the effect of the agent on NBC3 activity; in the previous paper, forskolin was added just before (estimated as 2 min) measurement of pH_i recovery rate. We found a lower degree of NBC3 inhibition by 8-Br-cAMP (38% ± 7%) and forskolin (44% ± 3%), which was independent of CFTR expression, since HEK293 cells do not endogenously express CFTR [219]. Combining the two data sets, it appears that cAMP mobilization inhibits NBC3 transport activity and that this inhibition is

potentiated in the presence of CFTR. Prolonged adrenergic stimulation results in NBC3 inhibition, even in the absence of CFTR.

The present report does conflict with the earlier report in the effect of the PKA inhibitor, H89. Here H89 fully blocked the inhibitory effect of forskolin on NBC3. In contrast, the earlier report found that H89 had a slight additional inhibitory effect on forskolin-treated NBC3, but blocked the inhibitory effect of CFTR on NBC3 activity. The basis for the difference in results is not clear. However, it may be related to methodology. In the present report, effects of compounds were internally controlled. That is, NBC3 transport rate was measured for NBC3 alone and again following treatment of the *same* set of cells. Summarized results presented in Fig. 2 are the average of these internally controlled data. The difference may also relate to the length of time of incubation with H89. We incubated with H89 for 5 min prior to treatment with forskolin, for a total of 15-20 minutes of H89 treatment. In the previous report H89 and forskolin were co-administered, which may have reduced the efficacy of H89.

Although our data do not support modulation of CAII binding as the mechanism by which cAMP regulates transport, our data do suggest that during extreme acidosis pH_i may regulate transport activity in part through increasing CAII binding to NBC3. Binding between CAII and NBC3 was pH-dependent, with an acidic maximum and reduced binding at alkaline pH, similar to what was previously found for the interaction of the AE1 Cl^-/HCO_3^- exchanger with CAII [134]. The increased interaction of CAII at acid pH would help to activate NBC3 during recovery from acid loads, a physiological function of the transporter.

We examined the regulation of the human NBC3 Na^+/HCO_3^- co-transporter by CAII, cAMP and pH_i. CAII binds amino acids D1135-D1136 in the C-terminal cytoplasmic tail of NBC3. Inhibition of the NBC3/CAII interaction, either by expression of functionally inactive CAII, or mutation of the CAII binding site on NBC3, reduced NBC3 activity, consistent with a model in which CAII interaction activates NBC3 transport activity. Since the CAII/NBC3 interaction increases at acid pH_i, the interaction contributes to pH-dependent regulation of NBC3 activity. Activation of the cAMP-coupled signalling pathway with 8-Br-cAMP or forskolin reduced NBC3 transport rate. However, we could find no evidence for phosphorylation of the NBC3 C-terminal tail by PKA. Similarly, the additivity of the 8-Br-cAMP and V143Y CAII effects led us to conclude that cAMP inhibits NBC3 activity through a mechanism independent of CAII.

Chapter 4

Summary and Future Directions

4.1 Summary

In 1999 when I began my training, NBC3 had just been discovered and very little was known about its physiology and even less about structure. It was clear at that point that cytoplasmic domains conveyed unique functionality to transport proteins and accounted for processes such as cell surface processing and membrane localization. However, very little direct work had been completed on these domains aside from the biochemical structural characterization of the AE1 N-terminal domain. I therefore sought to characterize the structure and function of one of the NBC3 cytoplasmic domains. Given that attempts at recombinant expression of N-terminal AE2 and AE3 cytoplasmic domains had thus far proved unsuccessful I chose to characterize the C-terminus of NBC3 (NBC3Ct). As this work was underway, the AE1/CAII interaction was first characterized and the consensus-binding motif identified. A screen of the NBC3Ct sequence identified two potential binding motifs and spurred the characterization of the NBC3/CAII interaction and extension of the membrane metabolon theory to include NBC family members.

4.1.1 Characterization of NBC3 Structure and Function

The sodium bicarbonate co-transporter (NBC3) is expressed in a range of tissues including heart, skeletal muscle, and kidney where it plays an important role in pH_i regulation and HCO_3^- metabolism. Hydropathy plot analysis and sequence alignment with AE1 suggest NBC3 has a three-domain structure consisting of a 67-kDa N-terminal cytoplasmic domain, a 57-kDa membrane domain, and an 11-kDa C-terminal cytoplasmic domain (NBC3Ct). The role of

C-terminal domains as important regulatory regions is an emerging theme in bicarbonate transporter physiology. In this study we determined the functional role of human NBC3Ct and characterized its structure using biochemical techniques. We first ascertained whether or not NBC3Ct is required for NBC3 transport activity. Deletion of the C-terminal domain diminished transport activity to 12 ± 5% of wild-type activity. Given the importance of cytoplasmic domains for cell surface processing, we next investigated the expression and intracellular distribution of the deletion mutant. The mutant accumulated to low levels and was almost completely retained inside the cell as assessed by immunoblots and confocal microscopy, suggesting a role for NBC3Ct in cell surface processing.

To characterize the structure of NBC3Ct, amino acids 1127 to 1214 of NBC3 were expressed as a GST fusion protein (GST.NBC3Ct). GST.NBC3Ct was cleaved with PreScission Protease™ and native NBC3Ct could be purified to 94% homogeneity. Gel permeation chromatography and sedimentation velocity ultracentrifugation of NBC3Ct indicated Stokes radii of 26 and 30 Å, respectively. By comparison with the CA control protein used to calibrate the GPC column (molecular weight 29 kDa, and Stokes radius 20 Å), NBC3Ct has a very extended structure. We thus sought to determine the approximate size of the domain using velocity ultracentrifugation and some computer modelling. In this way, we ascertained that NBC3Ct has a prolate shape with long and short axes of 19 and 2 nm, respectively. The related isoform NBC1 is sensitive to changes in pH_i but not extracellular pH, suggesting its cytoplasmic domains play a role in the pH sensitive regulation of this transporter. To investigate whether NBC3 undergoes a similar type of regulation via NBC3Ct, we looked for changes

in the circular dichroism spectra of NBC3Ct over the pH 6.2-7.8 range. No change in the spectra was observed, ruling out a large conformational change as a component of pH sensor function. Proteolysis with trypsin and chymotrypsin identified two proteolytically sensitive regions, R1129 and K1183-K1186, which may form protein interaction sites.

4.1.2 Regulation of NBC3 transport activity by CAII interaction and PKA-dependent phosphorylation

We investigated whether NBC3, like some Cl^-/HCO_3^- exchange proteins, could bind CAII and whether protein kinase A (PKA) could regulate NBC3 activity through modulation of CAII binding. CAII bound the C-terminal domain of NBC3, NBC3Ct, with the K_d=101 nM; the interaction was stronger at acid pH, which is consistent with a role for NBC3 in regulation of pH_i during acidosis. Co-transfection of HEK293 cells with NBC3 and CAII recruited CAII to the plasma membrane. Mutagenesis of consensus CAII binding sites revealed that the D1135-D1136 region of NBC3 is essential for CAII/NBC3 interaction and for optimal function since the NBC3 D1135N/D1136N retained only 29% ± 22% of wild-type activity. Co-expression of the functionally dominant negative CAII mutant V143Y with NBC3 or addition of 100 μM 8-Br-cAMP to NBC3 transfected cells reduced pH_i recovery rate by 31% ± 3%, or 38% ± 7%, respectively, relative to untreated NBC3 transfected cells. The effects were additive, together decreasing pH_i recovery rate by 69% ± 12%, which suggests that PKA reduces transport activity by a mechanism independent of CAII. Measurements of PKA-dependent phosphorylation by mass spectroscopy and labelling with γ-^{32}P-ATP

showed that NBC3Ct was not a PKA substrate. These results demonstrate that NBC3 and CAII interact to maximize the HCO_3^- transport rate. While PKA decreased NBC3 transport activity, it did so independent of the NBC3/CAII interaction and did not involve phosphorylation of NBC3Ct.

4.2 Future directions

Our finding that stimulation by PKA reduces NBC3 transport in transiently transfected HEK293 cells and that this process does not involve phosphorylation of NBC3Ct begs the question; how does PKA stimulate NBC3 transport activity? Preliminary studies failed to show a decrease in CAII binding to GST.NBC3Ct following pre-incubation of CAII with the catalytic domain of PKA and ATP, suggesting that PKA must phosphorylate some other structure that influences NBC3 transport activity. The next most obvious candidate is the N-terminal domain of NBC3, which possesses several consensus PKA phosphorylation sites. Fertile ground for an aspiring transport physiologist would be to construct a series of point mutants that knock out each consensus PKA phosphorylation site in the N-terminal domain and characterize the effect on NBC3 transport activity in the presence of PKA agonists. NBC3 interacts with the scaffolding protein NHERF, a known PKA binding protein; thus, NHERF also may be a potential target for PKA phosphorylation. My attempts to over-express NBC3Nt in *E. coli* and to purify it were unsuccessful. However, my attempts were not exhaustive and several combinations of vector and host remain to be tested. If the N-terminal domain can be purified, then a study parallel to the one presented in this thesis could be completed.

Preliminary studies have suggested that NBC3 activity is not regulated by PKC. Some reports on the regulation of NBC1 have suggested that acute changes in transport activity involve changes in V_{max}, which is consistent with an increase in transporter turnover rate or an increase in transporter number in the plasma membrane. Unfortunately, the NBC3 activity assay used in preliminary experiments was not robust enough to allow detailed kinetic characterization of NBC3 transport. Should an assay system with a better signal to noise ratio be developed, it would become possible to determine the transport kinetics of NBC3 in the presence of PKC agonists and calculate any change in V_{max}. This could potentially be a very exciting avenue of exploration. Recently, we modified our NBC3 transport assay to measure Na^+-stimulated intracellular pH recovery. These assays, in which buffer switches from zero Na^+ to Na^+ medium, yielded the most robust transport we have seen and hold promise for more detailed studies of NBC3 kinetics.

Attempts to obtain a crystallographic structure of NBC3Ct have thus far been unsuccessful. Approximately 70 crystallization conditions for purified NBC3Ct alone were assessed and a further 1500 conditions for an equal molar mixture of NBC3Ct and CAII assessed. In light of the proteolytic sensitivity of NBC3Ct, a protein product consisting of the proteolytically insensitive portion of NBC3Ct may yield a successful crystallization. In addition, if the N-terminal domain of NBC3 is ever successfully purified in milligram quantities, it also would be an interesting subject for crystallization trials.

On a more clinical level, the guard during ischemia against necrosis (GUARDIAN) clinical trial of cariporide, a specific NHE1 inhibitor, showed a 10% ($p=0.12$) risk reduction for cardiovascular events after 36 days of cariporide

(120 mg tid) treatment in high risk patients undergoing coronary artery bypass graft[220]. Benefits were maintained for 6 months (25% p=0.03). It is believed that although modest, this risk reduction may be improved with increased doses of cariporide, as neither risk reduction saturation nor an increase in the rate of adverse effects was observed at the concentrations studied. The rationale for the GUARDIAN trial is based on decreasing intracellular Na^+ loading during the reperfusion phase, following an acute ischemic episode. Since NBC3 is also present in cardiomyocytes and operates with a parallel mechanism to NHE1 it also is a potential target to reduce intracellular Na^+ accumulation. To date, no specific inhibitors of this transporter have been identified. However, the results demonstrated by this thesis lay the groundwork for identification of inhibitors that take advantage of CAII interaction blockade or mimicking the effects of PKA phosphorylation on NBC3.

Bibliography

1. Busa, W.B. and R. Nuccitelli, *Metabolic regulation via intracellular pH*. Am J Physiol, 1984. 246(4 Pt 2): p. R409-38.
2. Gross, E., N. Abuladze, A. Pushkin, I. Kurtz, and C.U. Cotton, *The stoichiometry of the electrogenic sodium bicarbonate cotransporter pNBC1 in mouse pancreatic duct cells is 2 HCO_3^-:1 Na^+*. J Physiol, 2001. 531(Pt 2): p. 375-82.
3. Edmonds, B.T., J. Murray, and J. Condeelis, *pH regulation of the F-actin binding properties of Dictyostelium elongation factor 1 alpha*. J Biol Chem, 1995. 270(25): p. 15222-30.
4. Ritter, M., E. Woll, D. Haussinger, and F. Lang, *Effects of bradykinin on cell volume and intracellular pH in NIH 3T3 fibroblasts expressing the ras oncogene*. FEBS Lett, 1992. 307(3): p. 367-70.
5. Hao, W., Z. Luo, L. Zheng, K. Prasad, and E.M. Lafer, *AP180 and AP-2 interact directly in a complex that cooperatively assembles clathrin*. J Biol Chem, 1999. 274(32): p. 22785-94.
6. Joseph, D., O. Tirmizi, X.L. Zhang, E.D. Crandall, and R.L. Lubman, *Polarity of alveolar epithelial cell acid-base permeability*. Am J Physiol Lung Cell Mol Physiol, 2002. 282(4): p. L675-83.
7. Nosek, T.M., K.Y. Fender, and R.E. Godt, *It is diprotonated inorganic phosphate that depresses force in skinned skeletal muscle fibers*. Science, 1987. 236(4798): p. 191-3.
8. Sterling, D. and J.R. Casey, *Bicarbonate transport proteins*. Biochem Cell Biol, 2002. 80(5): p. 483-97.
9. Halestrap, A.P. and N.T. Price, *The proton-linked monocarboxylate transporter (MCT) family: structure, function and regulation*. Biochem. J., 1999. 343 Pt 2: p. 281-299.
10. Fliegel, L. and J.R.B. Dyck, *Molecular Biology of the cardiac sodium/hydrogen exchanger*. Card. Res., 1995. 29: p. 155-159.
11. Adrogue, H.E. and H.J. Adrogue, *Acid-base physiology*. Respir Care, 2001. 46(4): p. 328-41.
12. Seidler, U., H. Rossmann, P. Jacob, O. Bachmann, S. Christiani, G. Lamprecht, and M. Gregor, *Expression and function of $Na^+HCO_3^-$ cotransporters in the gastrointestinal tract*. Ann N Y Acad Sci, 2000. 915: p. 1-14.
13. Hug, M.J., T. Tamada, and R.J. Bridges, *CFTR and bicarbonate secretion by [correction of to] epithelial cells*. News Physiol Sci, 2003. 18: p. 38-42.
14. Ishiguro, H., S. Naruse, J.I. San Roman, M. Case, and M.C. Steward, *Pancreatic ductal bicarbonate secretion: past, present and future*. J of Pancreas, 2001. 2(4 Suppl): p. 192-7.
15. Soleimani, M., *Na^+:HCO_3^- cotransporters (NBC): expression and regulation in the kidney*. J Nephrol, 2002. 15 Suppl 5: p. S32-40.
16. Romero, M.F., *The electrogenic Na^+/HCO_3^- cotransporter, NBC*. J of Pancreas, 2001. 2(4 Suppl): p. 182-91.

17. Gross, E. and I. Kurtz, *Structural determinants and significance of regulation of electrogenic Na^+-HCO_3^- cotransporter stoichiometry*. Am J Physiol Renal Physiol, 2002. 283(5): p. F876-87.
18. Yip, K.P., S. Tsuruoka, G.J. Schwartz, and I. Kurtz, *Apical H^+/base transporters mediating bicarbonate absorption and pH_i regulation in the OMCD*. Am J Physiol Renal Physiol, 2002. 283(5): p. F1098-104.
19. Gross, E., A. Pushkin, N. Abuladze, O. Fedotoff, and I. Kurtz, *Regulation of the sodium bicarbonate cotransporter kNBC1 function: role of Asp^{986}, Asp^{988} and kNBC1-carbonic anhydrase II binding*. J Physiol, 2002. 544(Pt 3): p. 679-85.
20. Alper, S.L., J. Natale, S. Gluck, H.F. Lodish, and D. Brown, *Subtypes of intercalated cells in rat kidney collecting duct defined by antibodies against erythroid band 3 and renal vacuolar H^+-ATPase*. Proc Natl Acad Sci U S A, 1989. 86(14): p. 5429-33.
21. Alper, S.L., *Genetic diseases of acid-base transporters*. Annu Rev Physiol, 2002. 64: p. 899-923.
22. Laski, M.E. and N.A. Kurtzman, *Characterization of acidification in the cortical and medullary collecting tubule of the rabbit*. J Clin Invest, 1983. 72(6): p. 2050-9.
23. Lee, M.G., W. Ahn, J.A. Lee, J.Y. Kim, J.Y. Choi, O.W. Moe, S.L. Milgram, S. Muallem, and K.H. Kim, *Coordination of pancreatic HCO_3^- secretion by protein-protein interaction between membrane transporters*. J o P, 2001. 2(4 Suppl): p. 203-6.
24. Romero, M.F., P. Fong, U.V. Berger, M.A. Hediger, and W.F. Boron, *Cloning and functional expression of rNBC, an electrogenic Na^+-HCO_3^- cotransporter from rat kidney*. Am. J. Physiol., 1998. 274(2 Pt 2): p. F425-32.
25. Kopito, R.R. and H.F. Lodish, *Primary structure and transmembrane orientation of the murine anion exchange protein*. Nature, 1985. 316: p. 234-238.
26. Alper, S.L., R.R. Kopito, S.M. Libresco, and H.F. Lodish, *Cloning and characterization of a murine Band 3-related cDNA from kidney and a lymphoid cell line*. J. Biol. Chem., 1988. 263: p. 17092-17099.
27. Kudrycki, K.E., P.R. Newman, and G.E. Shull, *cDNA cloning and tissue distribution of mRNAs for two proteins that are related to the Band 3 Cl^-/HCO_3^- exchanger*. J. Biol. Chem., 1990. 265: p. 462-471.
28. Burnham, C.E., H. Amlal, Z. Wang, G.E. Shull, and M. Soleimani, *Cloning and functional expression of a human kidney Na^+:HCO_3^- cotransporter*. J. Biol. Chem., 1997. 272(31): p. 19111-4.
29. Romero, M.F., M.A. Hediger, E.L. Boulpaep, and W.F. Boron, *Expression cloning and characterization of a renal electrogenic Na^+/HCO_3^- cotransporter*. Nature, 1997. 387(6631): p. 409-13.
30. Abuladze, N., I. Lee, D. Newman, J. Hwang, K. Boorer, A. Pushkin, and I. Kurtz, *Molecular cloning, chromosomal localization, tissue distribution, and functional expression of the human pancreatic sodium bicarbonate cotransporter*. J. Biol. Chem., 1998. 273(28): p. 17689-17695.
31. Bevensee, M.O., B.M. Schmitt, I. Choi, M.F. Romero, and W.F. Boron, *An electrogenic Na^+-HCO_3^- cotransporter (NBC) with a novel COOH-terminus, cloned from rat brain*. Am. J. Physiol., 2000. 278(6): p. C1200-C1211.

32. Choi, I., M.F. Romero, N. Khandoudi, A. Bril, and W.F. Boron, *Cloning and characterization of a human electrogenic Na^+-HCO_3^- cotransporter isoform (hhNBC).* Am. J. Physiol., 1999. 276(3 Pt 1): p. C576-584.
33. Choi, I., C. Aalkjaer, E.L. Boulpaep, and W.F. Boron, *An electroneutral sodium/bicarbonate cotransporter NBCn1 and associated sodium channel.* Nature, 2000. 405(6786): p. 571-5.
34. Ishibashi, K., S. Sasaki, and F. Marumo, *Molecular cloning of a new sodium bicarbonate cotransporter cDNA from human retina.* Biochem. Biophys. Res. Commun., 1998. 246(2): p. 535-538.
35. Pushkin, A., N. Abuladze, I. Lee, D. Newman, J. Hwang, and I. Kurtz, *Cloning, tissue distribution, genomic organization, and functional characterization of NBC3, a new member of the sodium bicarbonate cotransporter family.* J. Biol. Chem., 1999. 274(23): p. 16569-16575.
36. Pushkin, A., N. Abuladze, D. Newman, I. Lee, G. Xu, and I. Kurtz, *Cloning, characterization and chromosomal assignment of NBC4, a new member of the sodium bicarbonate cotransporter family.* Biochim Biophys Acta, 2000. 1493(1-2): p. 215-8.
37. Sassani, P., A. Pushkin, E. Gross, A. Gomer, N. Abuladze, R. Dukkipati, G. Carpenito, and I. Kurtz, *Functional characterization of NBC4: a new electrogenic sodium-bicarbonate cotransporter.* Am J Physiol Cell Physiol, 2002. 282(2): p. C408-16.
38. Virkki, L.V., D.A. Wilson, R.D. Vaughan-Jones, and W.F. Boron, *Functional characterization of human NBC4 as an electrogenic Na^+-HCO_3^- cotransporter (NBCe2).* Am J Physiol Cell Physiol, 2002. 282(6): p. C1278-89.
39. Xu, J., Z. Wang, S. Barone, M. Petrovic, H. Amlal, L. Conforti, S. Petrovic, and M. Soleimani, *Expression of the Na^+-HCO_3^- cotransporter NBC4 in rat kidney and characterization of a novel NBC4 variant.* Am J Physiol Renal Physiol, 2003. 284(1): p. F41-50.
40. Parker, M.D., E.P. Ourmozdi, and M.J. Tanner, *Human BTR1, a new bicarbonate transporter superfamily member and human AE4 from kidney.* Biochem Biophys Res Commun, 2001. 282(5): p. 1103-9.
41. Tsuganezawa, H., K. Kobayashi, M. Iyori, T. Araki, A. Koizumi, S.I. Watanabe, A. Kaneko, T. Fukao, T. Monkawa, T. Yoshida, D.K. Kim, Y. Kanai, H. Endou, M. Hayashi, and T. Saruta, *A new member of the HCO3- transporter superfamily is an apical anion exchanger of beta-intercalated cells in the kidney.* J Biol Chem, 2000. 1: p. 1.
42. Grichtchenko, II, M.F. Romero, and W.F. Boron, *Extracellular HCO_3^- dependence of electrogenic Na^+/HCO_3^- cotransporters cloned from salamander and rat kidney.* J Gen Physiol, 2000. 115(5): p. 533-46.
43. Romero, M.F., D. Henry, S. Nelson, P.J. Harte, A.K. Dillon, and C.M. Sciortino, *Cloning and characterization of a Na^+ driven anion exchanger (NDAE1): a new bicarbonate transporter.* J. Biol. Chem., 2000. 275(32): p. 24552-9.
44. Wang, C.Z. H. Yano, K. Nagashima, and S. Seino, *The Na^+-driven Cl^-/HCO_3^- exchanger: Cloning, tissue distribution, and functional characterization.* J Biol Chem, 2000.
45. Melvin, J.E., K. Park, L. Richardson, P.J. Schultheis, and G.E. Shull, *Mouse down-regulated in adenoma (DRA) is an intestinal Cl^-/HCO_3^- exchanger and is*

up-regulated in colon of mice lacking the NHE3 Na^+/H^+ exchanger. J. Biol. Chem., 1999. 274(32): p. 22855-22861.

46. Schweinfest, C.W., K.W. Henderson, S. Suster, N. Kondoh, and T.S. Papas, *Identification of a colon mucosa gene that is down-regulated in colon adenomas and adenocarcinomas*. Proc. Natl. Acad. Sci., 1993. 90(9): p. 4166-4170.
47. Soleimani, M., T. Greeley, S. Petrovic, Z. Wang, H. Amlal, P. Kopp, and C.E. Burnham, *Pendrin: an apical $Cl^-/OH^-/HCO_3^-$ exchanger in the kidney cortex*. Am J Physiol Renal Physiol, 2001. 280(2): p. F356-64.
48. Scott, D.A., R. Wang, T.M. Kreman, V.C. Sheffield, and L.P. Karnishki, *The Pendred syndrome gene encodes a chloride-iodide transport protein*. Nat Genet, 1999. 21(4): p. 440-3.
49. Xie, Q., R. Welch, A. Mercado, M.F. Romero, and D.B. Mount, *Molecular characterization of the murine Slc26a6 anion exchanger: functional comparison with Slc26a1*. Am J Physiol Renal Physiol, 2002. 283(4): p. F826-38.
50. Wang, Z., S. Petrovic, E. Mann, and M. Soleimani, *Identification of an apical Cl^-/HCO_3^- exchanger in the small intestine*. Am J Physiol Gastrointest Liver Physiol, 2002. 282(3): p. G573-9.
51. Waldegger, S., I. Moschen, A. Ramirez, R.J. Smith, H. Ayadi, F. Lang, and C. Kubisch, *Cloning and characterization of SLC26A6, a novel member of the solute carrier 26 gene family*. Genomics, 2001. 72(1): p. 43-50.
52. Lohi, H., M. Kujala, S. Makela, E. Lehtonen, M. Kestila, U. Saarialho-Kere, D. Markovich, and J. Kere, *Functional characterization of three novel tissue-specific anion exchangers SLC26A7, -A8, and -A9*. J Biol Chem, 2002. 277(16): p. 14246-54.
53. Vincourt, J.B., D. Jullien, S. Kossida, F. Amalric, and J.P. Girard, *Molecular cloning of SLC26A7, a novel member of the SLC26 sulfate/anion transporter family, from high endothelial venules and kidney*. Genomics, 2002. 79(2): p. 249-56.
54. Toure, A., L. Morin, C. Pineau, F. Becq, O. Dorseuil, and G. Gacon, *Tat1, a novel sulfate transporter specifically expressed in human male germ cells and potentially linked to rhogtpase signaling*. J Biol Chem, 2001. 276(23): p. 20309-15.
55. Burnham, C.E., M. Flagella, Z. Wang, H. Amlal, G.E. Shull, and M. Soleimani, *Cloning, renal distribution, and regulation of the rat Na^+-HCO_3^- cotransporter*. Am. J. Physiol., 1998. 274(6 Pt 2): p. F1119-26.
56. Thevenod, F., E. Roussa, B.M. Schmitt, and M.F. Romero, *Cloning and immunolocalization of a rat pancreatic Na^+ bicarbonate cotransporter*. Biochem. Biophys. Res. Commun., 1999. 264(1): p. 291-8.
57. Abuladze, N., M. Song, A. Pushkin, D. Newman, I. Lee, S. Nicholas, and I. Kurtz, *Structural organization of the human NBC1 gene: kNBC1 is transcribed from an alternative promoter in intron 3*. Gene, 2000. 251(2): p. 109-122.
58. Jensen, L.J., B.M. Schmitt, U.V. Berger, N.N. Nsumu, W.F. Boron, M.A. Hediger, D. Brown, and S. Breton, *Localization of sodium bicarbonate cotransporter (NBC) protein and messenger ribonucleic acid in rat epididymis*. Biol Reprod, 1999. 60(3): p. 573-9.

59. Schmitt, B.M., D. Biemesderfer, M.F. Romero, E.L. Boulpaep, and W.F. Boron, *Immunolocalization of the electrogenic Na^+-HCO_3^- cotransporter in mammalian and amphibian kidney*. Am J Physiol, 1999. 276(1 Pt 2): p. F27-38.
60. Schmitt, B.M., U.V. Berger, R.M. Douglas, M.O. Bevensee, M.A. Hediger, G.G. Haddad, and W.F. Boron, *Na^+/HCO_3^- cotransporters in rat brain: expression in glia, neurons, and choroid plexus*. J Neurosci, 2000. 20(18): p. 6839-48.
61. Marino, C.R., V. Jeanes, W.F. Boron, and B.M. Schmitt, *Expression and distribution of the Na^+-HCO_3^- cotransporter in human pancreas*. Am. J. Physiol., 1999. 277(2 Pt 1): p. G487-94.
62. Roussa, E., M.F. Romero, B.M. Schmitt, W.F. Boron, S.L. Alper, and F. Thevenod, *Immunolocalization of anion exchanger AE2 and Na^+-HCO_3^- cotransporter in rat parotid and submandibular glands*. Am J Physiol, 1999. 277(6 Pt 1): p. G1288-96.
63. Rossmann, H., O. Bachmann, D. Vieillard-Baron, M. Gregor, and U. Seidler, *Na^+/HCO_3- cotransport and expression of NBC1 and NBC2 in rabbit gastric parietal and mucous cells*. Gastroenterology, 1999. 116(6): p. 1389-1398.
64. Maunsbach, A.B., H. Vorum, T.H. Kwon, S. Nielsen, B. Simonsen, I. Choi, B.M. Schmitt, W.F. Boron, and C. Aalkjaer, *Immunoelectron microscopic localization of the electrogenic Na^+/HCO_3^- cotransporter in rat and ambystoma kidney*. J Am Soc Nephrol, 2000. 11(12): p. 2179-89.
65. Sun, X.C., J.A. Bonanno, S. Jelamskii, and Q. Xie, *Expression and localization of Na^+/HCO_3^- cotransporter in bovine corneal endothelium*. Am J Physiol Cell Physiol, 2000. 279(5): p. C1648-55.
66. Bok, D., M.J. Schibler, A. Pushkin, P. Sassani, N. Abuladze, Z. Naser, and I. Kurtz, *Immunolocalization of electrogenic sodium-bicarbonate cotransporters pNBC1 and kNBC1 in the rat eye*. Am J Physiol Renal Physiol, 2001. 281(5): p. F920-35.
67. Douglas, R.M., B.M. Schmitt, Y. Xia, M.O. Bevensee, D. Biemesderfer, W.F. Boron, and G.G. Haddad, *Sodium-hydrogen exchangers and sodium-bicarbonate co-transporters: ontogeny of protein expression in the rat brain*. Neuroscience, 2001. 102(1): p. 217-28.
68. Roussa, E., *H^+ and HCO_3^- transporters in human salivary ducts. An immunohistochemical study*. Histochem J, 2001. 33(6): p. 337-44.
69. Park, K., P.T. Hurley, E. Roussa, G.J. Cooper, C.P. Smith, F. Thevenod, M.C. Steward, and R.M. Case, *Expression of a sodium bicarbonate cotransporter in human parotid salivary glands*. Arch Oral Biol, 2002. 47(1): p. 1-9.
70. Abuladze, N., I. Lee, D. Newman, J. Hwang, A. Pushkin, and I. Kurtz, *Axial heterogeneity of sodium-bicarbonate cotransporter expression in the rabbit proximal tubule*. Am J Physiol, 1998. 274(3 Pt 2): p. F628-33.
71. Soleimani, M. and C.E. Burnham, *Physiologic and molecular aspects of the Na^+:HCO_3^- cotransporter in health and disease processes*. Kidney Int., 2000. 57(2): p. 371-84.
72. Lopes, A.G., A.W. Siebens, G. Giebisch, and W.F. Boron, *Electrogenic Na^+/HCO_3^- cotransport across basolateral membrane of isolated perfused Necturus proximal tubule*. Am J Physiol, 1987. 253(2 Pt 2): p. F340-50.

73. Soleimani, M. and P.S. Aronson, *Ionic mechanism of Na^+-HCO_3^- cotransport in rabbit renal basolateral membrane vesicles.* J Biol Chem, 1989. 264(31): p. 18302-8.
74. Soleimani, M., S.M. Grassi, and P.S. Aronson, *Stoichiometry of Na^+-HCO_3^- cotransport in basolateral membrane vesicles isolated from rabbit renal cortex.* J Clin Invest, 1987. 79(4): p. 1276-80.
75. Gross, E. and U. Hopfer, *Activity and stoichiometry of Na^+:HCO_3^- cotransport in immortalized renal proximal tubule cells.* J Membr Biol, 1996. 152(3): p. 245-52.
76. Sciortino, C.M. and M.F. Romero, *Cation and voltage dependence of rat kidney electrogenic Na^+-HCO_3^- cotransporter, rkNBC, expressed in oocytes.* Am. J. Physiol., 1999. 277(4 Pt 2): p. F611-23.
77. Gross, E., K. Hawkins, N. Abuladze, A. Pushkin, C.U. Cotton, U. Hopfer, and I. Kurtz, *The stoichiometry of the electrogenic sodium bicarbonate cotransporter NBC1 is cell-type dependent.* J Physiol, 2001. 531(Pt 3): p. 597-603.
78. Bernardo, A.A., F.T. Kear, A.V. Santos, J. Ma, D. Steplock, R.B. Robey, and E.J. Weinman, *Basolateral Na^+/HCO_3^- cotransport activity is regulated by the dissociable Na^+/H^+ exchanger regulatory factor.* J. Clin. Invest., 1999. 104(2): p. 195-201.
79. Steagall, W.K., T.J. Kelley, R.J. Marsick, and M.L. Drumm, *Type II protein kinase A regulates CFTR in airway, pancreatic, and intestinal cells.* Am J Physiol, 1998. 274(3 Pt 1): p. C819-26.
80. Sterling, D., R.A. Reithmeier, and J.R. Casey, *A transport metabolon: Functional interaction of carbonic anhydrase II and chloride/bicarbonate exchangers.* J Biol Chem, 2001. 17: p. 17.
81. Alvarez, B.V., F.B. Loiselle, C.T. Supuran, G.J. Schwartz, and J.R. Casey, *Direct extracellular interaction between carbonic anhydrase IV and the human NBC1 sodium/bicarbonate co-transporter.* Biochemistry, 2003. 42(42): p. 12321-9.
82. Amlal, H., Q. Chen, T. Greeley, L. Pavelic, and M. Soleimani, *Coordinated down-regulation of NBC-1 and NHE-3 in sodium and bicarbonate loading.* Kidney Int, 2001. 60(5): p. 1824-36.
83. Ruiz, O.S., R.B. Robey, Y.Y. Qiu, L.J. Wang, C.J. Li, J. Ma, and J.A. Arruda, *Regulation of the renal Na^+-HCO_3^- cotransporter. XI. Signal transduction underlying CO_2 stimulation.* Am J Physiol, 1999. 277(4 Pt 2): p. F580-6.
84. Amlal, H., C.E. Burnham, and M. Soleimani, *Characterization of Na^+/HCO_3^- cotransporter isoform NBC-3 [published erratum appears in Am J Physiol 1999 Sep;277(3 Pt 2):following table of contents].* Am J Physiol, 1999. 276(6 Pt 2): p. F903-13.
85. Robey, R.B., O.S. Ruiz, J. Baniqued, D. Mahmud, D.J. Espiritu, A.A. Bernardo, and J.A. Arruda, *SFKs, Ras, and the classic MAPK pathway couple muscarinic receptor activation to increased Na^+-HCO_3^- cotransport activity in renal epithelial cells.* Am J Physiol Renal Physiol, 2001. 280(5): p. F844-50.
86. Sandmann, S., M. Yu, E. Kaschina, A. Blume, E. Bouzinova, C. Aalkjaer, and T. Unger, *Differential effects of angiotensin AT1 and AT2 receptors on the expression, translation and function of the Na^+-H^+ exchanger and Na^+-HCO_3^- symporter in the rat heart after myocardial infarction.* J Am Coll Cardiol, 2001. 37(8): p. 2154-65.

87. Takeda, M., K. Yoshitomi, and M. Imai, *Regulation of Na^+-3HCO_3^- cotransport in rabbit proximal convoluted tubule via adenosine A1 receptor*. Am J Physiol, 1993. 265(4 Pt 2): p. F511-9.
88. Geibel, J., G. Giebisch, and W.F. Boron, *Angiotensin II stimulates both Na^+-H^+ exchange and Na^+/HCO_3^- cotransport in the rabbit proximal tubule*. Proc. Natl. Acad. Sci., 1990. 87(20): p. 7917-7920.
89. Soleimani, M., Y.J. Hattabaugh, and G.L. Bizal, *Acute regulation of Na^+/H^+ exchange, Na^+:HCO_3^- cotransport, and Cl^-/base exchange in acid base disorders*. J Lab Clin Med, 1994. 124(1): p. 69-78.
90. Gross, E. and U. Hopfer, *Effects of pH on kinetic parameters of the Na^+/HCO_3^- cotransporter in renal proximal tubule*. Biophys. J., 1999. 76(6): p. 3066-3075.
91. Cha, B., S. Oh, J. Shanmugaratnam, M. Donowitz, and C.C. Yun, *Two Histidine Residues in the Juxta-Membrane Cytoplasmic Domain of Na^+/H^+ Exchanger Isoform 3 (NHE3) Determine the Set Point*. J Membr Biol, 2003. 191(1): p. 49-58.
92. Ruiz, O.S., Y.Y. Qiu, L.J. Wang, L.R. Cardoso, and J.A. Arruda, *Regulation of renal Na^+-HCO_3^+ cotransporter: VIII. Mechanism of stimulatory effect of respiratory acidosis*. J Membr Biol, 1998. 162(3): p. 201-8.
93. Robey, R.B., O.S. Ruiz, D.J. Espiritu, V.C. Ibanez, F.T. Kear, O.A. Noboa, A.A. Bernardo, and J.A. Arruda, *Angiotensin II stimulation of renal epithelial cell Na^+/HCO_3^- cotransport activity: a central role for Src family kinase/classic MAPK pathway coupling*. J Membr Biol, 2002. 187(2): p. 135-45.
94. Horita, S., Y. Zheng, C. Hara, H. Yamada, M. Kunimi, S. Taniguchi, S. Uwatoko, T. Sugaya, A. Goto, T. Fujita, and G. Seki, *Biphasic regulation of Na^+-HCO_3^- cotransporter by angiotensin II type 1A receptor*. Hypertension, 2002. 40(5): p. 707-12.
95. Baetz, D., R.S. Haworth, M. Avkiran, and D. Feuvray, *The ERK pathway regulates Na^+-HCO_3^- cotransport activity in adult rat cardiomyocytes*. Am J Physiol Heart Circ Physiol, 2002. 283(5): p. H2102-9.
96. Espiritu, D.J., A.A. Bernardo, R.B. Robey, and J.A. Arruda, *A central role for Pyk2-Src interaction in coupling diverse stimuli to increased epithelial NBC activity*. Am J Physiol Renal Physiol, 2002. 283(4): p. F663-70.
97. Ruiz, O.S., Y.Y. Qiu, L.R. Cardoso, and J.A. Arruda, *Regulation of the renal Na^+-HCO_3^- cotransporter: IX. Modulation by insulin, epidermal growth factor and carbachol*. Regul Pept, 1998. 77(1-3): p. 155-61.
98. Ali, R., H. Amlal, C.E. Burnham, and M. Soleimani, *Glucocorticoids enhance the expression of the basolateral Na^+:HCO_3^- cotransporter in renal proximal tubules*. Kidney Int, 2000. 57(3): p. 1063-71.
99. Alvaro, D., A. Gigliozzi, L. Marucci, G. Alpini, B. Barbaro, R. Monterubbianesi, L. Minetola, M.G. Mancino, J.F. Medina, A.F. Attili, and A. Benedetti, *Corticosteroids modulate the secretory processes of the rat intrahepatic biliary epithelium*. Gastroenterology, 2002. 122(4): p. 1058-69.
100. Amlal, H., K. Habo, and M. Soleimani, *Potassium deprivation upregulates expression of renal basolateral Na^+-HCO_3^- cotransporter (NBC-1)*. Am J Physiol Renal Physiol, 2000. 279(3): p. F532-43.
101. Ruiz, O.S., Y.Y. Qiu, L.J. Wang, and J.A. Arruda, *Regulation of the renal Na^+-HCO_3^- cotransporter: V. mechanism of the inhibitory effect of parathyroid hormone*. Kidney Int, 1996. 49(2): p. 396-402.

102. Ruiz, O.S. and J.A. Arruda, *Regulation of the renal Na^+-HCO_3^- cotransporter by cAMP and Ca-dependent protein kinases*. Am J Physiol, 1992. 262(4 Pt 2): p. F560-5.
103. Pushkin, A., N. Abuladze, D. Newman, I. Lee, G. Xu, and I. Kurtz, *Two C-terminal variants of NBC4, a new member of the sodium bicarbonate cotransporter family: cloning, characterization, and localization*. IUBMB Life, 2000. 50(1): p. 13-9.
104. Tang, X.B., J. Fujinaga, R. Kopito, and J.R. Casey, *Topology of the region surrounding Glu681 of human AE1 protein, the erythrocyte anion exchanger*. J. Biol. Chem., 1998. 273(35): p. 22545-22553.
105. Fujinaga, J., X.-B. Tang, and J.R. Casey, *Topology of the membrane domain of human anion exchange protein, AE1. J. Biol. Chem.*, 1999. 274: p. 6626-6633.
106. Zhu, Q., Lee, D. W. K. and Casey, J. R., *Novel topology in C-terminal region of the human plasma membrane anion exchanger, AE1*. J. Biol Chem, 2003. 278: p. 3112-3120.
107. Tatishchev, S., N. Abuladze, A. Pushkin, D. Newman, W. Liu, D. Weeks, G. Sachs, and I. Kurtz, *Identification of membrane topography of the electrogenic sodium bicarbonate cotransporter pNBC1 by in vitro transcription/translation*. Biochemistry, 2003. 42(3): p. 755-65.
108. Aickin, C.C., *Regulation of intracellular pH in smooth muscle cells of the guinea-pig femoral artery*. J Physiol (Lond), 1994. 479(Pt 2): p. 331-40.
109. Aalkjaer, C. and E.J. Cragoe, Jr., *Intracellular pH regulation in resting and contracting segments of rat mesenteric resistance vessels*. J Physiol, 1988. 402: p. 391-410.
110. Aalkjaer, C. and A. Hughes, *Chloride and bicarbonate transport in rat resistance arteries*. J Physiol, 1991. 436: p. 57-73.
111. Kwon, T.H., A. Pushkin, N. Abuladze, S. Nielsen, and I. Kurtz, *Immunoelectron microscopic localization of NBC3 sodium-bicarbonate cotransporter in rat kidney*. Am. J. Physiol. Renal Physiol., 2000. 278(2): p. F327-36.
112. Park, M., S.B. Ko, J.Y. Choi, G. Muallem, P.J. Thomas, A. Pushkin, M.S. Lee, J.Y. Kim, M.G. Lee, S. Muallem, and I. Kurtz, *The cystic fibrosis transmembrane conductance regulator interacts with and regulates the activity of the HCO_3^- salvage transporter human Na^+-HCO_3^- cotransport isoform 3*. J Biol Chem, 2002. 277(52): p. 50503-9.
113. Loiselle, F.B., P. Jaschke, and J.R. Casey, *Structural and functional characterization of the human NBC3 sodium/bicarbonate co-transporter carboxyl-terminal cytoplasmic domain*. Mol Membr Biol, 2003. 20(4): p. 307-17.
114. Pushkin, A., K.P. Yip, I. Clark, N. Abuladze, T.H. Kwon, S. Tsuruoka, G.J. Schwartz, S. Nielsen, and I. Kurtz, *NBC3 expression in rabbit collecting duct: colocalization with vacuolar H^+-ATPase*. Am. J. Physiol., 1999. 277(6 Pt 2): p. F974-981.
115. Gluck, S.L., D.M. Underhill, M. Iyori, L.S. Holliday, T.Y. Kostrominova, and B.S. Lee, *Physiology and biochemistry of the kidney vacuolar H^+-ATPase*. Annu Rev Physiol, 1996. 58: p. 427-45.
116. Stevens, T.H. and M. Forgac, *Structure, function and regulation of the vacuolar H^+-ATPase*. Annu Rev Cell Dev Biol, 1997. 13: p. 779-808.

117. Milton, A.E. and I.D. Weiner, *Intracellular pH regulation in the rabbit cortical collecting duct A-type intercalated cell*. Am J Physiol, 1997. 273(3 Pt 2): p. F340-7.
118. Gresz, V., T.H. Kwon, H. Vorum, T. Zelles, I. Kurtz, M.C. Steward, C. Aalkjaer, and S. Nielsen, *Immunolocalization of electroneutral Na^+-HCO_3^- cotransporters in human and rat salivary glands*. Am J Physiol Gastrointest Liver Physiol, 2002. 283(2): p. G473-80.
119. Vorum, H., T.H. Kwon, C. Fulton, B. Simonsen, I. Choi, W. Boron, A.B. Maunsbach, S. Nielsen, and C. Aalkjaer, *Immunolocalization of electroneutral Na^+-HCO_3^- cotransporter in rat kidney*. Am J Physiol Renal Physiol, 2000. 279(5): p. F901-9.
120. Brylawski, B., http://www3.ncbi.nlm.nih.gov/Omim/. 2000.
121. Igarashi, T., J. Inatomi, T. Sekine, S.H. Cha, Y. Kanai, M. Kunimi, K. Tsukamoto, H. Satoh, M. Shimadzu, F. Tozawa, T. Mori, M. Shiobara, G. Seki, and H. Endou, *Mutations in SLC4A4 cause permanent isolated proximal renal tubular acidosis with ocular abnormalities*. Nat. Genet., 1999. 23(3): p. 264-266.
122. Ahmad, H., A.S. Tobola, A. Silva, and R. Castillo, *Glutathione S-transferase of goat lens: evidence for expression of only class mu isoenzymes*. Curr Eye Res, 1998. 17(11): p. 1097-101.
123. Olson, T.M. and M.T. Keating, *Mapping a cardiomyopathy locus to chromosome 3p22-p25*. J Clin Invest, 1996. 97(2): p. 528-32.
124. Bok, D., G. Galbraith, I. Lopez, M. Woodruff, S. Nusinowitz, H. BeltrandelRio, W. Huang, S. Zhao, R. Geske, C. Montgomery, I. Van Sligtenhorst, C. Friddle, K. Platt, M.J. Sparks, A. Pushkin, N. Abuladze, A. Ishiyama, R. Dukkipati, W. Liu, and I. Kurtz, *Blindness and auditory impairment caused by loss of the sodium bicarbonate cotransporter NBC3*. Nat Genet, 2003. 34(3): p. 313-9.
125. Sterling, D., R.A. Reithmeier, and J.R. Casey, *Carbonic anhydrase: in the driver's seat for bicarbonate transport*. J. of Pancreas, 2001. 2(4 Suppl): p. 165-70.
126. Supuran, C.T., A. Scozzafava, and A. Casini, *Carbonic anhydrase inhibitors*. Med Res Rev, 2003. 23(2): p. 146-89.
127. Pastorek, J., S. Pastorekova, I. Callebaut, J.P. Mornon, V. Zelnik, R. Opavsky, M. Zat'ovicova, S. Liao, D. Portetelle, E.J. Stanbridge, and et al., *Cloning and characterization of MN, a human tumor-associated protein with a domain homologous to carbonic anhydrase and a putative helix-loop-helix DNA binding segment*. Oncogene, 1994. 9(10): p. 2877-88.
128. Sly, W.S. and P.Y. hu, *Human carbonic anhydrases and carbonic anhydrase deficiencies*. Annu. Rev. Biochem., 1995. 64: p. 375-401.
129. Tureci, O., U. Sahin, E. Vollmar, S. Siemer, E. Gottert, G. Seitz, A.K. Parkkila, G.N. Shah, J.H. Grubb, M. Pfreundschuh, and W.S. Sly, *Human carbonic anhydrase XII: cDNA cloning, expression, and chromosomal localization of a carbonic anhydrase gene that is overexpressed in some renal cell cancers*. Proc Natl Acad Sci U S A, 1998. 95(13): p. 7608-13.
130. Zavada, J., Z. Zavadova, S. Pastorekova, F. Ciampor, J. Pastorek, and V. Zelnik, *Expression of MaTu-MN protein in human tumor cultures and in clinical specimens*. Int J Cancer, 1993. 54(2): p. 268-74.
131. Siffert, W. and G. Gros, *Carbonic anhydrase C in white-skeletal-muscle tissue*. Biochem J, 1982. 205(3): p. 559-66.

132. Breton, S., *The cellular physiology of carbonic anhydrases*. Jop, 2001. 2(4 Suppl): p. 159-64.
133. Noda, Y., Y. Takai, Y. Iwai, M.A. Meenaghan, and M. Mori, *Immunohistochemical study of carbonic anhydrase in mixed tumours from major salivary glands and skin*. Virchows Arch A Pathol Anat Histopathol, 1986. 408(5): p. 449-59.
134. Vince, J.W. and R.A.F. Reithmeier, *Carbonic anhydrase II binds to the carboxyl-terminus of human band 3, the erythrocyte Cl/HCO_3 exchanger*. J. Biol. Chem, 1998. 273(43): p. 28430-7.
135. Carter, N.D., A. Fryer, A.G. Grant, R. Hume, R.G. Strange, and P.J. Wistrand, *Membrane specific carbonic anhydrase (CAIV) expression in human tissues*. Biochim Biophys Acta, 1990. 1026(1): p. 113-6.
136. Sterling, D., B.V. Alvarez, and J.R. Casey, *The extracellular component of a transport metabolon. Extracellular loop 4 of the human AE1 Cl/HCO_3 exchanger binds carbonic anhydrase IV*. J Biol Chem, 2002. 277(28): p. 25239-46.
137. Wang, C.C., R. Moriyama, C.R. Lombardo, and P.S. Low, *Partial characterization of the cytoplasmic domain of human kidney band 3*. J. Biol. Chem., 1995. 270(30): p. 17892-17897.
138. Zhang, D., A. Kiyatkin, J.T. Bolin, and P.S. Low, *Crystallographic structure and functional interpretation of the cytoplasmic domain of erythrocyte membrane band 3*. Blood, 2000. 96(9): p. 2925-33.
139. Chang, S.H. and P.S. Low, *Identification of a critical ankyrin-binding loop on the cytoplasmic domain of erythrocyte membrane band 3 by crystal structure analysis and site-directed mutagenesis*. J Biol Chem, 2003. 278(9): p. 6879-84.
140. Cohen, C.M., E. Dotimas, and C. Korsgren, *Human erythrocyte membrane protein band 4.2 (pallidin)*. Semin Hematol, 1993. 30(2): p. 119-37.
141. An, X.L., Y. Takakuwa, W. Nunomura, S. Manno, and N. Mohandas, *Modulation of band 3-ankyrin interaction by protein 4.1. Functional implications in regulation of erythrocyte membrane mechanical properties*. J Biol Chem, 1996. 271(52): p. 33187-91.
142. Rybicki, A.C., R.S. Schwartz, E.J. Hustedt, and C.E. Cobb, *Increased rotational mobility and extractability of band 3 from protein 4.2-deficient erythrocyte membranes: evidence of a role for protein 4.2 in strengthening the band 3-cytoskeleton linkage*. Blood, 1996. 88(7): p. 2745-53.
143. Pasternack, G.R., R.A. Anderson, T.L. Leto, and V.T. Marchesi, *Interactions between protein 4.1 and band 3. An alternative binding site for an element of the membrane skeleton*. J Biol Chem, 1985. 260(6): p. 3676-83.
144. Rogalski, A.A., T.L. Steck, and A. Waseem, *Association of glyceraldehyde-3-phosphate dehydrogenase with the plasma membrane of the intact human red blood cell*. J Biol Chem, 1989. 264(11): p. 6438-46.
145. Jenkins, J.D., D.P. Madden, and T.L. Steck, *Association of phosphofructokinase and aldolase with the membrane of the intact erythrocyte*. J Biol Chem, 1984. 259(15): p. 9374-8.
146. Murthy, S.N., T. Liu, R.K. Kaul, H. Kohler, and T.L. Steck, *The aldolase-binding site of the human erythrocyte membrane is at the NH_2 terminus of band 3*. J Biol Chem, 1981. 256(21): p. 11203-8.

147. Walder, J.A., R. Chatterjee, T.L. Steck, P.S. Low, G.F. Musso, E.T. Kaiser, P.H. Rogers, and A. Arnone, *The interaction of hemoglobin with the cytoplasmic domain of Band 3 of the human erythrocyte membrane*. J. Biol. Chem., 1984. 259: p. 10238-10246.
148. Salhany, J.M. and R.L. Sloan, *Direct evidence for modulation of porter quaternary structure by transport site ligands*. Biochem. Biophys. Res. Comm., 1989. 159(3): p. 1337-1344.
149. Waugh, S.M. and P.S. Low, *Hemichrome binding to Band 3: nucleation of Heinz bodies on the erythrocyte membrane*. Biochem., 1985. 24: p. 34-39.
150. Harrison, M.L., C.C. Isaacson, D.L. Burg, R.L. Geahlen, and P.S. Low, *Phosphorylation of human erythrocyte band 3 by endogenous $P72^{syk}$*. J. Biol. Chem., 1994. 269: p. 955-959.
151. Sibanda, B.L., T.L. Blundell, and J.M. Thornton, *Conformation of beta-hairpins in protein structures. A systematic classification with applications to modelling by homology, electron density fitting and protein engineering*. J Mol Biol, 1989. 206(4): p. 759-77.
152. Kollert-Jons, A., S. Wagner, S. Hubner, H. Appelhans, and D. Drenckhahn, *Anion exchanger 1 in human kidney and oncocytoma differs from erythroid AE1 in its NH2 terminus*. Am J Physiol, 1993. 265(6 Pt 2): p. F813-21.
153. Ding, Y., J.R. Casey, and R.R. Kopito, *The major kidney AE1 isoform does not bind ankyrin (Ank1) in vitro. An essential role for the 79 NH_2-terminal amino acid residues of band 3*. J. Biol. Chem., 1994. 269(51): p. 32201-8.
154. Alper, S.L., M.N. Chernova, and A.K. Stewart, *Regulation of Na^+-independent Cl^-/HCO_3^- exchangers by pH*. J. of Pancreas, 2001. 2(4 Suppl): p. 171-5.
155. Humphreys, B.D., L. Jiang, M.N. Chernova, and S.L. Alper, *Functional characterization and regulation by pH of murine AE2 anion exchanger expressed in Xenopus oocytes*. Am. J. Physiol. Cell Physiol., 1994. 267: p. C1295-1307.
156. Humphreys, B.D., M.N. Chernova, L. Jiang, Y. Zhang, and S.L. Alper, *NH_4Cl activates AE2 anion exchanger in Xenopus oocytes at acidic pH_i*. Am J Physiol, 1997. 272(4 Pt 1): p. C1232-40.
157. Humphreys, B.D., L. Jiang, M.N. Chernova, and S.L. Alper, *Hypertonic activation of AE2 anion exchanger in Xenopus oocytes via NHE-mediated intracellular alkalinization*. Am J Physiol, 1995. 268(1 Pt 1): p. C201-9.
158. Jiang, T. and S.F. Steinberg, *Beta 2-adrenergic receptors enhance contractility by stimulating HCO_3^--dependent intracellular alkalinization*. Am J Physiol, 1997. 273(2 Pt 2): p. H1044-7.
159. Orlowski, J. and S. Grinstein, *Na^+/H^+ exchangers of mammalian cells*. J Biol Chem, 1997. 272(36): p. 22373-6.
160. Allen, D.G. and X.H. Xiao, *Role of the cardiac Na^+/H^+ exchanger during ischemia and reperfusion*. Cardiovasc Res, 2003. 57(4): p. 934-41.
161. Rossi, G.P., M. Cavallin, G.G. Nussdorfer, and A.C. Pessina, *The endothelin-aldosterone axis and cardiovascular diseases*. J Cardiovasc Pharmacol, 2001. 38 Suppl 2: p. S49-52.
162. Fliegel, L., *Regulation of myocardial Na^+/H^+ exchanger activity*. Basic Res Cardiol, 2001. 96(4): p. 301-5.

163. Li, X., B. Alvarez, J.R. Casey, R.A. Reithmeier, and L. Fliegel, *Carbonic anhydrase II binds to and enhances activity of the Na^+/H^+ exchanger*. J Biol Chem, 2002. 277(39): p. 36085-91.
164. Aharonovitz, O., H.C. Zaun, T. Balla, J.D. York, J. Orlowski, and S. Grinstein, *Intracellular pH regulation by Na^+/H^+ exchange requires phosphatidylinositol 4,5-bisphosphate*. J Cell Biol, 2000. 150(1): p. 213-24.
165. Lin, X. and D.L. Barber, *A calcineurin homologous protein inhibits GTPase-stimulated Na^+-H^+ exchange*. Proc Natl Acad Sci U S A, 1996. 93(22): p. 12631-6.
166. Wakabayashi, S., T. Pang, X. Su, and M. Shigekawa, *A novel topology model of the human Na^+/H^+ exchanger isoform 1*. J Biol Chem, 2000. 275(11): p. 7942-9.
167. Moor, A.N. and L. Fliegel, *Protein kinase-mediated regulation of the Na^+/H^+ exchanger in the rat myocardium by mitogen-activated protein kinase-dependent pathways*. J. Biol. Chem., 1999. 274(33): p. 22985-22992.
168. Clerk, A. and P.H. Sugden, *Activation of protein kinase cascades in the heart by hypertrophic G protein-coupled receptor agonists*. Am J Cardiol, 1999. 83(12A): p. 64H-69H.
169. Takahashi, E., J. Abe, B. Gallis, R. Aebersold, D.J. Spring, E.G. Krebs, and B.C. Berk, *$p90^{RSK}$ is a serum-stimulated Na^+/H^+ exchanger isoform-1 kinase. Regulatory phosphorylation of serine 703 of Na^+/H^+ exchanger isoform-1*. J. Biol. Chem., 1999. 274(29): p. 20206-20214.
170. Tominaga, T., T. Ishizaki, S. Narumiya, and D.L. Barber, *p160ROCK mediates RhoA activation of Na^+-H^+ exchange*. Embo J, 1998. 17(16): p. 4712-22.
171. Weinman, E.J., *New functions for the NHERF family of proteins*. J Clin Invest, 2001. 108(2): p. 185-6.
172. Reczek, D., M. Berryman, and A. Bretscher, *Identification of EBP50: A PDZ-containing phosphoprotein that associates with members of the ezrin-radixin-moesin family*. J Cell Biol, 1997. 139(1): p. 169-79.
173. Kurashima, K., F.H. Yu, A.G. Cabado, E.Z. Szabo, S. Grinstein, and J. Orlowski, *Identification of sites required for down-regulation of Na^+/H^+ exchanger NHE3 activity by cAMP-dependent protein kinase. phosphorylation-dependent and -independent mechanisms*. J Biol Chem, 1997. 272(45): p. 28672-9.
174. Zizak, M., G. Lamprecht, D. Steplock, N. Tariq, S. Shenolikar, M. Donowitz, C.H. Yun, and E.J. Weinman, *cAMP-induced phosphorylation and inhibition of Na^+/H^+ exchanger 3 (NHE3) are dependent on the presence but not the phosphorylation of NHE regulatory factor*. J Biol Chem, 1999. 274(35): p. 24753-8.
175. Weinman, E.J., D. Steplock, M. Donowitz, and S. Shenolikar, *NHERF associations with sodium-hydrogen exchanger isoform 3 (NHE3) and ezrin are essential for cAMP-mediated phosphorylation and inhibition of NHE3*. Biochemistry, 2000. 39(20): p. 6123-9.
176. Kleizen, B., I. Braakman, and H.R. de Jonge, *Regulated trafficking of the CFTR chloride channel*. Eur J Cell Biol, 2000. 79(8): p. 544-56.
177. Pushkin, A., N. Abuladze, D. Newman, V. Muronets, P. Sassani, S. Tatishchev, and I. Kurtz, *The COOH termini of NBC3 and the 56-kDa H^+-ATPase subunit are PDZ motifs involved in their interaction*. Am J Physiol Cell Physiol, 2003. 284(3): p. C667-73.

178. Boron, V.F., M.A. Hediger, E.L. Boulpaep, and M.F. Romero, *The renal electrogenic Na^+:HCO_3^- cotransporter*. J Exp Biol, 1997. 200(Pt 2): p. 263-8.
179. Lubman, R.L. and E.D. Crandall, *Regulation of intracellular pH in alveolar epithelial cells*. Am J Physiol, 1992. 262(1 Pt 1): p. L1-14.
180. Komukai, K., T. Ishikawa, and S. Kurihara, *Effects of acidosis on Ca^{2+} sensitivity of contractile elements in intact ferret myocardium*. Am J Physiol, 1998. 274(1 Pt 2): p. H147-54.
181. Juel, C., *Lactate/proton co-transport in skeletal muscle: regulation and importance for pH homeostasis*. Acta Physiol Scand, 1996. 156(3): p. 369-74.
182. Igarashi, P., R.F. Reilly, F. Hildebrandt, D. Biemesderfer, N.A. Reboucas, C.W. Slayman, and P.S. Aronson, *Molecular biology of renal Na^+/H^+ exchangers*. Kidney Int Suppl, 1991. 33: p. S84-9.
183. Chow, C.W., *Regulation and intracellular localization of the epithelial isoforms of the Na^+/H^+ exchangers NHE2 and NHE3*. Clin Invest Med, 1999. 22(5): p. 195-206.
184. Avkiran, M. and R.S. Haworth, *Regulation of cardiac sarcolemmal Na^+/H^+ exchanger activity by endogenous ligands. Relevance to ischemia*. Ann N Y Acad Sci, 1999. 874: p. 335-45.
185. Hume, J.R., D. Duan, M.L. Collier, J. Yamazaki, and B. Horowitz, *Anion transport in heart*. Physiol Rev, 2000. 80(1): p. 31-81.
186. Leviel, F., D. Eladari, A. Blanchard, J.S. Poumarat, M. Paillard, and R.A. Podevin, *Pathways for HCO_3^- exit across the basolateral membrane in rat thick limbs*. Am J Physiol, 1999. 276(6 Pt 2): p. F847-56.
187. Hara, C., H. Satoh, T. Usui, M. Kunimi, E. Noiri, K. Tsukamoto, S. Taniguchi, S. Uwatoko, A. Goto, L.C. Racusen, J. Inatomi, H. Endou, T. Fujita, and G. Seki, *Intracellular pH regulatory mechanism in a human renal proximal cell line (HKC-8): evidence for Na^+/H^+ exchanger, Cl^-/HCO_3^- exchanger and Na^+/HCO_3^- cotransporter*. Pflugers Arch, 2000. 440(5): p. 713-20.
188. Turner, H.C., L.J. Alvarez, and O.A. Candia, *Identification and localization of acid-base transporters in the conjunctival epithelium*. Exp Eye Res, 2001. 72(5): p. 519-31.
189. Wang, Z., L. Conforti, S. Petrovic, H. Amlal, C.E. Burnham, and M. Soleimani, *Mouse Na^+: HCO_3^- cotransporter isoform NBC-3 (kNBC-3): cloning, expression, and renal distribution*. Kidney Int, 2001. 59(4): p. 1405-14.
190. Ruetz, S., A.E. Lindsey, and R.R. Kopito, *Function and biosynthesis of erythroid and nonerythroid anion exchangers*. Society of General Physiologists Series, 1993. 48: p. 193-200.
191. Khandoudi, N., J. Albadine, P. Robert, S. Krief, I. Berrebi-Bertrand, X. Martin, M.O. Bevensee, W.F. Boron, and A. Bril, *Inhibition of the cardiac electrogenic sodium bicarbonate cotransporter reduces ischemic injury*. Cardiovasc Res, 2001. 52(3): p. 387-96.
192. Thomas, J.A., R.N. Buchsbaum, A. Zimniak, and E. Racker, *Intracellular pH measurements in Ehrlich ascites tumor cells utilizing spectroscopic probes generated in situ*. Biochemistry, 1979. 18(11): p. 2210-2218.
193. Roos, A. and W.F. Boron, *Intracellular pH*. Physiol. Rev., 1981. 61(2): p. 296-434.

194. Sterling, D. and J.R. Casey, *Transport activity of AE3 chloride/bicarbonate anion-exchange proteins and their regulation by intracellular pH*. Biochem. J., 1999. 344 Pt 1: p. 221-229.
195. Bradford, M.M., *A rapid and sensitive method for the quantitation of microgram quantities of protein utilizing the pricinple of protein-dye binding*. Anal. Biochem., 1976. 72: p. 248-254.
196. Laemmli, U.K., *Cleavage of structural proteins during assembly of the head of bacteriophage T4*. Nature, 1970. 227: p. 680-685.
197. Towbin, H., T. Staehelin, and J. Gordon, *Electrophoretic transfer of proteins from polyacrylamide gels to nitrocellulose sheets: procedure and some applications*. Proc. Natl. Acad. Sci., 1979. 76: p. 4350-4354.
198. Laue, T.M. and W.F. Stafford, 3rd, *Modern applications of analytical ultracentrifugation*. Annu Rev Biophys Biomol Struct, 1999. 28: p. 75-100.
199. Philo, J.S., *An improved function for fitting sedimentation velocity data for low-molecular-weight solutes*. Biophys J, 1997. 72(1): p. 435-44.
200. Lieberman, D.M. and R.A.F. Reithmeier, *Localization of the carboxyl terminus of Band 3 to the cytoplasmic side of the erythrocyte membrane using antibodies raised against a synthetic peptide*. J. Biol. Chem., 1988. 263: p. 10022-10028.
201. Sherman, M. and A.L. Goldberg, *Involvement of the chaperonin dnaK in the rapid degradation of a mutant protein in Escherichia coli*. Embo J, 1992. 11(1): p. 71-7.
202. Provencher, S.W. and J. Glockner, *Estimation of globular protein secondary structure from circular dichroism*. Biochemistry, 1981. 20(1): p. 33-7.
203. Weinman, E.J., C.M. Evangelista, D. Steplock, M.Z. Liu, S. Shenolikar, and A. Bernardo, *Essential role for NHERF in cAMP-mediated inhibition of the Na^+/HCO_3^- co-transporter in BSC-1 cells*. J Biol Chem, 2001. 276(45): p. 42339-46.
204. Kim, J.H., W. Lee-Kwon, J.B. Park, S.H. Ryu, C.H. Yun, and M. Donowitz, *Ca^{2+}-dependent inhibition of Na^+/H^+ exchanger 3 (NHE3) requires an NHE3-E3KARP-alpha-actinin-4 complex for oligomerization and endocytosis*. J Biol Chem, 2002. 277(26): p. 23714-24.
205. Vince, J.W. and R.A. Reithmeier, *Identification of the Carbonic Anhydrase II Binding Site in the Cl^-/HCO_3^- Anion Exchanger AE1*. Biochemistry, 2000. 39(18): p. 5527-5533.
206. Vince, J.W., U. Carlsson, and R.A. Reithmeier, *Localization of the Cl^-/HCO_3^- anion exchanger binding site to the amino-terminal region of carbonic anhydrase II*. Biochemistry, 2000. 39(44): p. 13344-9.
207. Gross, E., O. Fedotoff, A. Pushkin, N. Abuladze, D. Newman, and I. Kurtz, *Phosphorylation-induced modulation of pNBC1 function: distinct roles for the amino- and carboxy-termini*. J Physiol, 2003. 549(Pt 3): p. 673-82.
208. Sarkar, G. and S.S. Sommer, *The megaprimer method of site-directed mutagenesis*. Biotechniques, 1990. 8: p. 404-407.
209. Karmazyn, M., *The sodium-hydrogen exchange system in the heart: its role in ischemic and reperfusion injury and therapeutic implications*. Can. J. Cardiol., 1996. 12(10): p. 1074-82.

210. Boron, W.F. and P. De Weer, *Intracellular pH transients in squid giant axons caused by CO2, NH3, and metabolic inhibitors*. J Gen Physiol, 1976. 67(1): p. 91-112.

211. Silva, N.L., H. Wang, C.V. Harris, D. Singh, and L. Fliegel, *Characterization of the Na^+/H^+ exchanger in human choriocarcinoma (BeWo) cells*. Pflugers Arch, 1997. 433(6): p. 792-802.

212. Fujinaga, J., F.B. Loiselle, and J.R. Casey, *Transport activity of chimaeric AE2-AE3 chloride/bicarbonate anion exchange proteins*. Biochem J, 2003. 371(Pt 3): p. 687-96.

213. Fierke, C.A., T.L. Calderone, and J.F. Krebs, *Functional consequences of engineering the hydrophobic pocket of carbonic anhydrase II*. Biochemistry, 1991. 30(46): p. 11054-63.

214. Gross, E., K. Hawkins, A. Pushkin, P. Sassani, R. Dukkipati, N. Abuladze, U. Hopfer, and I. Kurtz, *Phosphorylation of Ser^{982} in the sodium bicarbonate cotransporter kNBC1 shifts the HCO_3^- : Na^+ stoichiometry from 3 : 1 to 2 : 1 in murine proximal tubule cells*. J Physiol, 2001. 537(Pt 3): p. 659-65.

215. Thurmond, D.C. and J.E. Pessin, *Molecular machinery involved in the insulin-regulated fusion of GLUT4-containing vesicles with the plasma membrane (review)*. Mol Membr Biol, 2001. 18(4): p. 237-45.

216. Kunimi, M., G. Seki, C. Hara, S. Taniguchi, S. Uwatoko, A. Goto, S. Kimura, and T. Fujita, *Dopamine inhibits renal Na^+:HCO_3^- cotransporter in rabbits and normotensive rats but not in spontaneously hypertensive rats*. Kidney Int., 2000. 57(2): p. 534-543.

217. Zaniboni, M., P. Swietach, A. Rossini, T. Yamamoto, K.W. Spitzer, and R.D. Vaughan-Jones, *Intracellular proton mobility and buffering power in cardiac ventricular myocytes from rat, rabbit, and guinea pig*. Am J Physiol Heart Circ Physiol, 2003. 285(3): p. H1236-46.

218. Vaughan-Jones, R.D. and K.W. Spitzer, *Role of bicarbonate in the regulation of intracellular pH in the mammalian ventricular myocyte*. Biochem Cell Biol, 2002. 80(5): p. 579-96.

219. Ward, C.L. and R.R. Kopito, *Intracellular turnover of cystic fibrosis transmembrane conductance regulator. Inefficient processing and rapid degradation of wild-type and mutant proteins*. Journal of Biological Chemistry, 1994. 269(41): p. 25710-8.

220. Theroux, P., B.R. Chaitman, N. Danchin, L. Erhardt, T. Meinertz, J.S. Schroeder, G. Tognoni, H.D. White, J.T. Willerson, and A. Jessel, *Inhibition of the sodium-hydrogen exchanger with cariporide to prevent myocardial infarction in high-risk ischemic situations. Main results of the GUARDIAN trial. Guard during ischemia against necrosis (GUARDIAN) Investigators*. Circulation, 2000. 102(25): p. 3032-8.